Cathodic protection system design framework for the petrochemical industry

DE Diedericks

21996032

Dissertation submitted in fulfilment of the requirements for the degree *Magister* in Electrical and Electronic Engineering at the Potchefstroom Campus of the North-West University

Supervisor: Prof G van Schoor

Co-supervisor: Dr EO Ranft

November 2015

ABSTRACT

The aim is to establish a cathodic protection (CP) system design framework for the petrochemical industry in South Africa. The CP system design framework is destined to be used as a guideline when designing CP systems for structures such as tanks, underground pipelines, and plant areas within the petrochemical industry.

The necessary understanding regarding corrosion and corrosion mitigation in the form of CP is compiled and presented in the form of literature study chapters. Standards published by standards organizations such as the National Association of Corrosion Engineers (NACE) and the International Organisation for Standardisation (ISO) contribute greatly towards the proposed CP system design framework. The empirical equations and certain approaches taken towards CP system design as presented in these standards and in other sources of literature are used to structure the design framework. It is important to note that an empirical approach is used in the CP system design framework.

Based on the design framework, the CP systems for the protection of a small tank farm and an underground pipeline are designed and documented. For verification purposes both these CP systems are implemented within BEASY™ CP and Corrosion. This software package, based on the Boundary Element Method (BEM) is used to visually evaluate the performance of the designed CP systems and to verify the design framework. An iterative approach is used throughout the verification process in order to adjust the design framework based on the results generated from the simulations.

The validation of the design framework is based on a comparison of the results obtained from the simulation of the CP system of the underground pipeline network and actual measurements of potential at available test points installed on the underground pipeline network. The correlation between the actual measured results and the simulated results proved that the design framework can be successfully implemented for the design of CP systems. The accuracy of the simulated results for a pipeline that has been in service for 15 years were also satisfactory and extends the use of the CP system design framework to simulate and determine the life expectancy of a given CP system based on the initial design parameters.

The cost of a given CP system will greatly influence the decision on the type of system to be installed. Although the dissertation mainly focuses on the technical challenges associated with CP system design, the important cost drivers for CP system design are highlighted throughout.

OPSOMMING

Die doel is om 'n katodiese beskerming (KB) stelsel ontwerpsraamwerk vir die petrochemiese bedryf in Suid-Afrika te ontwikkel. Die KB stelsel ontwerpsraamwerk is bestem om gebruik te word as 'n riglyn vir die ontwerp van KB stelsels vir strukture soos tenks, ondergrondse pyplyne, en fabrieksgebiede in die petrochemiese bedryf.

Die nodige begrip rakende roes en korrosie voorkoming, in die vorm van KB, is saamgestel en aangebied in die vorm van twee literatuurstudie hoofstukke. Standaarde gepubliseer deur standaarde organisasies soos die Nasionale Vereniging vir Korrosie Ingenieurs (NACE) en die Internasionale Organisasie vir Standaardisering (ISO) dra grootliks by tot die voorgestelde KB stelsel ontwerpsraamwerk. Die empiriese vergelykings en sekere benaderings tot KB stelsel ontwerp soos aangebied in hierdie standaarde en in ander bronne van literatuur word gebruik om die ontwerpsraamwerk te struktureer. Dit is belangrik om daarop te let dat 'n empiriese benadering gebruik word in die KB stelsel ontwerpsraamwerk.

Die ontwerpsraamwerk word gebruik om KB stelsels vir die beskerming van 'n klein tenk plaas asook 'n ondergrondse pyplyn te ontwerp en te dokumenteer. Vir verifikasie doeleindes word albei hierdie KB stelsels gesimuleer met behulp van BEASY™ CP and Corrosion. Hierdie sagteware pakket, gebaseer op die Grens Element Metode (GEM), word gebruik om die doeltreffendheid van die ontwerpe van beide KB stelsels visueel te evalueer en sodoende die ontwerpsraamwerk te verifieer. 'n Iteratiewe benadering word deur die verifikasie proses gebruik om die ontwerpsraamwerk aan te pas op grond van die simulasie resultate.

Die validasie van die ontwerpsraamwerk berus op ‘n vergelyking van die simulasie resultate van die ondergrondse pyplyn netwerk en werklike metings van potensiaal by beskikbare toets punte op die ondergrondse pyplyn. Die korrelasie tussen die gesimuleerde en werklike potensiaal metings het bewys dat die ontwerpsraamwerk suksesvol gebruik kan word vir die ontwerp van KB stelsels. Die akkuraatheid van die gesimuleerde resultate van die ondergrondse pyplyn, wat al 15 jaar in werking is, het bevestig dat die ontwerpsraamwerk suksesvol gebruik kan word om te bepaal wat die vlak van katodiese beskerming op ‘n struktuur sal wees soos die einde van die diens leeftyd nader. Hierdie inligting is gebaseer op aanvanklike ontwerpsparameters.

Die koste van 'n gegewe KB stelsel sal die besluit oor die tipe stelsel wat geïnstalleer moet word sterk beïnvloed. Alhoewel die verhandeling hoofsaaklik fokus op die tegniese uitdagings wat verband hou met KB stelsel ontwerp, word die belangrike kostedrywers vir KB stelsel ontwerp deurgaans uitgelig.

ACKNOWLEDGEMENTS

Firstly, I would like to thank all the parties involved at the North West University for the opportunity to further my studies. I would also like to thank you for all the support and encouragement during the course of my study.

I would also like to acknowledge the following people in no particular order for their contributions during the course of my study.

- Dr. Lafras Lamont for his time, guidance, and advice during the early stages of the study.
- Professor George van Schoor, my supervisor, for his support, guidance, encouragement, and advice throughout the course of this study.
- Dr. Eugén Ranft, my co-supervisor, for his advice, guidance, and input throughout.
- Elmarie Peters for her love, support, and understanding, especially during the difficult times.
- My parents, Wynand and Marinda Diedericks, for their help, advice, support, and love.
- My friend, Brando de Waal, for his loyalty, support, advice, and encouragement.

“For I know the plans I have for you, declares the Lord, plans for welfare and not for evil, to give you a future and a hope.” Jeremiah 29:11

TABLE OF CONTENTS

LIST OF TABLES

LIST OF FIGURES

LIST OF ABBREVIATIONS

BEM	Boundary Element Method
CP	Cathodic protection
CSE	Copper/Copper Sulphate reference Electrode
FBE	Fusion Bonded Epoxy
GDP	Gross Domestic Product
ICCP	Impressed Current Cathodic Protection
RE	Reference Electrode
SACP	Sacrificial Anode Cathodic Protection
SHE	Standard Hydrogen Electrode
SRB	Sulphate-Reducing Bacteria
TRU	Transformer Rectifier Unit
UK	United Kingdom
USA	United States of America

LIST OF SYMBOLS

A	Surface area
A	Amperes
a	Atomic weight
Al	Aluminium
α	Fraction of polarisation
B	Mobility
β_a	Anodic Tafel slope
β_c	Cathodic Tafel slope
c_i	Concentration
C_B	Solution concentration
c_{Ox}	Concentration of oxidising agent
c_{Red}	Concentration of reducing agent
d	Diameter
D	Diffusion constant
D_z	Diffusivity of reacting species
δ	Thickness of concentration gradient
e^-	Electron
E_A	Pipe anode potential
E_C	Pipe cathode potential
E_{corr}	Corrosion potential
E	Potential
$\vec{E}$	Electric field strength
ε_c	Cathodic polarisation
Fe	Iron
$Fe(OH)_2$	Iron (II) hydroxide
$\mathfrak{F}$	Faraday constant
ΔG	Free reaction enthalpy
ΔG_f^*	Forward reaction rate activation energy
ΔG_r^*	Reverse reaction rate activation energy
H	Hydrogen
H_3O	Hydronium
H_2	Dihydrogen
H_2O	Water

R_{PA}	Pipe anode resistance-to-earth
R_{PC}	Pipe cathode resistance-to-earth
I_{corr}	Current through electrolyte (corrosion current)
I'	External anode current
$R_A{}'$	External anode resistance-to-earth
$M(s)$	General oxidising element
OH^-	Hydroxide
z	Charge number
O_2	Oxygen
$\tilde{\mu}_i$	Electrochemical potential
μ_i	Partial molar free enthalpy
φ	Electric potential
z_i	Charge number
$\vec{w}_i$	Velocity in the migration direction
R	Gas constant
T	Absolute temperature
U^*	Nernst potential / Voltage in thermodynamic equilibrium
φ_B	Electrical potential of reference electrode
μ_B	Partial molar free enthalpy of reference electrode
U_H	Potential measured against SHE
V	Volts
Ω	Ohm
m	Mass
m	Meter
I	Current
t	Time / depth
n	Number of equivalents exchanged
r	Corrosion rate
i	Current density
η_a	Anodic overpotential
η_c	Cathodic overpotential
i_a	Anodic current density
i_c	Cathodic current density
i_o	Exchange current density

r_f	Forward reaction rate
r_r	Reverse reaction rate
K_f	Forward reaction rate constant
K_r	Reverse reaction rate constant
$i_{app,c}$	Net applied current
$\eta_{T,c}$	Total cathodic polarisation
$\eta_{act,c}$	Cathodic activation polarisation
η_{conc}	Concentration polarisation
i_L	Limiting current density
Zn	Zinc
ρ	Specific electrolyte resistivity
J	Current density
R_n	Total resistance of n anodes
R	Resistance
F	Interference factor
s	Spacing between anodes
v	Multiple of spacing between anodes
L	Length
R_v	Resistance of vertical anode / ground bed
R_h	Resistance of horizontal anode / ground bed
kg	Kilogram
Mg	Magnesium

1

CHAPTER

INTRODUCTION

This chapter provides an introduction to the corrosion process and the engineering technology known as cathodic protection. The chapter will present the reader with the problem statement along with the issues to be addressed and the research methodology. An overview of the document is also presented in this introductory chapter.

1.1 Background

Corrosion is one of the major challenges that faces the petrochemical industry in modern society. The cost of corrosion is well known in the petrochemical industry as tens of millions of dollars in lost income and treatment costs are reported annually. Projections to June 2013 indicated that the total corrosion related costs, direct and indirect, will have exceeded $1 trillion or roughly 6% of the GDP in the USA [1]. It is therefore clear why corrosion mitigation is so important in the petrochemical industry. Apart from the economic impact that corrosion has on the industry, there is also a social impact.

It is reported that corrosion causes great ecological damage to the environment along with the loss of human life [2]. According to a study conducted on available careers in corrosion mitigation it became apparent that highly skilled personnel in corrosion mitigation are pursued by employers. While job titles and specific duties vary from one position to another, cathodic protection (CP) skills are high in demand [3].

The aim of this research is to establish a knowledge base on cathodic protection (CP) to support the need for the expert skills in corrosion that is required in the petrochemical industry. In order to mitigate corrosion by designing and implementing a CP system for a given application, prior knowledge on corrosion and CP systems are essential. The physics phenomenon of corrosion as well as the method of CP to mitigate it, need to be understood.

Although not the focus of this study, it is of utmost importance that the optimal technical solution for a given application is implemented at the lowest possible cost. This is very important from a business perspective and will be mentioned where applicable throughout the dissertation.

1.1.1 Corrosion

Corrosion is a natural phenomenon that occurs across the globe and plays a major part in the failure of metal structures, especially in the petrochemical industry. All natural processes tend toward their lowest possible energy states and thus corrosion tends to return refined steel products to their lowest natural state, i.e. hydrated iron oxides. The hydrated iron oxides, commonly known as rust, are similar in chemical composition than the original iron oxide [4].

From a more technical point of view corrosion can be described as an electrochemical process. The electrochemical process describes the chemical reaction taking place between the metal and the surrounding electrolyte, where a flow of electric current is involved, in accordance with the laws of thermodynamics [5].

A schematic diagram of corrosion cells that is formed on the surface of a metal structure is displayed in Figure 1-1. In most instances where corrosion occurs, the metal is in close contact with an electrolyte, i.e. a corrosive medium. The electrolyte is responsible for the establishment of differences in the electric potential across the surface of the metal structure. The result is that a network of closed-circuit galvanic cells, or couples, are formed in which electric current can flow. The current will flow from the anodic areas to the adjacent cathodic areas. Corrosion will appear at the anodic areas in accordance with Faraday's laws [5].

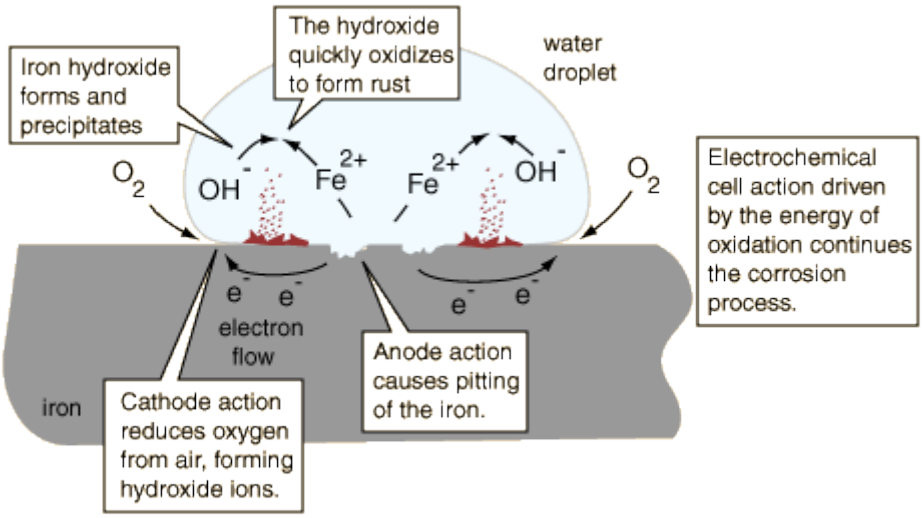

Figure 1-1: Schematic diagram of corrosion cells on iron **[6]**

Due to the electrical nature of the electrochemical cell, the mitigation of corrosion can be approached from either an electrochemical or an electrical point of view [5]. The use of CP in mitigating corrosion in the petrochemical industry has become common practice in most countries, due to its effectiveness if properly designed and implemented.

1.1.2 Cathodic protection

The history of CP is well documented within academic literature. The first use of CP is generally attributed to Sir Humphrey Davy in the early 1800's [7]. It is generally accepted in literature that the first use of CP in the petrochemical industry was documented in the USA around 1950. The introduction of CP in industry coincided with the introduction of thin-walled steel pipes for the underground transmission of oil and gas. The UK followed suit in the use of CP systems in the early 1950s. CP is a well-established technology today and is used to protect a wide variety of underground or immersed structures in the petrochemical industry.

The principle of CP can best be described in terms of polarisation. Once the anodic areas in the electrochemical cell can be polarised to, or beyond, the potential of the corresponding cathodic areas, corrosion will cease to exist. Two systems are readily used to achieve the polarisation of the anodic areas:

- Impressed current cathodic protection (ICCP)
- Sacrificial anode cathodic protection (SACP)

A functional illustration of an ICCP system is displayed in Figure 1-2. The figure illustrates how the external current applied to the structure mitigates corrosion. With the two CP systems in mind, i.e. ICCP and SACP, there is one major difference between the respective systems. ICCP uses an external power source with inert anodes, while SACP uses the naturally occurring electrochemical potential difference between the different metallic elements to provide protection.

The design and implementation of CP systems are complex procedures that require certain skills and the understanding of the principles behind CP. Furthermore, the soil is a very complex environment and the structures that are buried in soil affect one another in complicated ways.

The abovementioned interaction between structures buried in soil is fundamental when designing CP systems for a given application. No two CP systems are the same as the environment is always changing and certain challenges arise when calculations are made by means of empirical equations. The empirical and analytical equations have been proven to be accurate enough in calculations for design purposes. Contingency factors are often incorporated in empirical calculations to allow for the use of average soil resistivity values in the empirical equations. The average soil resistivity values are used to not overcomplicate the empirical calculations.

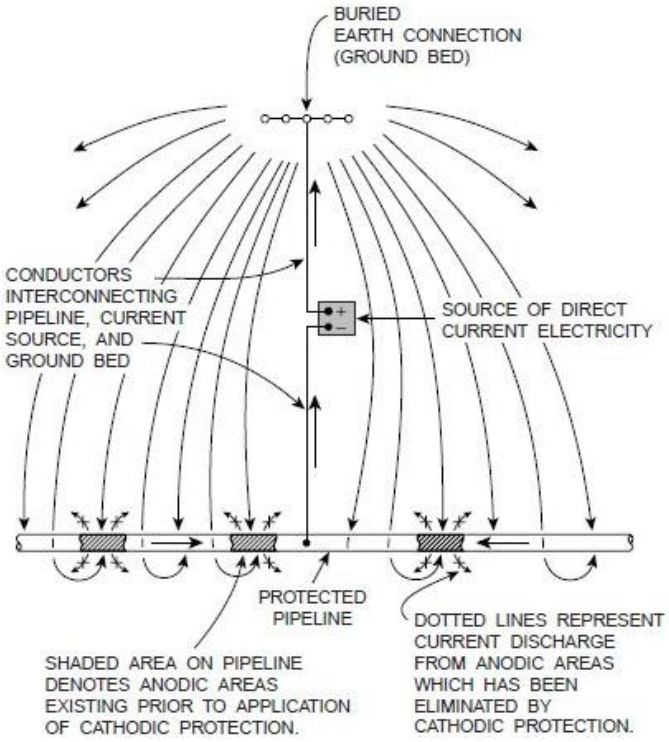

Figure 1-2: Functional illustration of an ICCP system **[8]**

The placement of the anodes with respect to the structure influences the performance of a prospective system, especially in terms of the resistance-to-earth of the anode ground bed. In cases where the anodes are not remotely placed with respect to the structure, some correction to the resistance is required [9]. The design of CP systems in the petrochemical industry is strongly dependent on specific standards. These standards provide guidelines to the design engineer in terms of empirical equations used in the design of CP systems and are based on previous experience with CP systems and the varying challenges.

1.2 Problem statement

The purpose of this project is to formulate a CP system design framework for the petrochemical industry in South Africa. The framework will be based on standard documents published for use in different parts of the world and will be used predominantly for CP system design in the petrochemical industry. Typical applications of the design framework include plant areas, tank farms and underground pipelines.

In order to put forward a verified and validated CP system design framework the underlying principles of corrosion and CP must be well understood. The study will include detailed literature that addresses the underlying principles while the end result will be the CP system design framework.

From a business perspective it is important to address the optimal design in terms of cost while still meeting the technical requirements. It is important to note that this study focusses on the most efficient technical solution and does not represent a techno-economic study. Implementing the CP system design framework into a feasible business plan will require the identification of the biggest cost drivers. These cost drivers will be identified throughout the dissertation to demonstrate how cost can influence CP system design but will not be the main focus of the study.

It is important to note that the CP system design framework developed throughout this dissertation will be developed with both SACP and ICCP systems in mind. The design approach for both these types of systems are essentially identical and will therefore contain the design procedure for both types of systems. For verification and validation purposes only ICCP systems are considered as the structures to be protected necessitate ICCP systems. The system to be used for validation purposes is of the ICCP type and therefore this dissertation mainly focuses on ICCP system design.

1.3 Issues to be addressed

The most important issues to be addressed throughout the dissertation are presented in the sections that follow. The issues to be addressed will be used to formulate the research methodology and will be presented in the form of a flow diagram at the end of this section.

1.3.1 Corrosion and CP strategies

The physics phenomenon behind the corrosion process and how corrosion can be mitigated need to be addressed. The basic thermodynamics and kinetics behind the corrosion process are important principles to understand and how it can be used in mitigating corrosion. CP is a proven technology in corrosion mitigation and the operating principles of the technology are essential in successfully implementing these systems. The two types of CP systems along with their respective applications must be compared in terms of advantages and disadvantages to ensure that the CP system installed for the protection of a metallic structure is fit for the application.

It is expected that different types of anodes are to be used depending on the type of CP system to be implemented, i.e. SACP or ICCP. The different anode types and anode sizes require consideration in terms of operating principles as well as implementation. The different anode ground bed configurations that are generally installed are another issue to be addressed. An assessment of the different configurations is required from a physics point of view in order to fully understand the role of the anode ground bed within the CP system.

1.3.2 CP system design framework

As stated in the problem statement, a CP system design framework is to be established for use within the petrochemical industry in South Africa. The CP system design framework will be used as a guide whenever designing CP system for various scenarios within the petrochemical industry. The framework will typically address the empirical design of CP systems along with a few other considerations regarding the design of CP systems.

Viewing the design framework from a business perspective, the argument exists that the cost of a CP system has to be included in such a framework. For the purpose of this study, the technical aspect, and more importantly, the technical accuracy of the design framework will be evaluated. The cost drivers regarding CP system design will be acknowledged throughout the dissertation where deemed necessary.

1.3.3 CP system design framework verification

The verification of the CP system design framework is an important step towards the validation of the CP system design framework. The verification phase will be used to determine whether the CP system design framework meets the requirements or not. During the verification phase of the CP system design framework it is possible that deficiencies within the framework will be recognised. In this case the CP system design framework will be amended to address the shortcomings if any exist.

1.3.4 CP system design framework validation

The validation of the CP system design framework is essential throughout this dissertation. The validation of the CP system design framework is required to ascertain whether the framework can generally be used as a guideline regarding CP system design within the petrochemical industry. The validation process will also ensure that deficiencies within the CP system design framework are recognised and corrected to the required level.

1.4 Research methodology

The research methodology that will be used throughout the dissertation will be documented in the sections to follow. The research methodology will serve as an extension of the issues to be addresses covered in the preceding section. The sequence of the research methodology is presented in the form of a high level flow diagram in Figure 1-3. The issues to be addressed are used within the flow diagram to give the reader some insight as to how the issues will be addressed and how the sequence of events will follow in the dissertation.

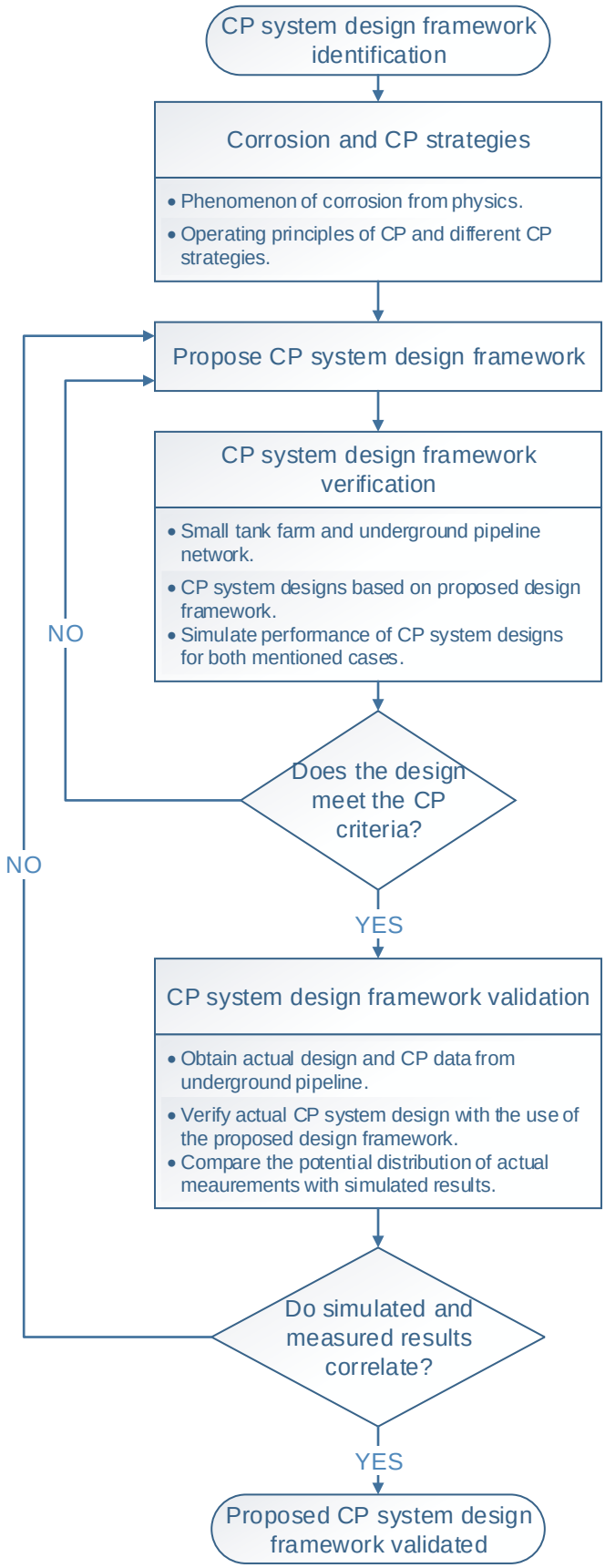

Figure 1-3: Flow diagram representing research methodology

1.4.1 Corrosion and CP strategies

The issues regarding corrosion and corrosion mitigation will be addressed in the form of a detailed literature study chapter that will focus on the corrosion process from a chemical perspective along with the most important aspects of corrosion mitigation. The operating principles of CP will also be covered in this literature chapter along with the respective advantages and disadvantages of SACP and ICCP systems respectively. The literature compilation will be used to become familiar with the physics phenomenon of corrosion and how CP is used to mitigate corrosion by applying CP. The operating principles of CP is deemed important in order to be able to effectively evaluate the performance of a given CP system and recognise shortages that may exist in the system.

Anodes and anode ground bed design will be addressed in the form of another literature chapter addressing the relevant issues. This literature chapter will also be used for the derivation of the equations that is used for the calculation of the grounding resistance of the anode ground bed. Anodes and anode ground beds are viewed as the most important components within a CP system. The literature regarding anodes and anode ground beds will be used to identify the different types of anodes that are generally used and identifying the different advantages and disadvantages associated with the different anodes.

1.4.2 CP system design framework

As was stated before, the aim is to develop a CP system design framework that can be used in general for CP system design in the petrochemical industry in South Africa. A proposed design framework will be developed by using the empirical equations found in literature and international standards and using these documents as a guideline. By designing CP systems for a small tank farm and an underground pipeline network, the design framework will be developed based on the procedure followed during the respective CP system designs.

After the design of the CP systems to protect the small tank farm and the underground pipeline respectively, it is expected that the design framework may have certain shortcomings. In order to identify any shortcomings a thorough verification and validation process is required.

1.4.3 CP system design framework verification

Measuring potential or polarisation levels brought about by the introduction of a CP system is the only practical way of verifying the design of a CP system. Other measurements that can be useful in the verification process will include current distribution and electric fields. Evaluating the

performance of the CP systems designed for the small tank farm and underground pipeline network in a suitable simulation software package will lead to the abovementioned results.

Computational Mechanics BEASY™ has a validated software package available for modelling the performance of a CP system. BEASY™ Corrosion and CP computes detailed data on potential shifts and current demand. The data acquired from the software will aid the formulation of the design framework. BEASY™ Corrosion and CP makes use of the boundary element method (BEM) in the computation of potential shifts and current demand.

BEASY™ Corrosion and CP will be used to visualise the results of the empirically designed CP systems to be implemented on the small tank farm as well as the underground pipeline network. This visualisation of the potential shift and/or current distribution on the surface of the metallic structures will be used during the evaluation and verification procedures to follow.

The two CP systems designed and on which the proposed CP system framework is based will be evaluated at the hand of the applicable CP criteria. The protection criteria that will be used for the verification of the design framework will include one or all of the following [8]:

- -850 mV with cathodic protection applied criterion
- Polarised potential of -850 mV criterion
- 100 mV of polarisation criterion

At this stage of the verification process the flow diagram will enter a loop in the case where the design does not meet the criteria. This sequence of events can be viewed in the flow diagram representing the research methodology and found in Figure 1-3. If the performance of the system does not meet the criteria the proposed design framework will be altered or adjusted where required in order to put forward a more efficient design. The performance of the altered design will once again be visualised with BEASY™ Corrosion and CP and re-evaluated. Once the CP criteria are met, the methodology can continue to validating the CP system design framework.

1.4.4 CP system design framework validation

The validation of the CP system design framework will include the use of actual potential measurements and/or current distributions of the underground pipeline network. These measurements will be compared to the results obtained from the simulations performed on the underground pipeline network. The purpose of the validation is to base the design of the CP system for the underground pipeline network on the CP system design framework developed earlier. The visualisation of the performance of this CP system will then follow in BEASY™

Corrosion and CP. The simulated results will then be compared to the actual potential measurements taken at the available test points.

As with the verification process the validation process will also enter a loop according to the functional flow diagram presented in Figure 1-3 in the case where the simulated results and actual measurements do not correlate. In the case where the simulated results and the actual measurements do not correlate the design framework

1.5 Overview of the dissertation

Chapter 2 contains a detailed literature study on corrosion and CP system design. The chapter starts off with an introduction on corrosion and why it is possible to mitigate corrosion from an electrical perspective. The operating principles of CP are addressed from a physics point of view. The operating principles of the two different CP systems are discussed along with the components of the respective systems. The limitations of CP systems, the advantages and disadvantages of the respective systems and certain required considerations are discussed. A critical review regarding the implementation of SACP and ICCP systems is included at the end of this chapter.

Chapter 3 serves as an additional literature study chapter that is used to provide the reader with all the necessary information regarding the anodes used in CP systems. The chapter also focuses on the design of anode ground beds in terms of the grounding resistance that is associated with each configuration of anode ground bed. A critical review of the literature contained in this chapter reaches conclusion on the most effective anodes and anode ground bed design.

Chapter 4 is dedicated to empirical CP system designs for a small tank farm and an underground pipeline network. The design of both systems are based on empirical equations generally associated with CP system design and documented in various sources of literature and international standards. The empirical design of the CP systems is used to establish a general design framework for CP design in the petrochemical industry. The equations presented in Chapter 3 of this document are used for the calculation of the grounding resistance of various anode types and sizes installed in different anode ground bed configurations.

Chapter 5 is dedicated to the verification of the design framework that was established in Chapter 4. The main focus of this chapter falls on the polarisation of the surface of the mentioned structures and the overall performance of the CP systems. The design framework is verified using the appropriate CP criteria in terms of the performance of the CP systems based on the design framework. The polarisation results used for verification purposes are obtained from simulations performed in BEASY™ Corrosion and CP.

Chapter 6 addresses the validation of the CP system design framework as proposed in this dissertation. The results obtained from the simulations performed during the verification of the design framework are compared to practical results obtained from the actual underground pipeline network. The results were taken from all the available test points installed on the underground pipeline network and compared to the relevant areas of interest obtained from the simulations.

Chapter 7 is used to conclude the research covered throughout the dissertation. The chapter will also be used to make certain recommendations regarding the use of the CP system design framework for designing CP systems for the petrochemical industry. The conclusions and recommendations made in this chapter are of high importance for successfully implementing the CP system design framework in the petrochemical industry.

Chapter 1 provided some background on corrosion and CP as a method of mitigating corrosion and supplied the reader with the problem statement. The issues to be addressed are discussed along with the research methodology that followed. The overview of the dissertation provided some insight into what to expect in the document. Chapter 2 follows and contains a detailed literature study. The literature study will be used to gather the relevant information in order to successfully complete the study on CP system design.

2

CHAPTER

CORROSION AND CORROSION MITIGATION

This chapter contains a detailed literature study on corrosion and CP system design. The chapter starts off with an introduction on corrosion and why it is possible to mitigate corrosion from an electrical perspective. The operating principles of CP are addressed from a physics point of view. The operating principles of the two different CP systems are discussed along with the components of the respective systems. The limitations of CP systems, the advantages and disadvantages of the respective systems and certain required considerations are discussed. A critical review regarding the implementation of SACP and ICCP systems is included at the end of this chapter.

2.1 Corrosion

Corrosion can be explained as the deterioration of a material due to the reactions the material has with the environment in which it is installed. The material most susceptible to corrosion is most often metal. Electrochemical reactions between the metal and the electrolyte in which it is immersed, i.e. chemicals present either in the soil and/or water, form corrosion cells. The corrosion cells formed are responsible for the degradation of the metallic surface [10]. Different types of corrosion can occur on the surface of a metal structure and can include one or all of the following types of corrosion [7, 11, 12]:

- Almost uniform weight loss corrosion
- Pitting corrosion
- Hydrogen-induced corrosion
- Stress corrosion
- Electrolytic corrosion
- Galvanic corrosion
- Inter-granular corrosion
- Erosion corrosion

A corrosion cell can be compared to a battery in an operational sense, and must therefore contain the same basic elements found in a battery: an anode, a cathode, a conductive electrolyte, and a metallic return path for the current. Corrosion can be prevented when one or more of the elements of the corrosion cell are removed [10].

In terms of the metal structure experiencing the effects of corrosion due to the development of a corrosion cell, the elements of the corrosion cell can be explained as follows:

- The anode is the area on the surface of the structure where positive metal (iron) ions leave the surface of the structure and enters the electrolyte. This is where corrosion takes place on the metal surface of the structure.
- The cathode is the area on the surface of the structure to which the positive metal ions are attracted to. At the cathode area on the surface of the structure corrosion is often eliminated or significantly reduced.
- The electrolyte, typically soil or water, is in contact with both the anode and the cathode. The electrolyte is conductive and provides a path for a current to flow between the anode and cathode.
- The metallic return path is provided by the metal of the structure found between the anodic and cathodic area on the surface of the structure. The metal serves as an electrical connection between the anode and cathode and completes the elements needed to form a corrosion cell.

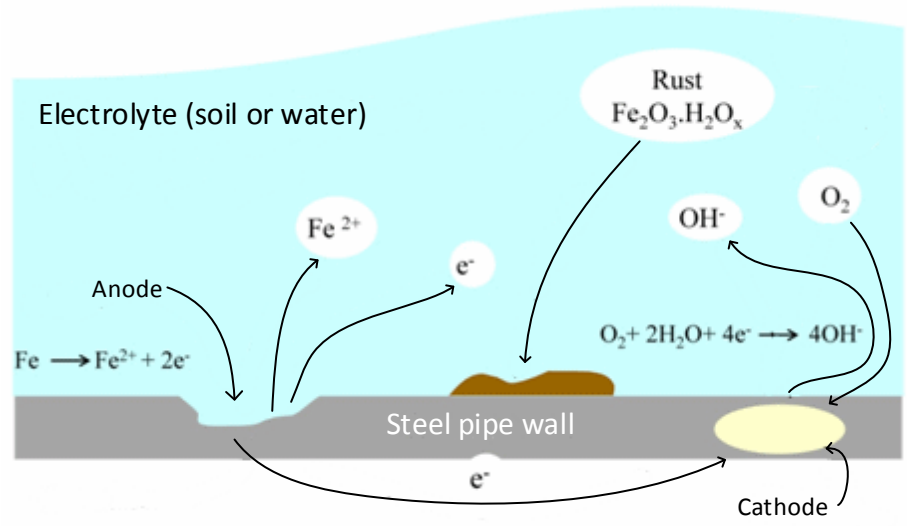

Figure 2-1: Corrosion cell on metallic surface

A basic corrosion cell causing material degradation on the surface of the metal structure is displayed in Figure 2-1. It can be seen that the surface of the metal, in this case a steel pipe wall, is degraded at the anodic area and the electrons set free by the electrochemical reaction are

attracted to the cathodic area on the surface of the steel pipe. Also present in the corrosion cell is a conductive electrolyte which is typically soil or water.

The value of the potential difference that exists between the anode and cathode of the corrosion cell reflects the difference in potential energy that an electron has at each of the two respective electrodes [13]. Different configurations can be responsible for developing a potential difference on a metal surface: whenever two different metals are immersed in the same electrolyte, the same metal is immersed in different electrolytes and interference from foreign structures or sources. In the corrosion cell, electrons always flow from the anodic area to the cathodic area, resulting in electrical current flow, and therefore it can be concluded that all corrosion results from the flow of electrical current [14].

At the anodic areas on the surface of the metal structure oxidation reactions takes place. Oxidation is normally explained as the loss of electrons by an atom, molecule or ion. The general anodic reaction occurring at the anode, as in Figure 2-1 can be described as follows:

$$M(s) \rightarrow M^{z+} + ze^{-}, \tag{2-1}$$

where $M(s)$ represents the element experiencing the loss of electrons, z represents the charge number, and e^{-} is representative of the free electron(s).

The reactions that occur at the cathodic areas on the surface of the metal structure are known as reduction reactions. Reduction is generally explained as the gain of electrons by an atom, molecule or ion [13]. Several possible half-reactions can take place at the cathodic areas. The reduction half-reactions that generally occur can be narrowed down to:

$$2H_3O^{+}(aq) + 2e^{-} \rightarrow H_2(g) + 2H_2O(l), \tag{2-2}$$

$$2H_2O(l) + 2e^{-} \rightarrow H_2(g) + 2OH^{-}(aq), \text{ and} \tag{2-3}$$

$$2H_2O(l) + O_2(g) + 4e^{-} \rightarrow 4OH^{-}(aq). \tag{2-4}$$

The rate at which the corrosion occurs is controlled by the rate of the cathodic process. From the above cathodic reactions, the reaction responsible for the fastest corrosion rate will be dependent on the acidity of the electrolyte and the amount of oxygen that is present in the electrolyte. In the presence of little or no oxygen in the electrolyte, when, for example the electrolyte is moist clay, the reduction reaction reduces hydrogen ions or water and the products from the reaction are H_2 (g) and hydroxide ions.

The following reactions are representative of the half-reactions occurring in the presence of little or the complete absence of oxygen in an electrolyte. In this case the anodic reaction (2-5), cathodic reaction (2-6), precipitation reaction (2-7), and the net reaction (2-8) follows:

$$Fe(s) \rightarrow Fe^{2+}(aq) + 2e^{-}, \quad \textbf{(2-5)}$$

$$2H_2O(l) + 2e^{-} \rightarrow H_2(g) + 2OH^{-}(aq), \quad \textbf{(2-6)}$$

$$Fe^{2+}(aq) + 2OH^{-} \rightarrow Fe(OH)_2(s), \text{ and} \quad \textbf{(2-7)}$$

$$Fe(s) + 2H_2O(l) \rightarrow H_2(g) + Fe(OH)_2(s). \quad \textbf{(2-8)}$$

In cases where both oxygen and water are present in an electrolyte, the chemistry of the corrosion process is different. The presence of oxygen in the electrolyte can cause the rate of corrosion to be 100 times faster compared to the corrosion rate in an electrolyte where oxygen is absent. In the presence of oxygen, the anodic reaction (2-9), cathodic reaction (2-10), precipitation reaction (2-11), and net reaction (2-12) follows:

$$2Fe(s) \rightarrow 2Fe^{2+}(aq) + 4e^{-}, \quad \textbf{(2-9)}$$

$$2H_2O(l) + 4e^{-} + O_2(g) \rightarrow 4OH^{-}(aq), \quad \textbf{(2-10)}$$

$$2Fe^{2+}(aq) + 4OH^{-} \rightarrow 2Fe(OH)_2(s), \text{ and} \quad \textbf{(2-11)}$$

$$2Fe(s) + 2H_2O(l) + O_2(g) \rightarrow 2Fe(OH)_2(s). \quad \textbf{(2-12)}$$

In the absence of oxygen and in the case where the electrolyte is neutral or near neutral in terms of acidity, corrosion virtually ceases. This is due to the fact that a reaction that enables the transfer of charges across the cathode surface cannot occur at an appreciable rate. Furthermore a layer of hydrogen develops at the cathode surface and assists in ceasing corrosion from taking place.

Another cathodic reaction occurs in the case where the electrolyte is acidic. In this instance a high concentration of hydrogen ions exist and the charges are transferred by the following reaction:

$$2H^{+} + 2OH^{-} + 2e^{-} \rightarrow H_2 + 2OH^{-}. \quad \textbf{(2-13)}$$

In both the reactions in (2-10) and (2-13) the liquid surrounding the cathodic surface tends to become more alkaline. The reaction presented in (2-13) is responsible for evolving hydrogen gas at the cathode. Virtually all corrosion of metal structures immersed in an electrolyte is affected by

the aforementioned mechanism [15]. The electrons that are set free from the chemical reactions make it possible to view the corrosion process from an electrical perspective.

To further support the statement that the corrosion process can be viewed from an electrical perspective a better understanding of corrosion from first principles is necessary. The most important aspects when analysing corrosion will present itself in the form of the basic thermodynamics behind the corrosion process and the corrosion kinetics. The basic thermodynamics of corrosion are used to better understand and analyse the energy associated with the corrosion process. The most important equation to be derived from the basic thermodynamics is the Nernst potential equation. The Nernst potential equation is used to derive the areas of stability for different phases on Pourbaix diagrams.

An overview of the basic thermodynamics associated with corrosion is provided in the section that follows. This overview is used to derive the Nernst potential equation to ultimately draw a simplified Pourbaix diagram iron in an aqueous solution.

2.1.1 Electrochemical kinetics of corrosion

The basis of electrochemical reactions is based on Faraday's Law. Electrochemical reactions either produce or consume electrons [16]. The flow of electrons is measured in ampere. The proportionality between the electron flow and the mass of metal reacted in an electrochemical reaction is given by Faraday's Law [16]:

$$m = \frac{Ita}{n\mathcal{F}},$$

(2-14)

where m is the mass reacted, I is the current in amperes, t is the time, a the atomic weight, n the number of equivalents exchanged, and $\mathcal{F}$ Faraday's constant. The rate of corrosion can be derived by dividing (2-14) by t and the surface area [16]:

$$r = \frac{m}{tA} = \frac{ia}{n\mathcal{F}},$$

(2-15)

where r represents the corrosion rate, A is the surface area, and i is defined as the current density, i.e. I/A. Equation (2-15) shows the proportionality between the loss of mass per unit area (e.g. $mg/dm^2/day$) and current density (e.g. $\mu A/cm^2$) [16].

2.1.2 Electrochemical polarisation

Overpotential is a term that is often used to refer to polarisation. The relationship between overpotential and the rate of the reaction represented by the current density is explained in the following equations [16]:

$$\eta_a = \beta_a \log \frac{i_a}{i_o}, \tag{2-16}$$

where η_a is the anodic overpotential, β_a is a positive Tafel constant, i_a the anodic current density, and i_o is the exchange current density equivalent to the reversible rate at equilibrium. For the cathodic reaction

$$\eta_c = \beta_c \log \frac{i_c}{i_o}, \tag{2-17}$$

where η_c is the cathodic overpotential, β_c is a negative Tafel constant, i_c the cathodic current density, and i_o is the exchange current density equivalent to the reversible rate at equilibrium. Equation (2-16) is representative of anodic polarisation, while (2-17) is representative of cathodic polarisation. Anodic polarisation is positive and cathodic polarisation is negative, and this is determined by the respective Tafel constants for half-cell reaction, i.e. β_a and β_c.

The Maxwell distribution law is used to express the reaction rates as a function of the respective activation energies. The reaction rate of the forward reaction is

$$r_f = K_f \exp\left[-\frac{\Delta {G_f}^*}{RT}\right], \tag{2-18}$$

where r_f represents the forward reaction rate, K_f is the forward reaction rate constant, $\Delta {G_f}^*$ the forward reaction rate activation energy, R the gas constant, and T the absolute temperature. The reaction rate of the reverse reaction is

$$r_r = K_r \exp\left[-\frac{\Delta {G_r}^*}{RT}\right], \tag{2-19}$$

where r_r represents the reverse reaction rate, K_r is the reverse reaction rate constant, $\Delta {G_r}^*$ the reverse reaction rate activation energy, R the gas constant, and T the absolute temperature. In the cases where (2-18) and (2-19) are at equilibrium

$$r_f = r_r = \frac{i_o a}{n\mathfrak{F}},$$

(2-20)

where i_o is the exchange current density equivalent to the reversible rate at equilibrium, a the atomic weight, n the number of equivalents exchanged, and $\mathfrak{F}$ is Faraday's constant. It follows from (2-20) that

$$i_o = K_f' \, exp\left[-\frac{\Delta G_f^*}{RT}\right] = K_r' \exp\left[-\frac{\Delta G_r^*}{RT}\right],$$

(2-21)

which clearly demonstrates that the exchange current density is a function of the activation energies [16]. The cathodic discharge reaction rate in terms of current density becomes [16]:

$$i_c = K_f' \exp\left[-\frac{\Delta G_f^* - \alpha n\mathfrak{F}\eta_c}{RT}\right],$$

(2-22)

where i_c represents the cathodic current density, K_f' the forward reaction rate constant in equilibrium, α is the fraction of η_c, the cathodic overpotential, taken by the discharge reaction. The anodic ionisation reaction rate becomes [16]:

$$i_a = K_r' \exp\left[-\frac{\Delta G_f^* + (1-\alpha)n\mathfrak{F}\eta_c}{RT}\right],$$

(2-23)

where i_a represents the anodic current density, K_r' the reverse reaction rate constant in equilibrium, $(1-\alpha)$ is the fraction of η_c, the cathodic overpotential, taken by the ionization reaction. The net applied current, $i_{app,c}$, is

$$i_{app,c} = i_c - i_a = i_o \exp\left[\frac{\alpha n\mathfrak{F}\eta_c}{RT}\right] - i_o \exp\left[\frac{-(1-\alpha)n\mathfrak{F}\eta_c}{RT}\right].$$

(2-24)

In the cases where η_c reaches high values, (2-24) simplifies to:

$$i_{app,c} = i_c - i_a = i_o \exp\left[\frac{\alpha n\mathfrak{F}\eta_c}{RT}\right].$$

(2-25)

The total cathodic polarisation is the sum of both the activation and concentration polarisation [16]:

$$\eta_{T,c} = \eta_{act,c} + \eta_{conc}\,,$$

(2-26)

where

$$\eta_{act,c} = \beta_c \log\left[\frac{i_c}{i_o}\right],$$

(2-27)

with $\eta_{act,c}$ the cathodic activation polarisation, and the concentration polarisation, η_{conc}, given by

$$\eta_{conc} = \frac{2.3RT}{n\mathbb{F}} \log\left[1 - \frac{i_c}{i_L}\right].$$

(2-28)

Equation (2-28) contains an undefined variable in the form of i_L, which is the limiting current density. The limiting current density is the measure of a maximum reaction rate that cannot be exceeded because of a limited diffusion rate of hydrogen ions in a solution [16]. The limiting current density is given by

$$i_L = \frac{D_z n\mathbb{F} C_B}{\delta},$$

(2-29)

where D_z is the diffusivity of the reacting species, n the number of equivalents exchanged, $\mathbb{F}$ Faraday's constant, C_B the solution concentration, and δ is the thickness of the concentration gradient in solution.

2.1.3 Corrosion potential and current density

Whenever a metallic structure is corroding in an electrolyte, both the anodic and cathodic half-cell reactions occur simultaneously on the surface of the metallic structure. Each of the reactions consist of its own half-cell electrode potential and exchange current density. This is an important statement, as these half-cell electrode potentials cannot coexist separately on an electrically conductive surface [16]. Each of the reactions must polarise to a common intermediate value. This intermediate value is referred to as the corrosion potential or mixed potential.

As the oxidising and reduction reactions, presented in (2-1) to (2-13), occurs on the surface of a metallic structure, the half-cell electrode potentials change respectively according to eq. (2-16) and (2-17). The polarisation on the same surface will continue until they become equal at the corrosion potential. At the corrosion potential, the rates of the anodic and cathodic reactions are equal and the rate of anodic dissolution is identical to the corrosion rate in terms of current density [16]:

$$i_c = i_a = i_{corr},$$

(2-30)

where i_c is the cathodic dissolution in terms of current density, i_a the anodic dissolution in terms of current density, and i_{corr} the corrosion rate in terms of current density. With the rate of corrosion well documented at this stage, the mitigation of corrosion follows. Cathodic polarisation is generally referred to as the underlying principle of CP and is discussed in the following section.

2.1.4 Cathodic polarisation

Whenever an excess of electron flow is applied to a corroding electrode, it causes the electrode potential to shift negatively [16]. This negative potential shift from the corrosion potential, E_{corr}, to a potential, E, where corrosion will cease, is defined as cathodic polarisation. The cathodic polarisation, ε_c, is given by

$$\varepsilon_c = E - E_{corr}\,.$$

(2-31)

The excess of electrons associated with cathodic polarisation suppresses the rate of the anodic reaction from i_{corr} to i_a and similarly increases the cathodic reduction reaction from i_{corr} to i_c [16]. The difference between the two reactions must be equal to the applied current, $i_{app,c}$, in order to fulfil the principle of charge conservation:

$$i_{app,c} = i_c - i_a.$$

(2-32)

Cathodic polarisation is explained in Figure 2-2. An excess of electron flow, $i_{app,c}$, is applied to a corroding electrode. The anodic reaction for the corroding electrode is defined by the blue line in Figure 2-2. The cathodic reaction is defined by the green line in Figure 2-2. The Tafel constants for both reactions, i.e. β_c and β_a, are assumed to be 0.1 V per decade. The corrosion potential, E_{corr}, and the rate of corrosion, i_{corr}, as a current density, are defined by mixed potential theory. The application of an excess electron flow causes a negative potential shift, ε_c, which causes the anodic ionization rate, i_a, to decrease and the cathodic discharge rate, i_c, to increase. Both these rate are defined as a current density in Figure 2-2.

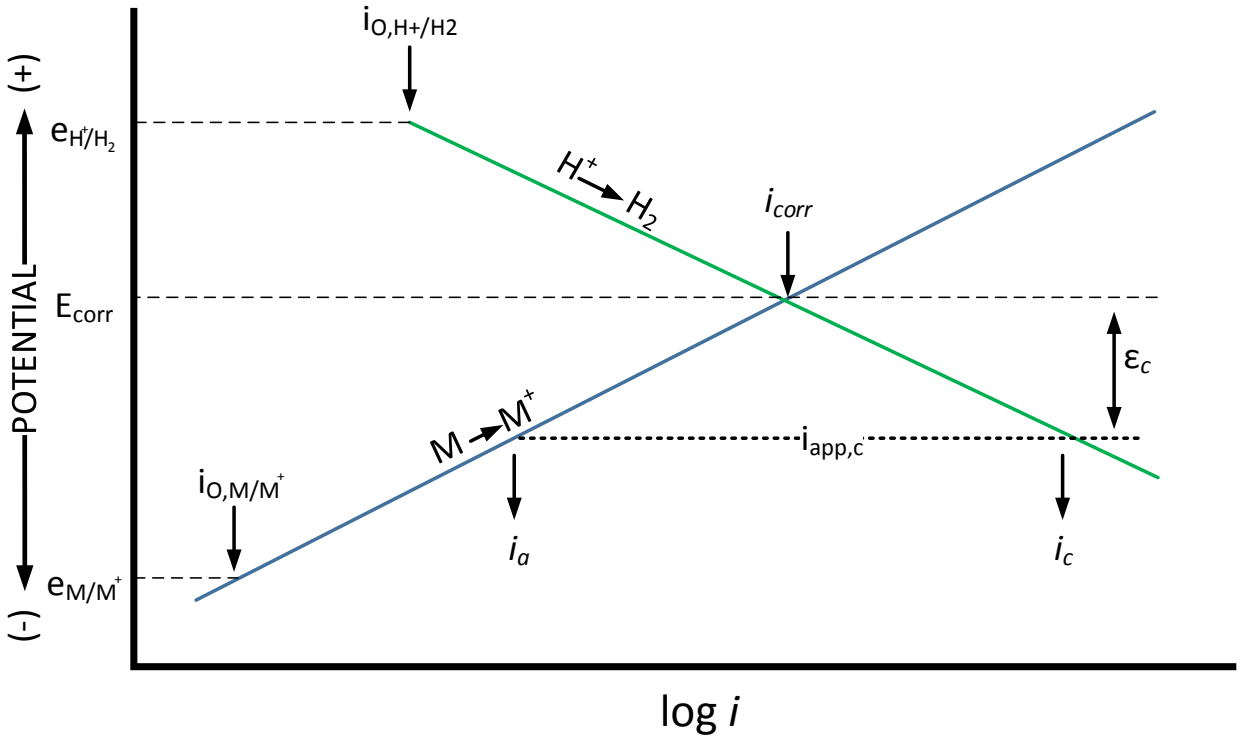

Figure 2-2: Cathodic polarisation of a corroding electrode in an electrolyte **[16]**

The preceding explanation along with Figure 2-2 will be used to explain the experimental polarisation curves that is contained in Figure 2-3. The polarisation curves defined in Figure 2-3 are based on the procedure that was explained with the aid of Figure 2-2.

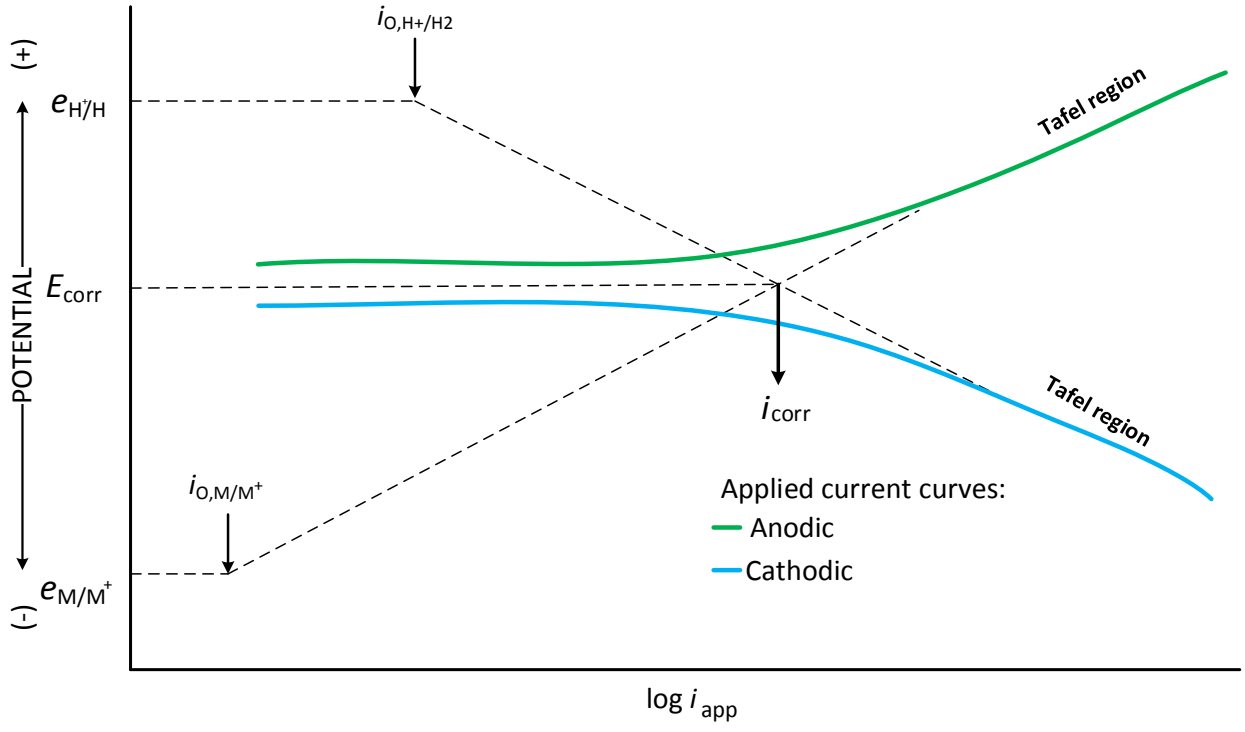

Figure 2-3: Experimental polarisation curves **[16]**

Figure 2-3 shows the external applied current for various values of ε_c. In cases where the potential shift is negative and small, i_c is only slightly higher than i_a, and $i_{app,c}$ is very low. The cathodic polarisation curve is defined by the blue line in Figure 2-3. As the potential shift increases, i_c increases while i_a decreases, both quite rapidly, until i_a becomes insignificant compared to i_c. At this point in the graph, the cathodic polarisation curve corresponds with the dashed line that represents the cathodic half-cell reaction's overpotential [16]. The linearity of the polarisation curve on a semi log plot at this point is termed Tafel behaviour. In the case where the potential shift is positive, the opposite of what was discussed regarding the cathodic polarisation curve is true. The green line in Figure 2-3 defines the anodic polarisation curve.

2.1.5 Equivalent electric circuit of corrosion cell

Now that the principles of corrosion had been discussed at the hand of corrosion cells and the chemical reactions taking place at the anodic and cathodic areas on the metallic surface respectively, an equivalent circuit of the corrosion cell can be developed.

At the interface between metal and soil there is an EMF, sometimes referred to as the standard potential. When current passes from the anode to the cathode, this EMF changes so that, to an approximation, the metal and soil can be represented by a resistance in series with a source of EMF. The following circuit will be used to represent an equivalent circuit for a simple corrosion cell in terms of resistances and sources [17].

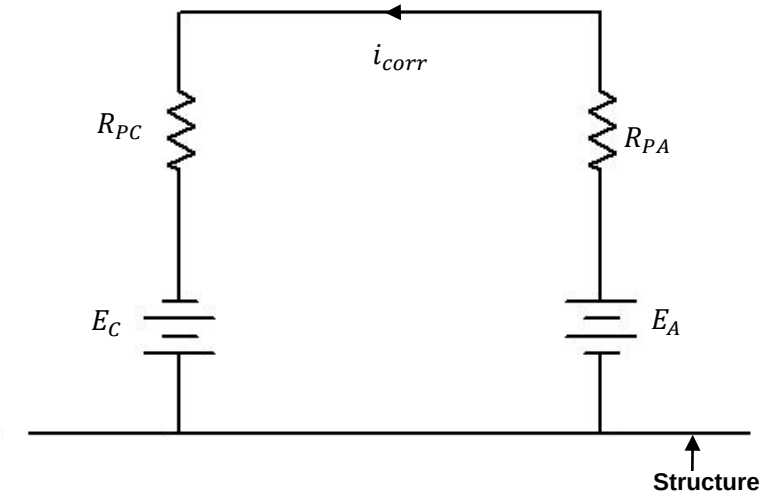

Figure 2-4: Equivalent circuit of corrosion cell **[17]**

The equivalent circuit of a corrosion cell is displayed in Figure 2-4. In the equivalent circuit of the corrosion cell the labels used indicate the following: E_A represents the open circuit potential of the anode electrode, E_C represents the open circuit potential of the cathode electrode, R_{PA} represents

the effective anode electrode resistance, R_{PC} represents the effective cathode electrode resistance, and i_{corr} indicates the corrosion current around the circuit.

The corrosion current referred to in Figure 2-4, assuming a zero resistance for the soil path, can be presented as follows:

$$i_{corr} = \frac{E_A - E_C}{R_{PA} + R_{PC}}.$$

(2-33)

2.2 Cathodic protection

Cathodic protection is an active form of corrosion control in which electrons are supplied to the metal structure to be protected [11]. Cathodic protection systems are synonymous with the implementation of an external anode. The external anode is used to allow current to flow from the anode, through the electrolyte, to the entire exposed surface of the metal structure to be protected. The flow of current forces the original anodic areas on the metal surface to become cathodic with respect to the external anode. The moment at which the original anodic areas become cathodic, corrosion is prevented since the metal surface no longer gives up electrons [9]. The equivalent circuit of a corroding cell with CP connected to it is displayed in Figure 2-5.

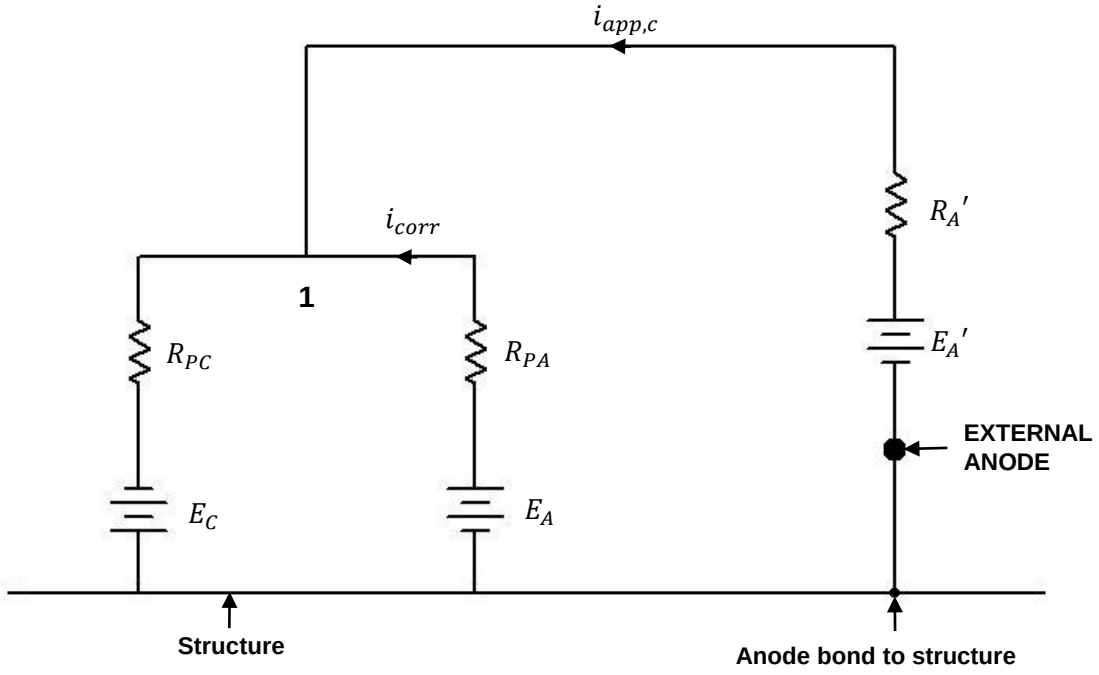

Figure 2-5: Equivalent circuit of corroding cell with "protection" current flowing from external source **[17]**

From the equivalent circuit presented in Figure 2-5, it can be seen that the current flow from the anode is decreased. The anode current is now $(i_{corr} - i_{app,c})$, while the current to the cathode is increased. Corrosion will cease in the case where no current leaves the anode, that is, whenever

($i_{corr} - i_{app,c} = 0$). In the case where this is in fact true, the potential across resistance R_{PA} will be zero. Since the potential at node 1 in Figure 2-5 must be the same by the two different paths, the following equation can be developed [17]:

$$E_A = E_C + R_{PC}(i_{corr} + i_{app,c})$$

(2-34)

According to (2-15), the potential of the structure being protected must be shifted to the open-circuit potential of the structure. For a pipeline, but not limited to only pipelines, the nominal desired potential range is between -850 and -1 200 mV, which has been proven to be scientifically sound [17]. This potential is measured with respect to a $Cu/CuSO_4$ reference electrode. Although the equivalent circuit represents a SACP system, it is also applicable to ICCP systems.

The use of equivalent electrical circuits to describe the corrosion cell and CP do have their limitations. These limitations boils down to the fact that simplifications have to be made in the actual physical arrangement in order to make it expressible in electrical terms [17]. The limitations are as follows [17]:

- The use of a simple resistance implies that the current density at all points of the electrode is constant. This is generally not true because the simple equivalent circuit gives no idea of the geometry of the system.
- Effects such as temperature, moisture content, liquid flow through the soil, oxygen concentration, bacterial action etc., are not directly incorporated, though they can be taken into account to some extent by selecting suitable values of electrode potentials if the appropriate contents are known.
- The shift in the pipe potentials due to CP, i.e. polarisation, is not linear with current, and hence it cannot be accurately represented by an ohmic resistance. Certain levels of capacitance and inductance are also present.

Despite the limitations of the use of equivalent electrical circuits in the assessment of CP systems, it holds some advantages to the corrosion engineer in terms of understanding the resistance to earth of the various components within the CP system.

2.2.1 Sacrificial anode cathodic protection

Sacrificial anode cathodic protection sacrifices one metal, referred to as the anode, in order to protect a given structure against corrosion. The galvanic anodes installed in a sacrificial anode

CP system will be consumed within a certain amount of time. Once the installed anodes are consumed, the replacement cost is less than that of the structure they protect.

Galvanic coupling is used to connect the anode to the metal structure. For the anode to provide effective protection against the effects of corrosion, the metal from which the anode is manufactured must be more anodic than the metal to be protected. Magnesium and zinc anodes are generally used as sacrificial anodes since it consists of a high negative potential and current density [11].

Sacrificial anode CP systems are relatively inexpensive and easy to install [18]. The difference between sacrificial anode CP systems and impressed current CP systems is that sacrificial anode CP systems don't require an external power source. This eliminates the need for acquiring expensive electrical equipment. When installing a sacrificial anode CP system, current cannot be supplied in the wrong direction and damage cannot be caused to neighbouring structures. The lack of damage caused to foreign structures is due to the low driving voltage of the sacrificial anode.

Once a sacrificial anode CP system is installed, very little maintenance is required. It is only recommended that the potential and protective currents are monitored occasionally. Safety concerns are quite limited when installing sacrificial anode CP systems. This is due to the low voltages associated with such a system. Sacrificial anode CP systems are therefore the preferred corrosion protection system in areas where the danger of explosions exist [7].

In cases where sacrificial anode protection systems are installed to protect structures buried in soil, the anodes can be installed in close proximity to the structure. This can save costs, as no further excavations will be required for the installation of the anodes, and they can be installed in the excavation made for the structure. Whenever structures are immersed in electrolytes with poor conductivity, the use of sacrificial anode CP systems are limited. This is due to the low driving voltage associated with these systems. The moment, at which the current delivery of the system becomes insufficient, external power sources are needed and the system have to be altered or an alternative system installed.

A simplified schematic of the current flow in a sacrificial anode CP system is displayed in Figure 2-6. The schematic is a representation of a pipeline buried in soil along with the sacrificial anode. The protective current is seen to flow from the active sacrificial (galvanic) anode through the soil to the pipeline. The direction of the current is indicated with the aid of arrows. Once again it can be seen that no external power source is present in a sacrificial anode CP system. The flow

of current from the anode to the protected structure is the result of the driving potential difference between the metals and the presence of a conductive electrolyte.

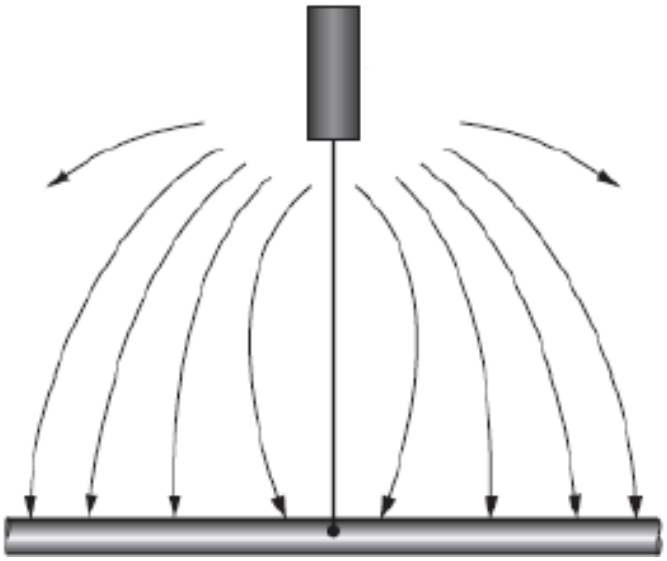

Figure 2-6: Schematic portraying current flow in a basic sacrificial anode CP system **[18]**

To summarise the advantages and limitations that are associated with sacrificial anode CP systems, the following lists are used [19]:

2.2.1.1 Advantages

- No external power source is requirement.
- Installation is uncomplicated.
- Cathodic interference is small compared to ICCP systems.
- Anodes can be readily added to the system.
- SACP systems are low maintenance systems.
- Uniform current distribution is achieved through these systems.
- The installation of anodes, during the construction of the structure to be protected, is relatively inexpensive.
- SACP systems use protective current efficiently.
- Fewer regulations are of importance.
- Right-of-way/easement costs are a minimum.

2.2.1.2 Limitations

- The driving potential of the anodes is limited.
- The current output of a SACP system is limited and often on the low side.

- In cases where the anodes are to be installed after the initial construction of the structure to be protected, the installation cost can be expensive.
- The number of anodes, required for sufficient protection, increase for poorly coated structures.
- When installed in a high-resistivity environment, SACP systems can be ineffective.

SACP systems are preferred over ICCP systems in certain cases. Although the installation costs of SACP systems may seem to be less than that of ICCP systems, careful consideration is needed when choosing between the two systems. From the limitations of SACP systems, it is visible that these systems have some shortcomings. ICCP systems are used in most cases to overcome these shortcomings. ICCP systems are to be discussed in greater detail along with the advantages and limitations of these systems.

2.2.1.3 Applications

General uses

Sacrificial anodes are generally used for applications where the required protective current is small (typically less than 1 A) and the resistivity of the electrolyte in the area is low enough (typically less than 10 000 Ω-cm) to permit their use [20]. In cases where the protective current (typically more than 1 A) requires a large number of sacrificial anodes to meet the demand, it may be more economical to install an ICCP system. This will only be possible if all the requirements of an ICCP can be met.

Specific uses

Specific and most general applications of SACP systems are as follows [20]:

- For protecting structures in areas where alternative power sources, required for ICCP systems, is unavailable.
- Clearing interferences in areas where the magnitude of the interference is not too great.
- Providing protection to well-coated sections of a structure, especially well-coated pipelines.
- For providing protection in areas where hot-spots on the structure exist and the use of complete CP is impractical or financially not viable.
- For supplementing ICCP systems in certain areas on the structure where unprotected areas still exist due to shielding effects or other reasons.
- For temporary protection, typically during the construction of a structure and an ICCP system is to be installed after the construction has been completed.
- For the mitigation of induced AC currents.

2.2.2 Impressed current cathodic protection

Impressed current CP systems require an external direct current source, which is connected between the external anode and the structure to be protected. The external source is used to provide the required driving power to the external anode. Generally, a number of external anodes are installed along with an impressed current CP system, referred to as a ground bed of anodes. The anode ground bed is forced to discharge as much CP current as is desirable by connecting the positive terminal of the external source to the anode ground bed. The negative terminal of the external source is connected to the structure to be protected.

Whenever the positive terminal of the external power source is wrongfully connected to the structure to be protected, it can have disastrous consequences. This will cause the structure to become anodic and experience an active form of corrosion.

The anode ground beds installed along with an impressed current system will corrode due to the current discharge experienced by these anodes. Desirably, materials with low consumption rates are installed as anodes in impressed current CP systems. The low consumption rate of the chosen anodes means that the anodes will have a long life expectancy.

A simplified schematic description of an impressed current CP system is displayed in Figure 2-7. The external power source can be seen at the top of the figure, with the positive terminal of the external power source connected to the external anode. The negative terminal of the external power source is connected to the structure to be protected. Although only one external anode is displayed in Figure 2-7, it must be remembered that anode ground beds are generally installed in impressed current CP systems.

The basic manner in which a structure is protected by means of ICCP and how CP is accomplished is displayed in Figure 2-8. The figure is used to display how the originally corroding section of the structure is caused to become a cathode. Whenever the given structure becomes cathodic, the cancellation of all the current discharging areas on the surface of the structure occurs. This process can be represented using the schematic to follow.

A simplified schematic of a basic impressed current CP system along with the current flow of such a system is displayed in Figure 2-8. Once again the schematic represents a buried pipeline, which is connected to an impressed current CP system. The external power source is represented by the rectifier in the middle of the schematic. The direction of the current flow from the anode ground bed is indicated by arrows. The shaded areas on the pipeline indicate the anodic areas prior to

the installation of the CP system. The current discharge from the anodic areas, now eliminated by the application of CP, is indicated by dotted lines.

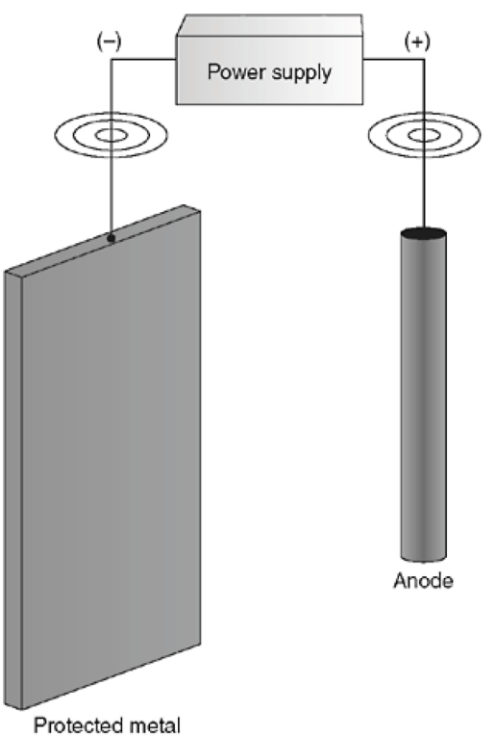

Figure 2-7: Schematic description of an impressed current CP system [18]

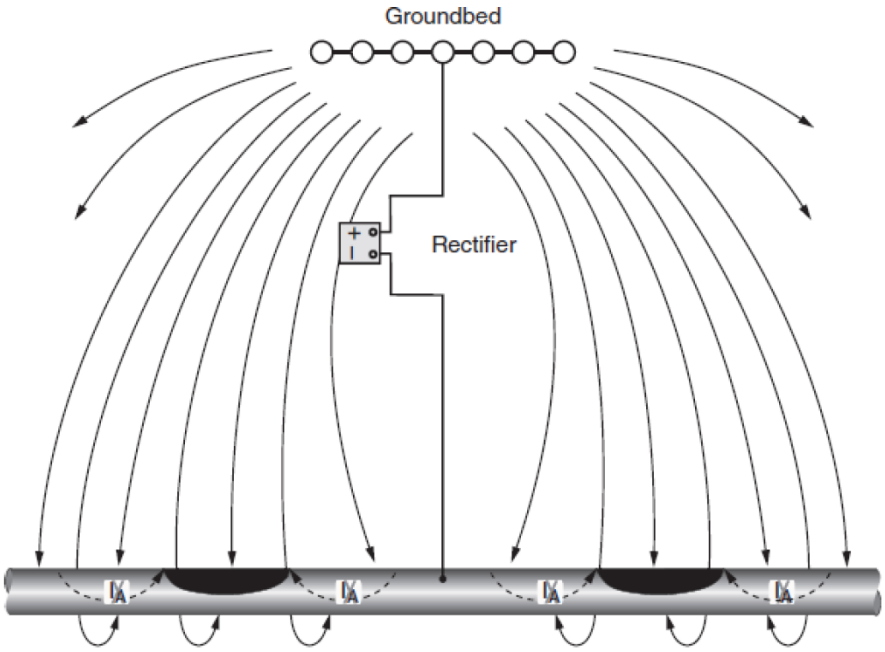

Figure 2-8: Schematic of current flow in basic impressed current CP system **[18]**

Overprotection, discussed in terms of buried pipelines, generally occur to portions of the pipeline that are closest to the anode. At the same time under-protection can occur at potions of the pipeline that is furthest away from the anode. These effects are due to the differences in the ohmic resistance along the pipeline whenever current is flowing. The under-protected portions of the pipeline are subject to corrosion. The overprotected regions can experience hydrogen embrittlement or stepwise cracking, which is associated with hydrogen evolution, occurring at these regions. Hydrogen evolution is a known cause of pipeline failure due to overprotection and should therefore be avoided.

To summarise the advantages and limitations that is associated with impressed current CP systems, the following lists are used [19]:

2.2.2.1 Advantages

- ICCP systems can be designed for wide ranges of voltage and current outputs.
- A single ground bed can be responsible for a high ampere year output.
- A single installation can be used to protect large areas or long ranges of pipelines.
- The voltage and current outputs can be varied as the need arises.
- ICCP systems are preferred in high resistivity environments.
- Effective protection is achieved on poorly coated or uncoated structures.

2.2.2.2 Limitations

- ICCP systems are prone to cause cathodic interference on adjacent pipelines and/or nearby structures.
- In certain instances, ICCP systems can be subject to power failures and/or vandalism.
- Periodic inspection and maintenance are required with the installation of ICCP systems.
- An external power source, which involves costs, is required for the system to operate.
- Incorrectly designed ICCP systems are prone to overprotection, which in turn can cause coating damage and even accelerate the corrosion process.

At first glance it may appear that SACP systems are the preferred choice in providing active corrosion protection for a given structure. This may be due to the absence of external power sources in SACP systems. Careful design and economic considerations are required when choosing between the two different active protection systems. ICCP systems are typically the preferred choice for the protection of extensive pipelines. Major advantages that ICCP systems enjoy over SACP systems are summarized:

- The wide range of voltage and current outputs that can be achieved by implementing an ICCP system.
- The large areas that can be protected from a single location.
- The effectiveness of ICCP systems on poorly coated or uncoated structures.

2.2.3 CP and protective coatings

CP systems are generally used in conjunction with protective coatings. The protective coatings serve as the primary protective measure, while the CP system is used to provide protection at those areas where coating defects occur. The current demand from the CP system will be at its lowest for a period following the application of the coating. As the coating is subjected to the corrosive environment and other forces, deterioration of the coating will appear. As the coating deteriorates, the current demand from the impressed current CP system will increase. These current requirement increases can be as much as 100 times that of the initial current requirements. This is one of the most well-known reasons for CP system failure.

2.2.3.1 Types of protective coatings

When coatings consisting of a high electrical resistance are used at the metal-electrolyte interface, the total current required for protection is reduced. The high electrical resistance of the coating also improves the distribution of the applied current to the surface of the structure [15]. The use of coatings with high electrical resistances will ensure that the potential distribution at the surface of the interface is more uniform. Various coatings are used for this purpose, each with its own advantages and limitations, which will not be discussed in detail:

- Coal tar or asphalt (bitumen) enamel coatings
- Coal tar epoxy coatings
- Conventional 2-pack epoxy coatings
- Fusion bonded epoxy coatings (FBE)
- 3-Layer Polyolefin coatings (3LPO, 3LPE)
- Thermal metal spray
- Polychloroprene (Neoprene) coatings
- Foamed coatings
- Liquid epoxy

2.2.3.2 Field joints

Field joints are considered the weakest part of any pipeline coating system. Various reasons are supplied for this with the main reasons comprising: improperly applied coatings, use of unsuitable coating types, or the selection of incompatible materials [21]. Special care should be taken to ensure that the correct procedures were followed during the application of field joints as mistakes can compromise the integrity of the entire system.

2.3 Distibution of current and potential in a stationary electric field

This section contains some important equations for corrosion protection. The equations that are derived are relevant to the stationary electric fields that are present in an electrolytically conducting medium. Soil and aqueous solutions are examples of electrolytically conducting media. The equations are also applicable to low frequencies in limited areas, provided no noticeable current displacement is caused by the electromagnetic field [7].

The stationary electric field is described by the following equations [7]:

- The vector Ohm's Law

$$E = J\rho, \tag{2-35}$$

from which because

$$E = -\nabla\varphi = -\frac{d\varphi}{dr}, \tag{2-36}$$

the potential, φ, in polar coordinates is given by

$$\varphi(r) = -\int E\, dr, \tag{2-37}$$

where E is the electric field strength, J the current density, ρ the specific resistivity of the electrolyte, φ the electric potential, and r representing a radius.

- The field outside a local current lead is source free. This means that the surface integral is equal to a current introduced by a ground:

$$I = \int_S J(r)\, dS = J(r) \times 4\pi r^2 \tag{2-38}$$

Equations (2-37) and (2-38) correspond to Kirchhoff's laws for electrical networks [7]. The derived equations will be used in the derivation of the equations to be used for the calculation of the grounding resistance of anodes and grounds.

2.4 Other important calculations

Important calculations and procedures integral in CP system design will follow in the chapters to follow where they are applicable. These calculations include:

- Surface area calculations
- Current requirements
- Resistance-to-electrolyte of the metal structure to be protected
- Resistance of electric cables
- Soil resistivity
- Transformer rectifier unit (TRU) requirements

Ohm's Law plays an important role in some of these calculations and it will become more evident in the calculations to follow.

2.5 Critical review of corrosion and corrosion mitigation

The basic thermodynamics of corrosion is used to identify the energy that is associated with the corrosion process. The available equations are used to draw up Pourbaix diagrams that provide important information regarding the various reactions taking place. Pourbaix diagrams do have certain limitations regarding corrosion as the thermodynamic equations are only accurate at high temperatures. This is not the case with corrosion and therefore the use of Pourbaix diagrams is limited. The information provided by corrosion kinetics are more useful as it can be used to determine the rate of corrosion.

Electrochemical kinetics of corrosion are used to calculate the rate of occurring corrosion. This leads to the definition of electrochemical polarisation. Electrochemical polarisation is used to identify the cathodic and anodic overpotentials respectively. The mentioned overpotentials are further used to determine the cathodic and anodic current densities respectively. Ultimately, the required current to be applied to mitigate corrosion is a function of both the cathodic and anodic current densities. The required level of cathodic polarisation is then identified and polarisation curves can be developed. The development and comprehension of these polarisation curves are very important as these polarisation curves are fundamental when simulating CP systems. For this reason it is essential to include and comprehend the electrochemical kinetics of corrosion.

The type of CP system to be installed will be dependent on the application of the CP system. SACP systems are limited to low current applications and are the preferred choice in offshore applications. The biggest advantage that SACP systems hold over ICCP systems is that SACP can be relatively inexpensive compared to ICCP systems. The major disadvantage is the low current output and low driving voltage associated with SACP systems which limits their use to low current applications and installations for temporary protection.

Because of the fact that ICCP systems make use of an external power source there exist no limiting factor on the output current and voltage of these systems. ICCP systems are generally preferred for all onshore applications and for the protection of large underground metallic structures.

The operating principles of SACP and ICCP systems are essentially identical with the only difference being the source of the output voltage. The cost of CP systems is also an important parameter to consider when designing these systems. The number of required anodes and TRUs, in the case of ICCP systems, are very important parameters to consider as it will greatly influence the total cost of a prospective CP system. Other cost drivers include labour, equipment, and cabling. The placement of anodes and TRUs with respect to the structures being protected will influence the length and size of cables, while the type of cable is determined by the surrounding environment and electrolyte.

Chapter 2 contains research on the fundamentals of corrosion and how and why corrosion occurs on metallic surfaces submerged in an electrolyte. How and why CP is used in the mitigation of corrosion were also discussed in this chapter. Most importantly, the fundamental principles of operation of CP systems was researched and how these systems are used to counter corrosion. The critical review of the literature contained in this chapter was used to identify the major differences between ICCP and SACP and which system is used for specific applications. The focus now shifts to the different anodes used in CP systems.

.

3

CHAPTER

ANODES AND ANODE GROUND BED DESIGN

This chapter serves as an additional literature study chapter that is used to provide the reader with all the necessary information regarding the anodes used in CP systems. The chapter also focuses on the design of anode ground beds in terms of the grounding resistance that is associated with each configuration of anode ground bed. A critical review of the literature contained in this chapter reaches conclusion on the most effective anodes and anode ground bed design.

3.1 Anodes

Two types of CP systems have been discussed in the preceding chapter with their differences in operation outlined. The type of anodes that are used in SACP and ICCP systems also differs. SACP systems make use of, as the name suggests, sacrificial anodes which is also generally referred to as galvanic anodes. ICCP systems are associated with the use of inert anodes. The major difference between the two types of anodes are highlighted by the following definitions:

- Sacrificial anodes are easily corroded materials deliberately installed in a pipe or tank to be sacrificed to corrosion, leaving the rest of the system relatively corrosion free [22]. The sacrificial anode will be used as the source of the CP current due to the higher electrical potential (natural potential or driving voltage) compared to the protected structure.
- An inert anode is an anode that is insoluble in the electrolyte under conditions obtained in electrolysis. Inert anodes are non-consumable [22]. Inert anodes are powered by the external source of DC current. Careful consideration of the electrolyte is required when selecting the type of inert anode to protect a given structure.

A detailed discussion regarding the different types of anodes can be found in Appendix D. The discussion focuses on parameters such as the types of materials used in the manufacturing of different types of anodes and the forms of anodes generally manufactured. Important detail contained within in this discussion include the consumption rates of the different materials used to manufacture sacrificial anodes and the driving voltages of the different materials.

Inert anodes, also referred to as impressed current anodes, are also discussed in Appendix D. The manufacturing materials used along with the different forms of impressed current anodes are discussed and supported by the different uses of each form of anodes.

Important to note at this point is that the anodes to be installed for a specific application will be one of the cost drivers in the final cost of a CP system. Depending on the type of CP system to be installed and the number of anodes to be installed the cost of a CP system can vary considerably.

The total number of anodes to be installed will be dependent on a number of parameters. Along with the expected lifetime of the anodes to be installed, the grounding resistance of the anodes will significantly influence the design of a specific CP system. For this reason it is important to understand the calculation of the grounding resistance of anodes and the equations used in these calculations.

3.2 Grounding resistance of anodes and grounds

It is necessary to understand the equations that are used for the calculation of resistance-to-earth values of anodes from first principles. This is especially important in understanding the shortcomings of certain empirical equations and what the effect of certain simplifications will be on the accuracy of the calculated values. The resistance-to-earth of the simplest case, i.e. the grounding resistance of a spherical anode in surrounding space will be derived.

Before commencing with the derivation of the equations used to calculate the grounding resistance of anodes, a few important details require mentioning:

The resistance between the spherical anode of radius, r, and a very distant, very large counter electrode (remote ground) is termed the grounding resistance of the anode. The major part of the resistance lies in the soil in the immediate vicinity of the anode. The total grounding resistance of the anode, that is, the resistance between its lead and the infinitely large and distant remote ground is composed of three terms [7]:

- The resistance in the lead and the anode itself, which usually is so small that it can be neglected: with extended cable connections, anodes or pipelines, the voltage drop in the metal must, of course be taken into account [7].
- The transition resistance between the surface of the metal and the electrolyte: with uncoated iron anodes in coke backfill, the transition resistance is usually low. With metals in soil, it can be increased by films of grease, paint, rust or deposits. It contains in addition an

electrochemical polarisation resistance that depends on the current [7]. This electrochemical polarisation resistance is due to electrochemical kinetics.

- The grounding resistance that is given by the current and potential distribution in the electrolyte will be considered in detail in what follows [7].

In order to derive the grounding resistance equation for the simplest case, a spherical-shaped anode of radius, r_0, will be considered. The anode is immersed very deep in an electrolyte ($t \gg r_0$). The current from the anode radiates uniformly outward in all directions. Between this spherical anode and the infinitely large and distant remote ground, a voltage U is applied, which involves a current $I = U/R$. R is the grounding resistance of the anode [7].

The impressed current, I, flows from the spherical anode radially in a symmetrical field, i.e. the equipotential lines represent spherical shells. With the expansion of eq. (2-35)

$$E = \rho J(r) = \frac{\rho I}{4\pi r^2},$$

(3-1)

where E is the electric field strength, ρ the specific resistivity of the electrolyte, J the current density, I the current, and r the radius. The potential, φ, at position, r, relative to the remote ground ($r \to \infty$) is given from eq. (2-37):

$$\varphi(r) = -\int_r^{\infty} E\, dr = -\frac{\rho I}{4\pi}\int_r^{\infty} r^{-2}\, dr = \frac{\rho I}{4\pi r}.$$

(3-2)

From this, the voltage, U_0, of the anode with $r = r_0$ is given by

$$U_0 = \varphi(r_0) = \frac{\rho I}{4\pi r_0}.$$

(3-3)

And therefore the grounding resistance, R, of the spherical anode is

$$R = \frac{U_0}{I} = \frac{\rho}{4\pi r_0}.$$

(3-4)

If the spherical anode is situated at a finite depth, t, the resistance is higher than for ($t \to \infty$) and lower than for $t = 0$, i.e. hemisphere is situated at the surface of the electrolyte. Its value is obtained by the mirror image of the anode at the surface ($t = 0$), so that view gives an equipotential line distribution similar to that shown in Figure 3-1. The figure is only used as a

reference regarding the mirror image of the anode and the equipotential line distribution, as it is the same as that represented in Figure 3-1 [7].

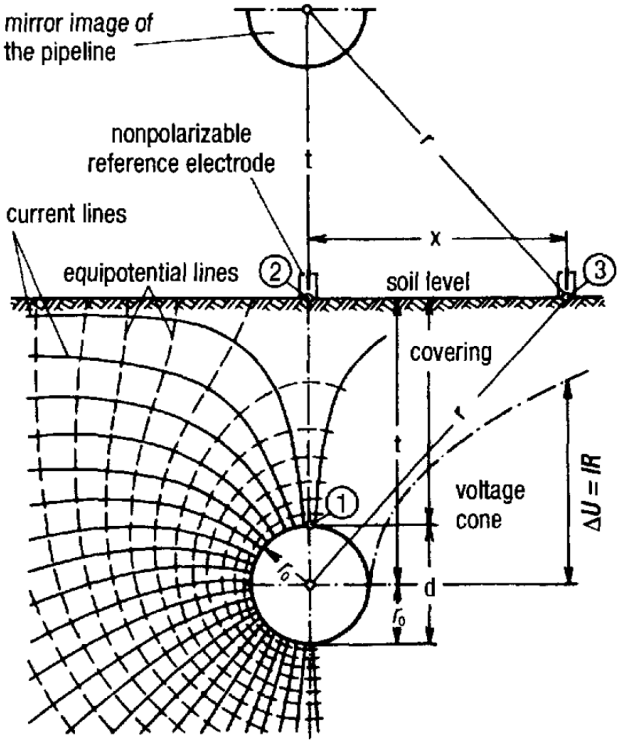

Figure 3-1: Cylindrical field around an uncoated pipeline in soil **[7]**

The equipotential line distribution remains unchanged if the upper half is removed, i.e. only the half space is considered. For the anode voltage, it follows from eq. (3-3), with $2r_0 = d$:

$$U_0 = \frac{\rho I}{4\pi r_0} + \frac{\rho I}{8\pi t} = \frac{\rho I}{2\pi}\left(\frac{1}{d} + \frac{1}{4t}\right)$$

(3-5)

The grounding resistance is therefore given by:

$$R = \frac{U_0}{I} = \frac{\rho}{2\pi}\left(\frac{1}{d} + \frac{1}{4t}\right)$$

(3-6)

The equations to be used for the calculation of the grounding resistance for simple anode shapes are included in Table B-1. These equations can be derived for the different shaped anodes on the basis of the derivation that was previously presented.

3.2.1 Interference factor with several anodes

The mutual interference of several individual anodes installed for CP of a structure can be treated by the potential distribution of a spherical anode. This case is only true for cases where the

spacing of anodes, s, is larger than the length, L, of the anode, i.e. $s > L$. Although the anodes are covered to a certain depth in practice, the equation for the grounding resistance is mostly used, i.e. in half space. This is due to the soil resistivity being frequently greater in the upper layers of the soil [7].

The total resistance of *n* anodes is given by

$$R_n = \frac{R}{n} F,$$

(3-7)

where R_n is the total grounding resistance for n anodes, n the number of anodes, R the grounding resistance of a single anode, and F the interference factor. The interference factor is defined in (3-12). It is important to note that this equation is only accurate as long as the anodes are of the same shape and size and installed in the same orientation.

The total grounding resistance of a group of anodes is obtained by summing the resistance contribution of individual anodes spaced at an equal spacing, vs, and dividing by the number of anodes [7]. This average resistance is added to each anode that physically corresponds to a uniform current loading of all the anodes. Naturally this average value assigns too low a current to the outer anodes and too high a current to the inner anodes. An approximate average value is given by [7]:

$$R_n = \frac{1}{n}\left[R + \frac{2}{n}\sum_{v=1}^{n-1}(n-v)\,R(vs)\right],$$

(3-8)

where R_n is the total grounding resistance for n anodes, n the number of anodes, R the grounding resistance of a single anode, v a multiple of the spacing, and s the distance between the anodes. Because $s > L$, it follows from the equation for the grounding resistance of a hemisphere in Table B-1 that

$$R(vs) = \frac{\rho}{2\pi vs}.$$

(3-9)

Thus, the total grounding resistance of the group of anodes is given by

$$R_n = \frac{1}{n}\left[R + \frac{\rho}{\pi s}\sum_{v=2}^{n}\frac{1}{v}\right] = \frac{R}{n}F.$$

(3-10)

The following relation exists between the harmonic series of the above equation and the Euler constant ($\gamma = 0.5772$) for large values of n:

$$\sum_{v=2}^{n} \frac{1}{v} \approx \gamma + \ln n - 1 = \ln(0.66n),$$

(3-11)

where v is a multiple of the distance between anodes, γ is Euler's constant, and n the number of anodes. The interference factor is the approximated as

$$F \approx 1 + \frac{\rho}{\pi s R} \ln(0.66n),$$

(3-12)

where F is the interference factor, ρ the specific resistivity of the electrolyte, R the grounding resistance of a single anode, s the distance between the anodes, and n the number of anodes.

3.2.2 Other forms for calculating grounding resistance

Based on research performed by H.B. Dwight as early as 1936 on the calculation of resistances to ground, CP system designers have used the research to derive equations for calculating the resistance-to-earth of various anode shapes. The accuracy of the equations developed by Dwight varies considerably, but is sufficiently good that the methods should be helpful when dealing with problems of grounding [23]. The most applicable equations to be used in CP system design are presented in the following:

For one ground rod:

$$R = \frac{\rho}{2\pi L}\left(\log\frac{4L}{d} - 1\right),$$

(3-13)

where R is the grounding resistance for a single rod, ρ the specific resistivity of the electrolyte, L the length of the rod, and d the diameter of the rod.

For two ground rods, ($s > L$):

$$R = \frac{\rho}{4\pi L}\left(\log\frac{4L}{d} - 1\right) + \frac{\rho}{4\pi s}\left(1 - \frac{L^2}{3s^2} + \frac{2}{5}\frac{L^4}{s^4} \ldots\ldots\right),$$

(3-14)

where R is the grounding resistance of two rods installed with a given distance between the two rods, ρ the specific resistivity of the electrolyte, L the length of the rods, d the diameter of the

rods, and s the distance between the two rods. The same classification of symbols is applicable to (3-15).

For two ground rods, $(s < L)$:

$$R = \frac{\rho}{4\pi L}\left(\log\left(\frac{4L}{d}\right) + \log\left(\frac{4L}{s}\right) - 2 + \frac{s}{2L} + \frac{s^2}{16L^2} + \frac{s^4}{512L^4} \ldots\ldots\right).$$

(3-15)

The abovementioned equations were used to derive the equations to follow. The equations to follow are known as Dwight's Formula and are generally used when calculating the grounding resistance of anodes. For a single vertical anode installation:

$$R_v = \frac{0.1588\rho}{L}\left[2.3\log\left(\frac{8L}{d}\right) - 1\right],$$

(3-16)

where R_v is the grounding resistance of a single vertical anode installation, ρ the specific soil resistivity of the electrolyte, L the length of the anode, and d the diameter of the anode. Resistance of several vertical anodes in parallel, n, can be calculated by the following equation [8]:

$$R_v = \frac{0.1588\rho}{nL}\left[2.3\log\left(\frac{8L}{d}\right) - 1 + \frac{2L}{s}(2.3\log 0.656n)\right],$$

(3-17)

where R_v is the grounding resistance for several anodes installed in parallel, n the number of anodes, L the length of the anodes, d the diameter of the anodes, and s the distance between the anodes.

The applicable equation to use for the calculation of the grounding resistance of a horizontal anode installation (also derived from H.B. Dwight equations) is the following:

$$R_h = \frac{0.1588\rho}{L}\left[2.3\log\left(\frac{4L^2 + 4L\sqrt{t^2 + L^2}}{dt}\right) + \frac{t}{L} - \frac{\sqrt{t^2 + L^2}}{L} - 1\right],$$

(3-18)

where R_h is the grounding resistance of a single horizontal anode installation, ρ the specific resistivity of the electrolyte, L the length of the anode, t the depth to the centre of the anode measured from the surface of the electrolyte, and d the diameter of the anode.

The calculation of the grounding resistance for a number of horizontal anodes installed in parallel is based on calculating the vertical resistance of these anodes for a specific spacing. The

grounding resistance for a single horizontal anode is calculated and then divided by the number of anodes installed in parallel. This result is then multiplied by the result of the vertical resistance for the same number of vertical anodes in parallel divided by the resistance of a single vertical anode divided by the number of anodes in parallel.

3.2.3 Anode ground beds

Anode ground beds are installed along with CP systems, both for impressed current systems, as well as sacrificial anode systems, to achieve maximum efficiency from the anodes used in these systems. Depending on the type of CP system used for the protection of a structure, different configurations of anode ground beds are used. The choice of ground bed to be employed along with a specific type of CP system is dependent on a few factors. Typically, the most important factors that need to be considered when ground beds are designed include: anode consumption rate and soil resistivity.

The anodes to be used in the different anode ground beds are placed in different positions varying according to the application of the CP system. The resistivity of soil is usually higher near the surface and decreases at deeper depths. This, along with the anode consumption rate, is used to determine how many anodes are required in the ground bed as well as the optimal distance between the anodes. These considerations are necessary for achieving an optimal projected anode lifetime during the design of such systems and accompanying anode ground beds.

In order to protect large metallic structures against the effects of corrosion, impressed current CP systems are mostly used. Impressed current anodes are generally used to achieve good protective current distribution across the structure being protected. The anode ground beds are required to be installed at a closely prescribed distance from the structure [24]. The different configurations of anode ground beds that are regularly implemented are to be discussed.

3.2.3.1 Shallow ground beds

Shallow anode ground beds are generally used in applications where the anodes are not required to be deeper than 15 m below the surface of the earth. The anodes installed in shallow anode ground beds can be installed in two different orientations: horizontally or vertically. The orientation of the anodes is dependent on the type of environment in which the anode ground bed is to be installed in. The number of anodes to be installed in an anode ground bed will be dependent on the following factors: soil resistivity, environmental conditions, size of structure, and available space.

3.2.3.2 Horizontal shallow ground beds

Horizontal shallow ground beds refer to the horizontal orientation in which the anodes are installed in. The anodes are laid horizontally in cases where the necessary ground space is available, along with a low soil resistivity in the upper layers of the soil in the specific ground space.

The trench or trenches in which the anodes are to be laid in, is typically dug by using excavators or mechanical trench diggers. Typically, a trench in which anodes are laid horizontally is 0.3 to 0.5 m wide and 1.5 to 1.8 m deep [7]. The length of the trench will depend on the number of anodes to be installed along with the distance between the individual anodes. The anodes are installed on top of a layer of backfill material, which is laid on the bottom of the trench. The backfill material is typically coke and is laid with a thickness of about 200 mm [7].

The anodes are connected in parallel, each anode connected to a single cable, from which every three to four anode cables are connected to the anode header cable. These connections are then encapsulated in an epoxy splice kit to provide an economical service life at high output currents [7]. It is of high importance to ensure that the cable connecting the anode ground bed to the transformer rectifier unit is properly insulated. Failing to ensure proper insulation will lead to the copper in the cable being anodically attacked and cause cable failure. Thus the connection to the transformer rectifier unit will be lost and the CP system will effectively stop to protect the given structure.

A typical horizontal shallow anode ground bed, providing protection to a pipeline, is displayed in Figure 3-2. It can be seen that the anode ground bed in the figure is installed perpendicular to the pipeline in this case. The horizontal orientation of the anodes can be seen along with the respective distances between the respective anodes. The distance and number of anodes are dependent on the current requirement and density of the structure being protected.

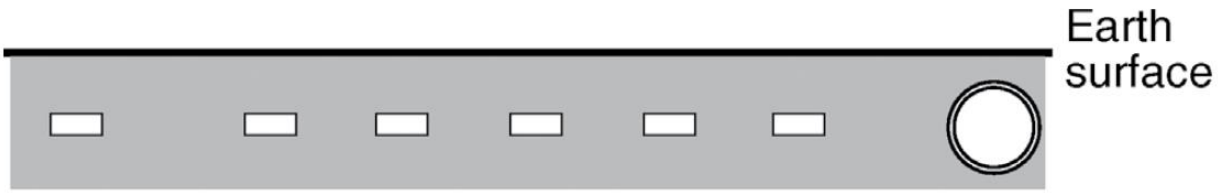

Figure 3-2: Typical horizontal shallow anode ground bed **[25]**

Typical installations of horizontal shallow anode ground beds require the anode bed to be parallel or perpendicular to one side of, for example, a pipeline. The parallel orientation, in close proximity to the structure, results in a drop in the protective current spread from the anode ground bed to the structure. Furthermore, the polarization of the whole piping network becomes more difficult

[24]. Also, it is difficult to install horizontal shallow anode ground beds in areas where limited ground space is available and in congested areas. Shallow ground beds are known to cause interference on nearby foreign structures due to the layout between the ground bed and the protected structure. The anode tension hill of various configurations of anode ground beds are generally used to determine the interference of the ground bed with respect to foreign structures.

3.2.3.3 Vertical shallow ground beds

Vertical shallow anode ground beds are often also referred to as single anode installations. This type of shallow anode ground bed is generally installed in areas where the installation of a continuous anode bed is not possible. Furthermore, these ground beds are usually used in small protection current applications. The anodes are individually placed centrally in respective boreholes. The boreholes are typically 2 m deep, and 300 mm in diameter [7]. The respective holes can either be dug by hand or by mechanical drilling machines.

The bottom of the respective boreholes is filled with backfill material, 200 mm thick, onto which the anode is placed in a vertical position. The rest of the hole is then filled with backfill material up to 200 mm above the top of the anode.

The grounding resistance of a shallow vertical anode ground bed with n anodes, spaced a distance, s, apart, compared to that of a continuous horizontal anode bed with length, $L = sn$, only shows little deviations. Although single anodes with a finite spacing have mutual interference up to a distance of 10 m, the total grounding resistance of such installations are much higher than anodes connected in parallel with infinite spacing [7].

A typical vertical shallow anode ground bed layout is displayed in Figure 3-3. The anodes, in individual boreholes, can be seen to be installed perpendicular, in this case, to the pipeline. This is not the most efficient orientation with respect to the pipeline as the current distribution on the protected structure is not even. The interference factor of this type of anode bed is influenced by the grounding resistance and is a function of the spacing between the vertical anodes.

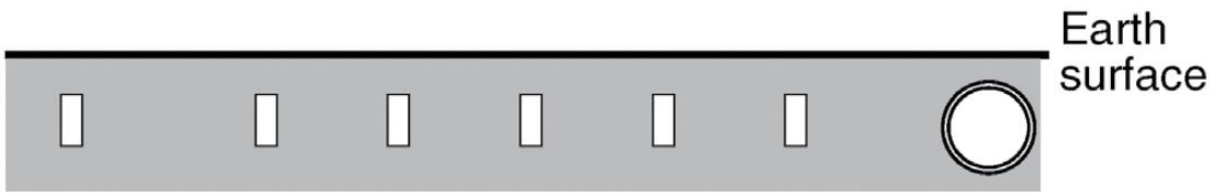

Figure 3-3: Typical vertical shallow anode ground bed **[25]**

3.2.3.4 Deep ground beds

The installation of deep anode ground beds requires the drilling of a vertical hole by means of a motor-driven drilling machine. The vertical hole is also referred to as a well, which is 200 to 250 cm in diameter. The depth of the hole to be drilled will be determined by the current requirements of the impressed current CP system. Two anode configurations are associated with deep anode ground beds:

(i) Individual anodes, with their respective individual cable connections, are located at specific depths in the hole; or
(ii) All of the anodes to be installed in the vertical hole are connected to a single cable connection.

The second of the two abovementioned anode configurations are preferred. This is because only one cable in the hole, which eases the installation and backfilling of the anodes. Another advantage the second configuration holds is the fact that the gases generated by the anodic reactions, can escape more easily. Deep anode ground beds also hold a few advantages over conventional shallow ground beds and comprise:

- This type of anode bed can be installed in a limited space as it does not take up a big space.
- The soil resistivity decreases with the increasing depth of the anode bed, which improves the overall current flow and distribution. As the soil resistivity decrease, the grounding resistance of the anode bed decreases along with it and is less than that of a shallow ground bed. This in turn means that a smaller transformer rectifier can be used to provide the same, or even better distributed, protection to the structure.
- No splices between anode and anode ground bed cables are to be maintained, as is the case with shallow ground bed configurations.
- Deep anode ground beds are installed perpendicular to the structure to be protected.
- Increased efficiency compared to shallow ground beds.
- Deep anode ground beds do not cause the same amount of interference to foreign structures as shallow ground beds.
- Better polarization of the structure can be achieved with deep anode ground beds. Better polarization means that a large structure area can be protected with the same current, compared to a shallow ground bed [24].

A simplified current flow diagram of a deep anode ground is provided in Figure 3-4. From the figure it can be seen that the ground bed is installed perpendicular with reference to the pipeline

in this case. The positive terminal of the transformer rectifier unit is connected to the anodes cable and the pipeline cable is connected to the negative terminal of the rectifier unit. The protective range of deep anode ground beds is greater, compared to that of shallow ground beds. This in turn results in less transformer rectifier unit maintenance because the installation of deep ground beds requires fewer rectifiers than is the case with shallow ground beds. Deep anode ground beds are typically installed in two different configurations namely open hole and closed hole deep ground beds. The differences between the different configurations are to be discussed.

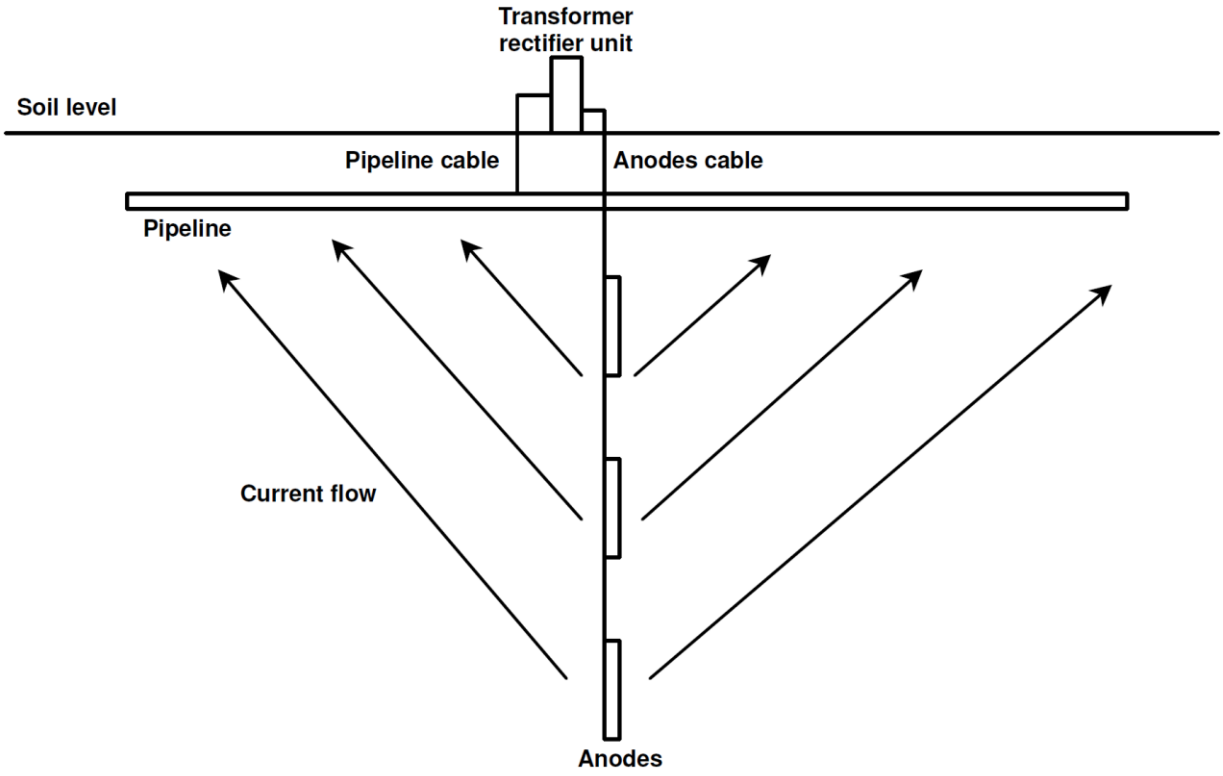

Figure 3-4: Current flow in a deep ground bed **[24]**

3.2.3.5 Open-hole deep ground beds

Some advantages that open-hole deep anode ground beds have compared to closed-hole deep anode ground beds have include:

- No backfill material is required to fill the hole after installation
- No anode supporting structure is required in open hole installations
- The need for venting facilities is cancelled due to the fact that the gasses evolved at the anodes can escape through the open hole.
- Open hole deep anode ground beds allow for the easy inspection, repair, and replacement of installed anodes.

- Furthermore, open-hole deep anode ground beds require no additional drilling cost after the practical operation lifetime of anode strings have expired and the strings require to be replaced.

3.2.3.6 Closed-hole deep ground beds

Some advantages that closed-hole deep anode ground beds compared to open-hole deep anode ground beds have, include:

- Closed-hole deep anode ground beds can be applied in the absence of water, while open-hole deep ground beds can be applied in the presence of water only.
- The earthing resistance of closed-hole deep anode ground beds is lower than that of open-hole deep anode ground beds.
- Closed-hole deep anode ground beds require no sump to be formed during installation, and thus reduce initial installation expenses.
- During the installation of open hole deep anode ground a perforated, non-conductive casing is required. This is necessary when considering the cave-in of the ground bed. This type is casing is not necessary in closed-hole deep anode ground bed installations.

Closed hole deep anode ground beds are generally filled with backfill material after the installation of the required anode strings. As backfill materials are also used in the installation of shallow ground beds, the different backfill materials are to be discussed.

3.2.4 Remoteness of ground beds

Whenever a CP system is installed to protect a structure against the effects of corrosion, a potential difference will exist between the earth and the protected structure. Typically in this case, the earth and structure will be positive (+) and negative (-) respectively. The mentioned potential difference is important for the criteria that are used for determining the degree of CP that is required for a given structure. It is possible to develop the desired potential difference between the earth and the pipeline using one of the following methods:

(i) The pipeline is made negative with respect to earth, or
(ii) The earth is made positive with respect to the pipe in local areas.

The abovementioned potential difference between the pipeline and remote earth is accomplished by installing either remote ground beds or close ground beds. Single anodes can also be implemented to accomplish the same result as with close ground beds.

3.2.4.1 Remote ground beds

The ground bed that is installed in a CP system, comprise an anode or a group of anodes. The ground bed is responsible for the current discharge that stops the protected structure from corroding. This current discharge from the ground bed will cause voltage drops in the earth. The voltage drops will occur between points along lines radiating from the ground bed [8]. These voltage drops will have a maximum value, per unit of distance, in close proximity of the ground bed. As the distance from the ground bed increases, the voltage drop per unit of distance decreases. The voltage drop will decrease to the point where no significant voltage drop can be observed. The term remote earth is used to describe this point, as no further interference from the ground bed is experienced. A detailed description and visual explanation of the operation of remote anode ground beds are presented in Figure 3-5.

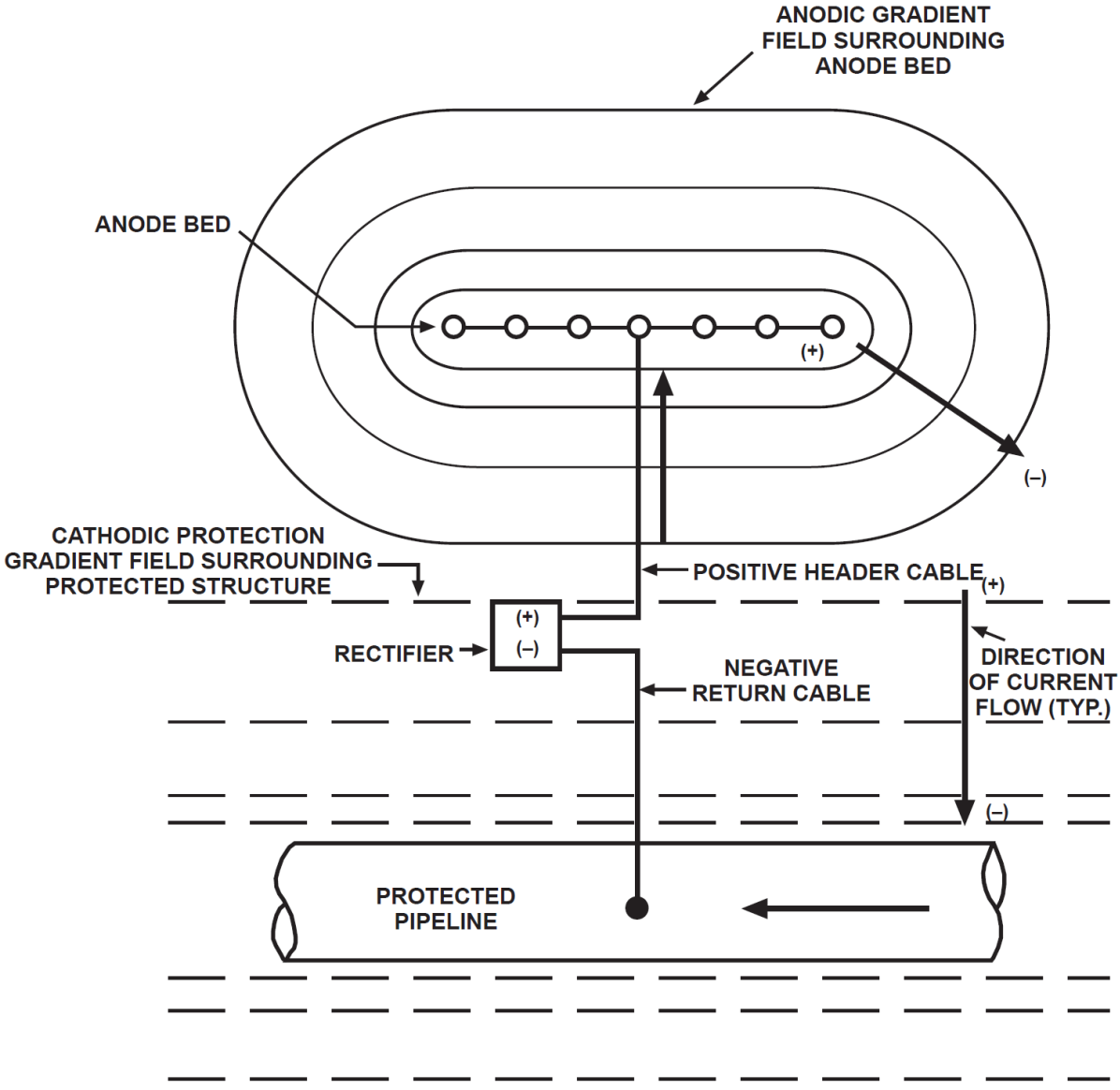

Figure 3-5: Remote anode ground bed operation explained **[20]**

The current discharge from the ground bed to the protected structure will also cause a voltage drop in the soil adjacent to the protected structure. Due to the voltage drop adjacent to the pipeline, an area of interference will surround the structure. A few considerations are required under these conditions, as current will flow from the ground bed into the surrounding earth. These considerations include that the earth is considered equivalent to a resistance-less, or even more, an infinite conductor [8].

This equivalent conductor will be utilised for current flow toward the structure to be protected. The current flow through the conductor, which is still the earth, will cause the desired voltage drop across the structure and the conductor. The voltage drop across the mentioned resistance will ensure that the structure will be more negative with respect to the remote earth. Once the structure reaches a sufficiently negative potential, effective CP will be a direct result.

In cases where a pipeline is to be protected by means of a CP system accompanied by a remote ground bed, the incremental longitudinal resistance of the pipeline has the biggest effect on the distance of pipeline that can be protected by a single ground bed. Limitations associated with the use of remote ground beds include:

- The minimum potential required for adequate protection at the most remote point with respect to the ground bed.
- Close to the ground bed, over protection can occur and special precaution is required to ensure that the pipe-to-soil polarised potential is maintained.

3.2.4.2 Close ground beds

Close ground beds typically refer to the use of anodes in close proximity to the structure to be protected. Close ground beds can consist of single anodes or a series of anodes. The use and functions of close ground beds differ greatly from those of remote ground beds. Different from remote ground beds, the success of close ground beds in protecting a structure depends on the area of influence that surrounds any given anode.

To simplify this concept, the current discharged from the anode to the earth is at its highest in close proximity of the anode. The current density will decrease as the distance from the anode increases. The high current density, very close to the anode, will cause the greatest point-to-point potential drop with respect to remote earth. Thus, the biggest potential drop exists within the first meter or so of remote earth surrounding the anode.

An equation developed by Rudenberg (1945), can be used to draw up curves for different sized anodes to be installed in close ground beds [8]. The curves, constructed from this equation, plot the total resistance or potential drop as a function of distance from an anode that is discharging current [79]. From the literature, the mentioned equation:

$$V_x = \frac{0.115824 \times I \times \rho}{x} log_{10}\left(\frac{y + \sqrt{y^2 + x^2}}{x}\right),$$

(3-19)

where V_x is the potential at point x on the surface of the soil, I the anode current, ρ the specific resistivity of the soil, y the length of the anode in the soil, and x the distance from the anode measured on the surface of the soil. In cases where x is greater than $10y$, the following approximation of the equation can be used:

$$V_x = \frac{0.00158496 \times I \times \rho}{x}.$$

(3-20)

It is important to keep in mind that the shape of the mentioned curve can be changed due to non-uniform soil conditions. Due to the nature of Ohm's law, these curves can also be used to indicate the percentage of total voltage drop as well as resistance.

The curve that is defined in Figure 3-6 is based on (3-19). The curve is a representation of the percentage anode voltage or resistance from remote earth to a point that is located "x" meters from the anode. This specific curve is a representation of an anode of 1524 mm in length, installed in soil with an average resistivity value of 1000 Ω cm. The anode discharges a current of 2 A, and these values were substituted in (3-19).

The same curve can be used in further calculations in order to determine the possible protective range that can be achieved by a single anode or close ground bed. To determine the possible protective range that can be achieved by a single anode or close ground bed, it will be assumed that the pipeline has a potential to earth of -0.5 V. This potential difference between the pipeline and earth is assumed before the anode is energised.

The remoteness of anode ground beds is very important with respect to neighbouring structures and other CP systems. This is due to the interference caused by the ground beds, both shallow and deep ground beds. The interference that will be caused by the anode ground beds can be calculated by the anode tension hill, or as sometimes referred to, the anode voltage cone. The anode tension hill will be used to calculate the potential between the soil and the anode ground

bed at various distances from the ground bed. These calculations can then be used to determine the safe distance at which anode ground beds can be installed without interfering with neighbouring structures.

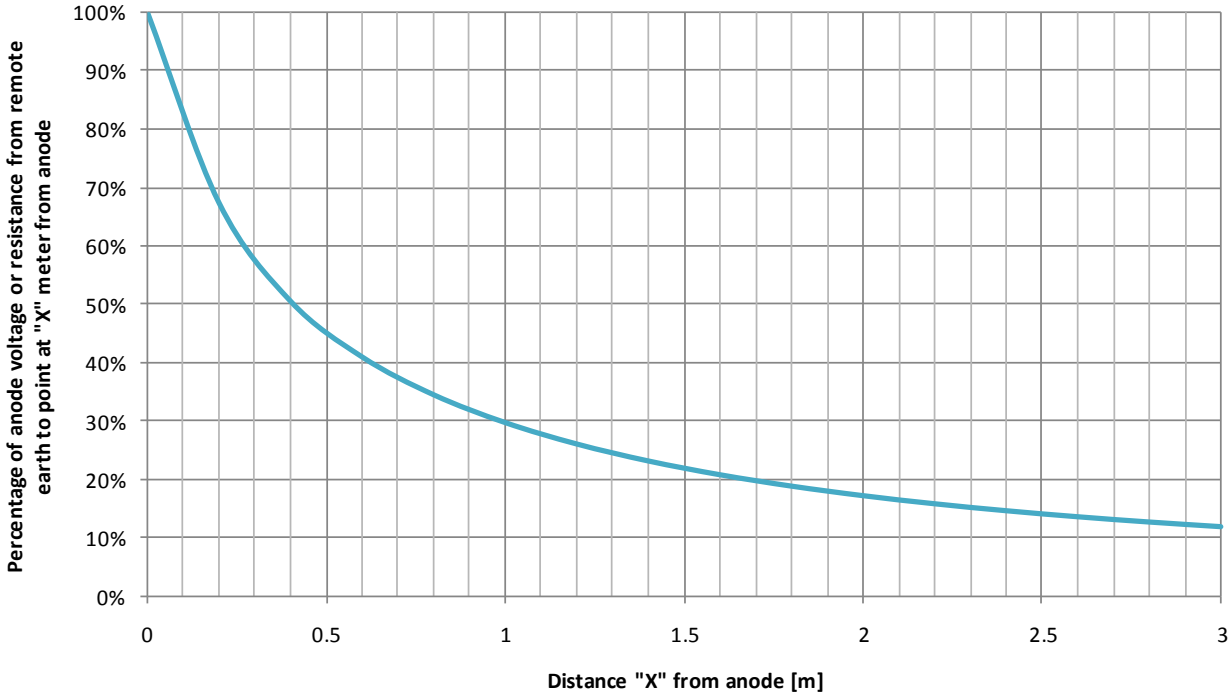

Figure 3-6: Gradients at a close ground bed **[8]**

The curve that is defined in Figure 3-7 displays the protective potentials impressed on a pipeline by a close ground bed anode. It can be seen from the figure that the area of protection provided by the close ground bed anode is rather limited. This type of configurations is implemented in hot spot areas where stray currents or coating damage occurs. Another important observation to be made from this figure is that other foreign structures in close proximity to this type of configuration may experience interference. It is therefore advisable to choose the location for these applications very carefully.

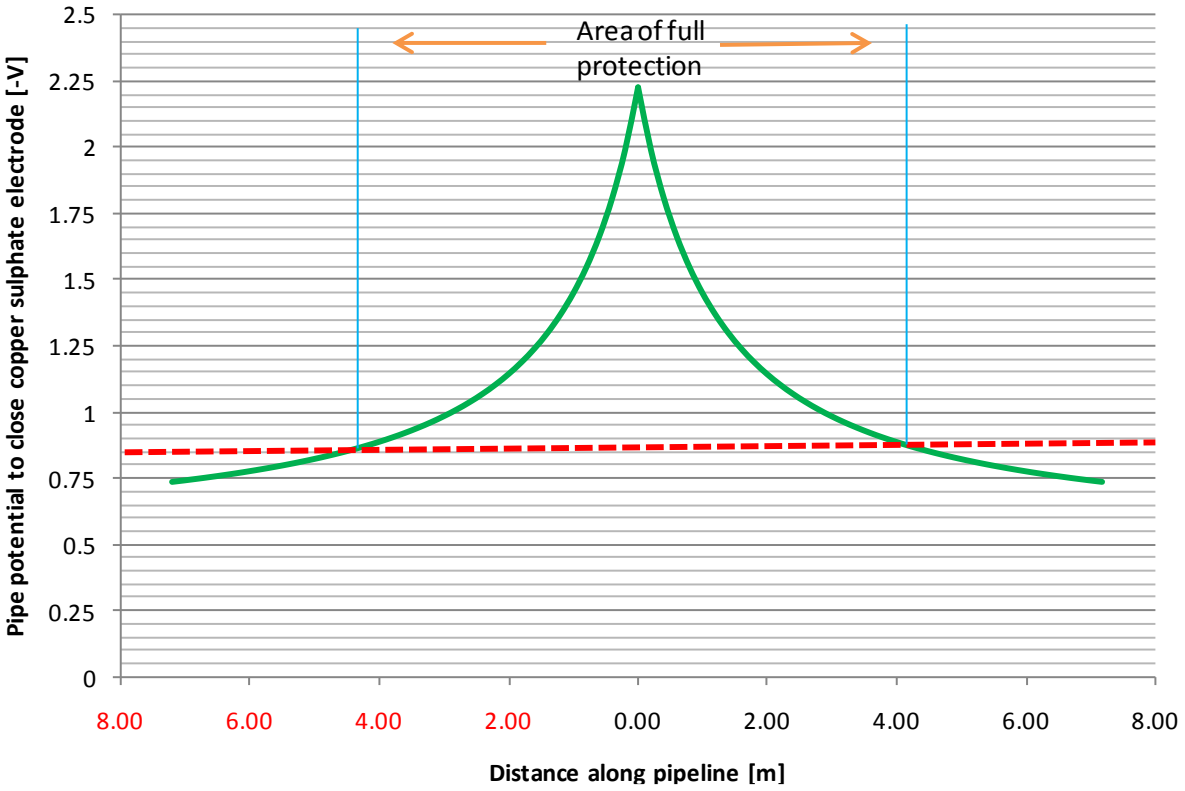

Figure 3-7: Protective potentials impressed on a pipeline by a close ground bed anode **[8]**

3.2.5 Backfill used in ground beds

Two types of backfill are generally available for use in anode ground beds. The type of backfill material to be used is dependent on the type of anode installed in a specific anode ground bed configuration. The two types of backfill materials are categorised as follows:

- Chemical backfills, and
- Carbonaceous backfills.

Chemical backfills are generally used in anode ground beds where sacrificial anodes are installed. The chemical backfill is used to provide an environment to the sacrificial anode which is conducive to anode dissolution. An environment which is conducive to anode dissolution improves the overall performance of the sacrificial anode.

Carbonaceous backfills are generally used in anode ground beds where impressed current anodes are installed. Carbonaceous backfill include materials such as coke breeze, calcined petroleum coke, and natural graphite. Surrounding an impressed current anode with carbonaceous backfill creates a surface around the anode on which oxidation reactions can occur more frequently. More advantages are associated with the use of carbonaceous backfill material include the prolonging of anode life and the increasing of the effective size of the anode. By

increasing the effective size of the anode, the grounding resistance of the anode are lowered considerably which is preferred in CP system design.

Other reasons why backfill materials are used in conjunction with impressed current anodes include:

- Restricts the formation of surface films, while also preventing electro osmotic dehydration.
- The backfill material provides a uniform current delivery.
- Backfill material is installed to ensure the uniform consumption of anode material.

Standard chemical backfill materials consist of a mixture containing 75% gypsum, 20% bentonite, and 5% sodium sulphate [7]. The backfill material is usually poured into the borehole, in deep ground bed applications, or used to backfill the trenches of shallow ground beds. Other applications where backfill material is used include anodes enclosed in bags of permeable material filled with backfill material. These bags can be installed in either shallow or deep anode ground beds.

The size and shape of particles in a specific type of backfill material are important parameters to consider when choosing a backfill material for a specific application. These parameters will determine the area of contact between the anode and the surrounding soil. In deep anode ground bed applications, the size and shape of the backfill particles will influence the porosity of the column.

A general purpose coke breeze is used in horizontal and vertical shallow ground beds, has a resistivity of around 35 Ω cm [7]. For deep anode ground bed applications, a special calcined petroleum coke breeze is generally used. The resistivity of this coke breeze is typically in the range of 15 Ω cm [7]. An advantage of the special calcined petroleum coke breeze is that the backfill material can be pumped and thus further advances its usage in deep anode ground beds.

3.3 Critical review of anodes and anode ground beds

The critical review of anodes and anode ground bed design is based on the information contained in this chapter as well as the information found in Appendix D. The critical review will first focus on the different types of anodes generally used in CP applications.

The most important parameters to consider when reviewing sacrificial anodes include the consumption rates and driving voltages of the different materials used in sacrificial anode manufacturing. Based on the relevant information it is evident that the preferred sacrificial anode

in a wide range of applications is a magnesium anode. Magnesium has the highest driving voltage of all the materials used to manufacture sacrificial and is therefore the preferred sacrificial anode. Zinc and aluminium anodes do have their uses but are generally limited to offshore applications.

MMO anodes outweighs the other impressed current anodes in most aspects. This is evident in all modern CP systems as MMO anodes have become the preferred choice for a number of reasons. Most notably, MMO anodes have a high current output along with favourable anode lifetime expectations. Compared to other impresses current anodes in terms of the amount of material used during the manufacturing process and the consumption rate, MMO anodes hold the advantage. MMO anodes are manufactured in various forms and sizes and makes it possible to be used in almost all ICCP applications.

The different anode bed configurations are more difficult to compare as the configuration of the anode ground bed to be installed is dependent on a number of parameters. The most notable parameter to have an influence on the type of anode ground bed to be installed is the environment surrounding the structure to be protected. In most cases each of the CP systems to be designed and installed will be unique. The choice on the anode ground bed to be installed will come down to the number of anode ground beds required, space available for the installation of the anode ground bed, surrounding structures, practicality, safety, and performance. From a business point of view cost will also be a contributing factor in the decision on the type of anode ground bed.

Optimally it is desired to install the anode ground bed configuration with the lowest grounding resistance. This will ensure that the required TRU output voltage is as low as possible and that the number of required TRUs are kept to a minimum. Certain trade-offs are to be made when the decision on the configuration of the anode ground bed to be installed is made. The type and amount of backfill to be installed in the ground bed will also be a contributing factor in this decision. As the anode ground bed configuration is one of the biggest cost drivers in CP system design, it is not surprising that optimal performance will occasionally be compromised to reduce the total cost of a specific system.

Chapter 3 served as another literature study chapter that was used to cover the various different anodes associated with CP systems and the specific uses of the different anodes. When these anodes are installed within a CP system, the grounding resistance of the anodes are of utmost importance to the design engineer. The different anode ground bed configuration also featured in this literature chapter with the advantages and disadvantages underlined.

It became evident in Chapter 3 that the grounding resistance of the anode ground beds are influenced by the configuration used and how the different configurations can affect the performance of the CP system in terms of current distribution. This phenomenon became evident in the derivation of the grounding resistance of anodes from first principles. Different equations are generally used for the calculation of the grounding resistance of a specific anode configuration and are dependent on the type of configuration used.

This chapter also underlined the difference between close ground beds and remote ground beds. This is a very important aspect to take into account when designing CP systems and anode ground beds in particular. The operating principles of close ground beds vary considerably when compared to remote ground beds. With these operating principles and anode ground bed configurations well documented, the empirical design of CP systems can be approached with confidence.

4

CHAPTER

EMPIRICAL CP SYSTEM DESIGN

This chapter is dedicated to empirical CP system design. The chapter will be used to empirically design CP systems for a small tank farm and an underground piping network. The design of both systems will be based on empirical equations generally associated with CP system design and documented in various sources of literature and international standards. The empirical design of the CP systems is used to establish a general design framework for CP design in the petrochemical industry. The equations presented in Chapter 3 of this document are used for the calculation of the grounding resistance of various anode types and sizes installed in different anode ground bed configurations.

4.1 Site survey data

Before commencing with the CP system design, it is necessary to gather important information from the site at which the CP system will be installed. A site survey is conducted to acquire specific detail regarding the structure to be protected and the surrounding environment. The information gathered from the site survey must be factored into the design and typically include the following [20]:

(i) From what material is the structure manufactured? What is the known electrical resistance of the structure?

(ii) Is the structure coated or bare? In the case of the structure being coated, what type of coating material and coating specification were used?

(iii) Is there a leak record on an existing line? The information on the location and date of the leak can be used to identify more serious problem areas of corrosion.

(iv) Are there any changes in the diameter, wall thickness and weight per meter along the route of the structure?

(v) Do test locations and construction details of the test locations exist for an existing structure? This information can be helpful in identifying locations where contact can be made with the structure for test purposes.

(vi) What is the construction method used on the couplers of the structure, all-welded or mechanical structures?

(vii) What are the locations of branch taps?

(viii) What are the locations of purposely isolating flanges or couplers?

(ix) Are there route and detail maps of the structure available? These maps are to include as much information available on the structure. Relevant information include lengths, diameters, heights, type of coating, and locations of any existing test points and/or TRUs etc.

(x) Are there any other foreign cathodically protected structures in close proximity to the structure? This information is important for identifying any other stray current sources.

(xi) Are there any other man-made sources of stray current in close proximity to the structure? These sources include DC electric transit systems, mining operations, and high-voltage electric transmission lines. In these cases it is important to identify the length of exposure, the distance between the structure and the source, the voltage that the HV line operates at, and the method of grounding used on transmission line towers.

(xii) At what temperature is the structure operated? This is especially important for pipelines as high temperatures can cause deterioration of the applied coating. In this case the current requirement to achieve corrosion prevention will increase.

(xiii) Is AC power available to provide power to a transformer rectifier unit or is an alternative DC power source required?

4.1.1 Soil resistivity

During the site survey, it is important to acquire the soil resistivity of the soil surrounding the structure to be protected. The soil resistivity test is also to be used when identifying the best possible location to install the anode ground bed. Typically, the anode ground bed is installed at the location with the lowest resistivity as this will greatly lower the resistance-to-earth value of the anode ground bed and subsequently the size of the external power source.

Various methods are available to measure soil resistivity. The most widely used and accepted soil resistivity measurement technique recommended for CP purposes is the Wenner method [26, 27, 28]. More information on how to implement and use the Wenner method for soil resistivity measurements is available in Annexure A, along with other methods used when measuring soil resistivity.

4.2 Small tank farm

The small tank farm that is considered in this instance constitutes 5 tanks that is spaced at an equal distance as illustrated in Figure 4-1. The most important information regarding the tanks are as follows:

- Tank diameter: 14 m
- Depth of tank in soil: 3 m
- Number of tanks: 5
- Average soil resistivity: 100 Ω-m
- Centre-to-centre distance between tanks: 34 m

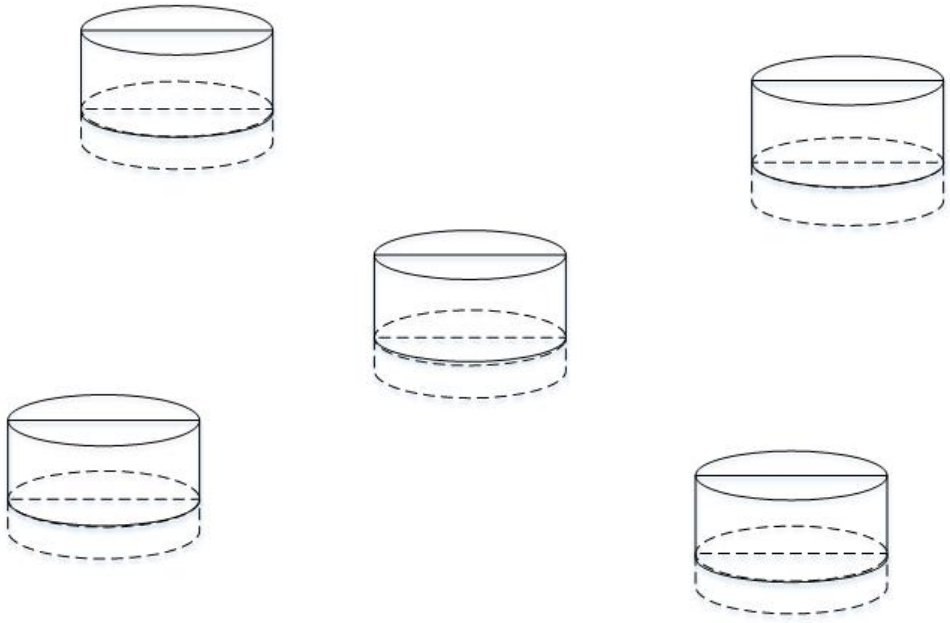

Figure 4-1: Layout of the 5 tanks in the small tank farm

It is important to note that only the average soil resistivity was made available for the purpose of CP system design. The use of the average value for soil resistivity in certain areas, especially when calculating resistance-to-earth values of the anodes may impact on the performance of the system. For countering the effect that the use of the average soil resistivity will have on certain calculations it is recommended that contingency factors are included in the calculations.

4.2.1 Empirical design

The empirical design of the CP system to be used to protect the tank bottoms from corroding is presented in this section. The calculations to be included are conducted with equations recommended in standard documents as well as literature. The design framework used to design CP systems is based on the following calculations:

- Surface area calculations
- Current requirement
- Required number of anodes
- System life calculations
- Grounding resistance calculations
- Current density
- Total circuit resistance
- TRU output voltage and power

4.2.2 Surface area calculations

The first requirement for the empirical design of the CP system is to determine the surface area of the structure to be protected. The only areas of the tanks to be protected are the areas that are in contact with of below the surface of the earth. These areas are defined by the dashed lines displayed in Figure 4-1. The calculation of the surface area of the tanks will therefore consist of the sum of the two respective surface areas. Calculating the surface area for the tank bottoms:

$$5(\pi r^2) = 5\pi(7^2) = 769.69\ \mathrm{m}^2. \quad \textbf{(4-1)}$$

The surface area of the sides of the tanks is calculated as follows:

$$5(2\pi rh) = (5\pi)(7)(3) = 659.74\ \mathrm{m}^2. \quad \textbf{(4-2)}$$

The total surface area of the 5 tanks is the sum of the results in (4-1) and (4-2) respectively:

$$S_A = 769.69 + 659.735 = 1426.43\ \mathrm{m}^2. \quad \textbf{(4-3)}$$

4.2.3 Current requirement calculations

The current requirement calculations are highly dependent on the total surface area that requires protection along with the environment surrounding the structure. The required potential shift along with the required current density is the main contributors toward the current required from the external anode ground bed to efficiently protect the structure. The cathodic polarisation curve of the material from which the tanks are manufactured will be used to determine the required current density to sufficiently polarise the surface of the structure.

The surfaces of the tanks are uncoated and therefore the polarisation curve for bare steel in soil will be considered to determine the required current density to sufficiently polarise the metal to the desired potential. The polarisation curve for bare steel in soil is displayed in Figure 4-2. The polarisation potential is presented on the vertical axis and the current density is presented on the horizontal axis of the graph. It is important to note that the potential is measured against an Ag/AgCl reference electrode.

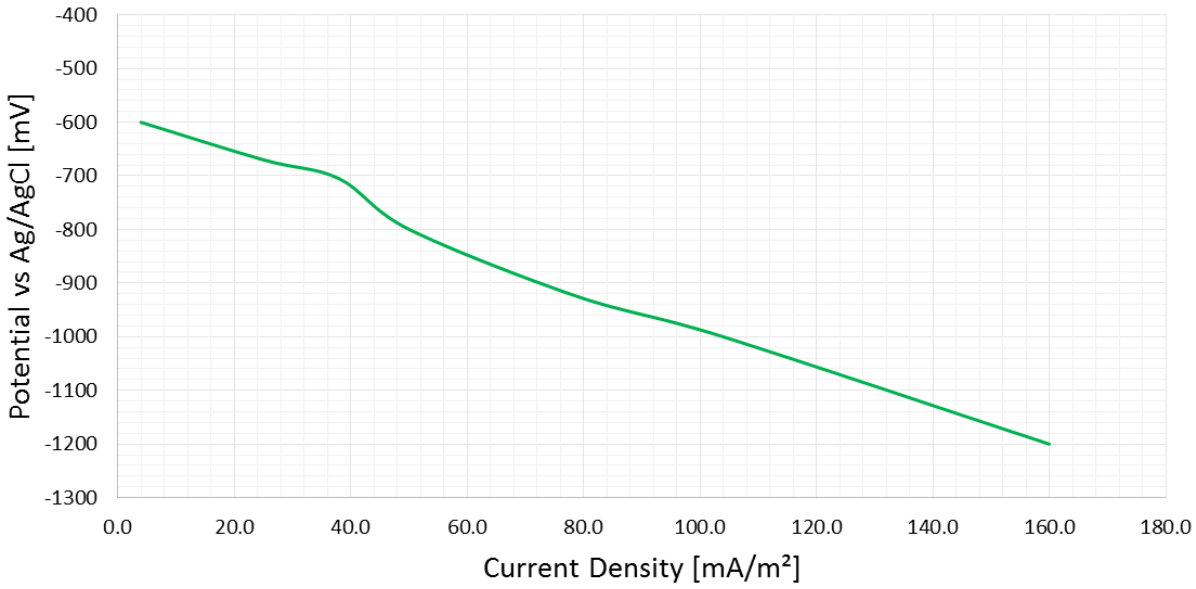

Figure 4-2: Polarisation curve for bare steel in soil

The potential of onshore structures are typically measured against $Cu/CuSO_4$ electrodes but for simulation purposes the potential is measured against Ag/AgCl electrodes. The desired protection potential for onshore structures, measured against $Cu/CuSO_4$ electrodes, is -850 mV. This value of polarisation potential has been proven scientifically sound and is accepted as the threshold potential for structures under CP [29].

To ensure adequate protection is achieved, the desired potential of the tanks must be shifted to approximately -900 mV, measured against a $Cu/CuSO_4$ reference electrode (CSE). As the potential displayed on the polarisation curve was measured against an Ag/AgCl reference electrode it is necessary to adjust the potential reading to be in reference to $Cu/CuSO_4$. The universal adjustment formula that is used for this purpose is presented as:

$$Reading\ adjusted\ to\ CSE\ potential = P(RE) - P(CSE) + (reading\ vs. RE), \tag{4-4}$$

where $P(RE)$ is the electrode potential of the electrode in use (vs. SHE), $P(CSE)$ is the electrode potential of a CSE (vs. SHE) and "reading vs. RE" is the voltage reading taken by the electrode in use [30]. With the use of (4-4), the required potential on the polarisation curve displayed in Figure 4-2, adjusted to CSE potential of -900 mV, can be determined as follows:

$$-900\ \text{mV} - (-316\ \text{mV} + 199\ \text{mV}) = -783\ \text{mV}. \tag{4-5}$$

In order to polarise the tank surfaces to the result obtained from (4-5), the required current density can be obtained from Figure 4-2 to be approximately 50 mA/m^2. The required current is then calculated as follows:

$$I_S = S_A \times J_S = 1429.43\ \text{m}^2 \times 50\ \text{mA/m}^2 = 71.47\ \text{A}. \tag{4-6}$$

The required current that is calculated in (4-6) is too close to the optimal required current to be safely implemented. For this reason it is necessary to include a contingency factor in the design. The contingency factor is used to compensate for factors such as possible non-uniform current distribution, attenuation and shielding. The most conservative of CP system designers suggest a contingency factor of 1.25. Incorporating the contingency factor into the calculation of the total required current results into the following:

$$I_T = I_S \times k_c = 71.47 \times 1.25 = 89.34\ \text{A} \approx 90\ \text{A}. \tag{4-7}$$

The current requirement is high and warrants the use of an ICCP system. To install a SACP system to protect the tanks would be expensive and will not be as effective as the ICCP system.

4.2.4 Required number of anodes

The type of anodes and the type of ground bed in which the anodes are to be installed in are the most important decisions when designing an ICCP system and CP systems in general. Another

important factor to keep in mind is that of the TRU or alternative power unit and the maximum current and voltage outputs respectively. In most cases TRUs can deliver a maximum of 100 A at an output voltage of 100 V. The type of ground bed and the resistance of the respective ground bed with respect to the electrolyte will determine the required output voltage of the TRU and are therefore a very important aspect of the design process.

In recent times the most used anodes in ICCP applications are silicon iron (Fe/Si) and mixed metal oxide (MMO) anodes. Both types of anodes are available in different lengths and diameters, with each size of anode capable of delivering a certain amount of output current for a specific design life. The type and number of anodes to be installed in a ground bed will be dependent on the required current of the structure to be protected.

For the design of the CP system to be implemented in the tank farm, MMO anodes are chosen. MMO anodes are manufactured in various shapes and sizes. For most anode installations, MMO tubular anodes are the preferred choice for a wide range of applications. These anodes are typically installed in petroleum coke or carbonaceous backfill in order to enlarge the anode contact surface area with the soil and lower the resistance-to-earth value of the anode ground bed.

Typical characteristics of tubular MMO anodes installed in petroleum coke, soil or freshwater are displayed in Table 4-1. According to the manufacturer datasheet [31], the maximum design current density for these anodes in the mentioned environments is 100 A/m². The current output is based on the design life of the system along with the maximum design current density of the anodes and the surface areas of the respective anodes.

Table 4-1: MMO tubular anode characteristics in calcined petroleum coke, soil or freshwater **[31]**

Anode size (d x L) [mm]	Current output [A]	Anode life [years]
25 x 500	4	20
19 x 1200	7	20
25 x 1000	8	20
25 x 1200	9.6	20
25 x 1500	12	20
32 x 1200	12	20

When these anodes are installed in carbonaceous backfill, the manufacturer suggests a maximum design current density of 50 A/m². The maximum design current density of 50 A/m² is for a design life of 20 years. According to the data sheet the manufacturer is able to increase or decrease the coating loadings in order to increase or decrease the design life respectively [31].

The data contained in Table 4-1 can be adapted for a maximum design current density of 50 A/m² and the maximum admissible current output of the anodes is presented in Table 4-2.

Table 4-2: MMO tubular anode characteristics in carbonaceous backfill **[31]**

Anode size (d x L) [mm]	Current output [A]	Anode life [years]
25 x 500	2	20
19 x 1200	3.6	20
25 x 1000	3.9	20
25 x 1200	4.7	20
25 x 1500	5.9	20
32 x 1200	6	20

Considering the number of anodes that will be required to sufficiently polarise the surface of the tanks will include the maximum current output of each anode size in a given installation. The required number of anodes to be installed for sufficient polarisation of the surface of the tanks is presented in Table 4-3 and Table 4-4 respectively. The required number of anodes is determined by dividing the total required current through the maximum admissible current output of the relevant anodes.

Table 4-3: Required number of MMO anodes installed in calcined petroleum coke, soil or freshwater

Anode size (d x L) [mm]	Current output [A]	Number of anodes	Anode life [years]
25 x 500	4	23	20
19 x 1200	7	13	20
25 x 1000	8	12	20
25 x 1200	9.6	10	20
25 x 1500	12	8	20
32 x 1200	12	8	20

Table 4-4: Required number of MMO anodes installed in carbonaceous backfill

Anode size (d x L) [mm]	Current output [A]	Number of anodes	Anode life [years]
25 x 500	2	45	20
19 x 1200	3.6	25	20
25 x 1000	3.9	24	20
25 x 1200	4.7	20	20
25 x 1500	5.9	16	20
32 x 1200	6	15	20

An assessment of the resistance-to-earth of the different anode bed configurations is required to make the decision on the type of anode ground bed to be installed along with the number of anodes. Other factors influencing the decision on the type of ground beds to be installed comprise:

- Practicality
- Total cost
- Accessibility
- Safety concerns
- Surrounding environment

4.2.5 Decision on ground bed configuration for small tank farm

Based on the available information regarding the environment surrounding the small tank farm the use of a remote ground bed is ruled out due the interference it will cause to surrounding structures. The most effective ground beds to be implemented will be that of close ground beds in close vicinity to the tanks in the small tank farm. The decision between horizontal and vertical ground beds comes down to accessibility, practicality, and total cost.

It is not possible to access the site where the anodes are to be installed with a tractor-loader-backhoe (TLB). This implies that if horizontal anode ground beds are to be installed the excavation are to be performed by means of manual labour. In the case of vertical anode grounds to be installed, an on-site drill rig is available. Depending on the depth at which the anodes are to be installed, the decision on the type of anode ground bed is dependent on practicality, cost and if one method is associated with any risks. These risks include compromising the structural integrity of the tanks or the safety of any employees.

The anodes are to be installed in close vicinity to the tanks at a depth of 3.5 m. This is due to the tank bottoms being at a depth of 3 m. Excavating a horizontal trench up to the required depth for the installation of a horizontal anode can compromise both the structural integrity of the tank as well as the safety of employees performing the excavations. The cost of excavations up to the required depth can become high depending on the number of ground beds required. Due to the availability of the on-site drill rig and the fact that close vertical ground beds won't compromise the structural integrity of the tanks it is decided to proceed with the design using vertical anode ground beds.

The next step is the calculation of the resistance-to-earth of the ground beds to be installed to be able to determine the required output voltage of the TRU to be installed.

4.2.6 Grounding resistance calculations

The calculation of the resistance-to-earth values of the anode ground beds is covered in this section. The aim is to keep the resistance-to-earth of anode grounds to as low a value as possible. The grounding resistance of the vertical anode ground beds is calculated with the aid of (4-8).

$$R = \frac{\rho}{2\pi L} \ln \left[\frac{2L}{d} \sqrt{\frac{4t + 3L}{4t + L}} \right].$$

(4-8)

where R is the resistance, ρ the soil resistivity, L the length of the anode in the ground, d the outside diameter of the anode, and t the depth of the anode below the surface of the earth.

Equation (4-8) is used to calculate the resistance of a single vertical anode ground bed. The parallel resistance of the number of anodes surrounding a single tank is calculated in the same manner used with parallel resistances in an electrical circuit. The anodes surrounding a single tank will be viewed as a single ground bed for reference purposes. This implies that five anode ground beds will be installed with the number of anodes installed around each tank depending on the information provided in the previous section.

Based on the information contained in Table 4-3 the number of anodes required to protect a single tank are presented in Table 4-5. The resistance-to-earth of the number of vertical anode ground beds required to protect a single tank will be viewed as a single anode ground surrounding a single tank when calculating the total resistance-to-earth of all the anode ground beds.

Table 4-5: Required number of MMO anodes installed in calcined petroleum coke to protect a single tank

Anode size [mm]	Current output [A]	Number of anodes	Anode life [years]
25 x 500	4	5	20
19 x 1200	7	3	20
25 x 1000	8	3	20
25 x 1200	9.6	2	20
25 x 1500	12	2	20
32 x 1200	12	2	20

Based on the anode sizes presented in Table 4-5 the resistance-to-earth of a single vertical anode ground bed installation at a depth of 3.5 m is calculated for every available anode size. The resistance-to-earth is calculated using (4-8) and is presented visually in Figure 4-3. A typical vertical anode ground bed configuration is displayed in Figure 4-4. When calculating the

resistance-to-earth of the anode ground bed, the dimensions of the column is substituted in the respective equations.

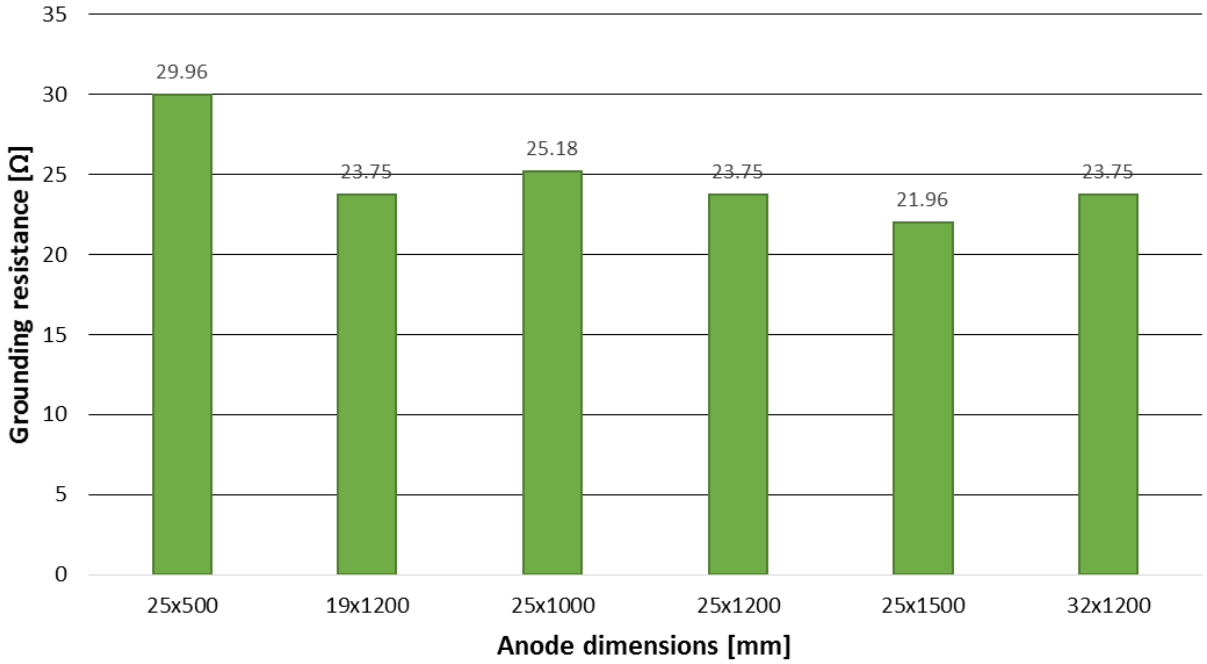

Figure 4-3: Grounding resistance for a single vertical anode ground bed at a depth of 3.5 m

The grounding resistance for vertically installed anodes at a depth of 3.5 m in the soil surrounding the tanks is displayed in Figure 4-3. The grounding resistance of the respective ground beds is based on the size of the column in which the anodes are installed. The number of required anodes per tank, as presented in Table 4-5, are installed in individual columns symmetrically around the tank and forms an anode ground bed.

A typical vertical anode installation is displayed in Figure 4-4. The vertical anode is installed in an auger hole with a diameter of 200 mm and filled with backfill material according to the dimensions displayed in Figure 4-4. The cable trench and the rest of the auger hole is filled with well tamped soil after the connections are completed. When calculating the grounding resistance of anode ground beds, the dimensions of the columns are used in the respective equations.

The grounding resistance values that are presented in Figure 4-3 are based on a single vertical anode ground bed. In order to calculate the parallel resistance of the number of required anodes installed for the protection of a single tank is calculated with the aid of (4-9):

$$R_{GB} = \left[\frac{1}{R_{A1}} + \frac{1}{R_{A2}} + \frac{1}{R_{A3}} + \cdots + \frac{1}{R_{An}}\right]^{-1}. \quad \textbf{(4-9)}$$

The number of anodes required for the protection of a single tank, as presented in Table 4-5, installed in individual vertical columns around the tank are referred to as an anode ground bed. The resistance-to-earth of the anode ground bed, depending on the required number of anodes installed around the tank as presented in Table 4-5, is visually displayed in Figure 4-5.

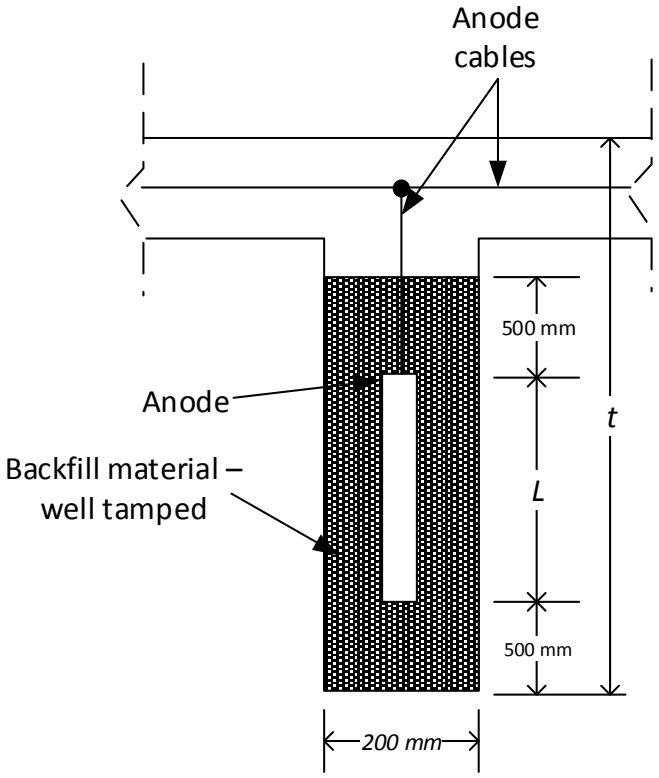

Figure 4-4: Typical vertical anode installation

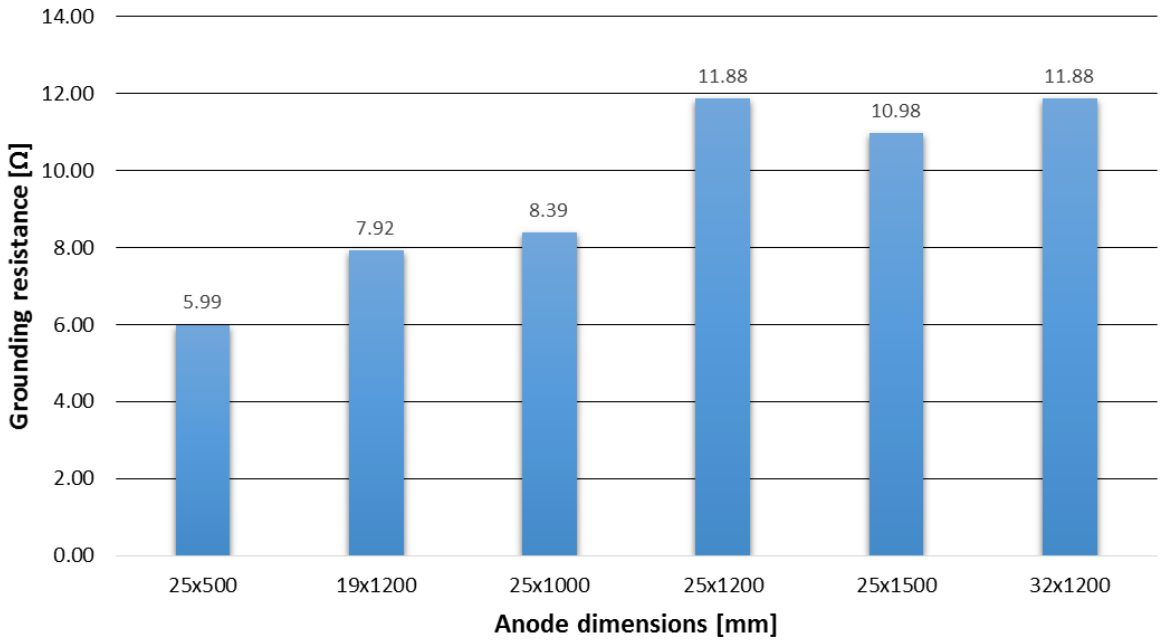

Figure 4-5: Grounding resistance of required number of anodes installed around a single tank

The resistance-to-earth value of interest is that of the total number of required anodes to be installed for the protection of all the tanks in the small tank farm. This resistance value is calculated by paralleling five anode ground beds that each have an equivalent resistance as displayed in Figure 4-5. The total resistance-to-earth value for the anodes to be installed, depending on the required number of anodes, is visually displayed in Figure 4-6.

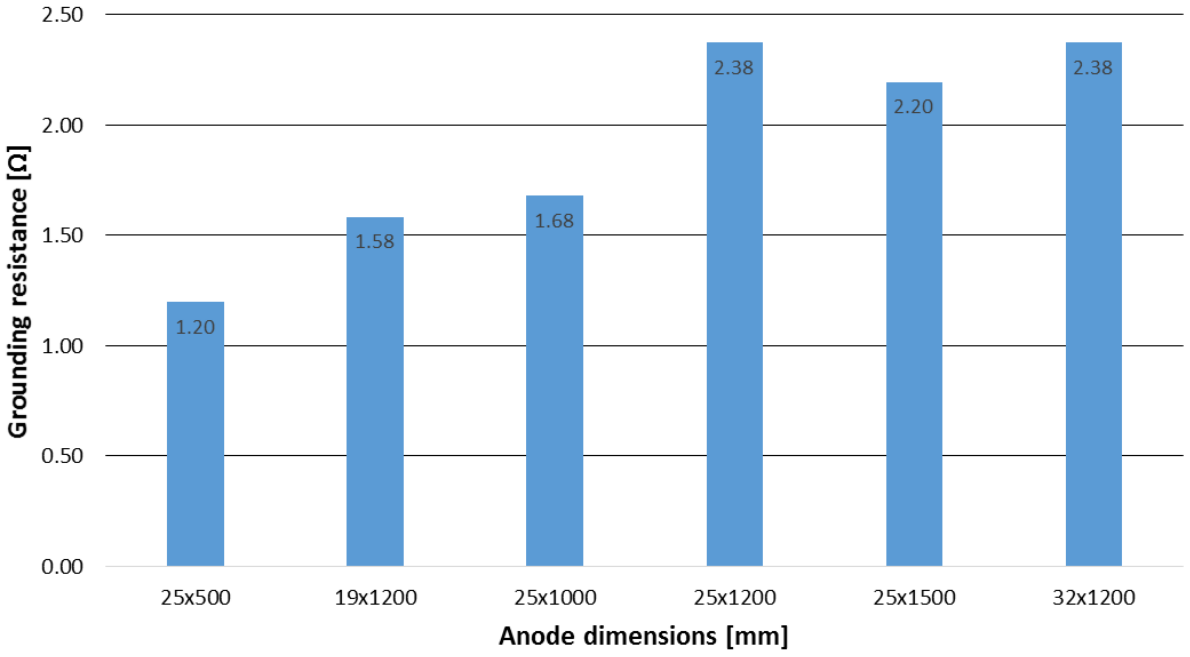

Figure 4-6: Total resistance-to-earth of required number of anodes according to **Table 4-5**

The total resistance-to-earth of the anodes required for the protection of the tanks in the small tank farm, based on the size of the respective anodes, is displayed in Figure 4-6. In order to keep the output voltage from the TRU as low as possible and within the specifications it is desired to install the anodes with the lowest resistance-to-earth value. For this reason 25 anodes with anode dimensions of 25 x 500 mm are chosen for this installation.

4.2.7 Total resistance of CP system circuit

The total resistance of the CP system circuit is the sum of all the resistance components in the system. This includes the grounding resistance of the anode ground beds, the grounding resistance of the tanks in parallel, and the resistance of the interconnecting cables.

The lowest grounding resistance for the vertical anode ground beds is found to be five anode grounds containing five anodes each with anode dimensions 25 x 500 mm. The value of the anode ground beds in parallel is therefore

$$R_A = 1.20\ \Omega\,.$$

(4-10)

The grounding resistance of the structure can be calculated by using the required potential shift and dividing by the required current of the structure. As the tanks will also be connected in parallel to the TRU in this case, it is necessary to first calculate the grounding resistance for a single tank. Using the polarisation curve for the tank material in soil, the required potential shift can be determined as

$$\Delta V_g = -600 - (-900) = 300\ \text{mV}.$$

(4-11)

The required current for a single tank is found by dividing the total required current by the number of tanks:

$$I_{Tank} = \frac{I_T}{5} = \frac{90}{5} = 18\ \text{A}.$$

(4-12)

The grounding resistance of a single tank is therefore:

$$R_{Tank} = \frac{\Delta V_g}{I_{Tank}} = \frac{300\ \text{mV}}{18\ \text{A}} = 0.017\ \Omega\,.$$

(4-13)

The total grounding resistance of all the tanks will therefore be five resistances, with the value found in (4-13), in parallel. The grounding resistance of the cathode is therefore

$$R_C = \left[\frac{1}{0.017} + \frac{1}{0.017} + \frac{1}{0.017} + \frac{1}{0.017} + \frac{1}{0.017}\right]^{-1} = 3.4\ \text{m}\Omega\,.$$

(4-14)

The other major contributing factor towards the total resistance of the circuit is the resistance of the cables interconnecting the anodes and tanks to the TRU. The resistance of these cables is dependent on the size and length of the cables. The size of the cables is determined by the amount of current flowing through the cables, while the length of the respective cables is dependent on the location of the TRU with respect to the tanks and anode ground beds.

By connecting the required number of anodes for the protection of each respective tank in parallel and viewing it as a single anode ground bed installation, the size of the cables required can be kept to a minimum. This in turn will require 5 anode junction boxes (AJB) for the paralleling of the anodes surrounding each tank and connecting the anodes to the TRU. By installing a cathode junction box (CJB) for the parallel connection of the tanks, the cable lengths can also be

minimised. The cable connected to the CJB must be able to handle a maximum current of 90 A at the output voltage of the TRU. Estimating the voltage output of the TRU for cable sizing purposes, the following calculation can be made:

$$I_T \times R_A = 90 \times 1.2 = 108 \text{ V}.$$

(4-15)

The preliminary estimation of the output voltage of the TRU indicates that the total resistance of the circuit must be lowered in order to lower the output voltage of the TRU to an acceptable value. As the anodes are the major contributors towards the total resistance of the CP circuit, it is possible to lower this resistance value by increasing the number of anodes to be installed. By increasing the number of anodes to be installed around each tank to 8, the following resistance-to-earth value will be applicable:

$$R_A = 0.75\ \Omega\,.$$

(4-16)

Performing the same estimation calculation of the output voltage of the TRU, as in (4-15), the following value is obtained:

$$I_T \times R_A = 90 \times 0.75 = 67.5 \text{ V}.$$

(4-17)

The output voltage of the TRU estimated in (4-17) is the minimum value the output voltage of the TRU can take on as it is only based on the resistance-to-earth value of the anode ground beds. The total resistance of the CP circuit will increase with the connection of the cables and the addition of the cathode resistances. This output voltage is very important to consider when deciding on the size of the cable as the voltage drop across the length of the cable must be taken into account.

The voltage drop across the length of the cables is very important to take into account when deciding on the size of the cables to be installed. To keep the voltage drop across the cables connecting the anodes to the AJB to a minimum the AJB is installed in close proximity to the tanks. Due to the placement of the AJBs with respect to anodes, it is possible to connect the anodes to the AJBs using 4 mm^2 cables. The voltage drop across these cables will not have any significant influence on the performance of the CP system.

The maximum current to be supplied to each AJB will influence the size of the cable connecting the AJB to the TRU. The maximum current to be supplied to the AJB is 20 A. The distance from

the respective AJBs to the TRU is 150 m. Different cable sizes with the associated voltage drop across a length of 150 m at a rated current of 20 A are presented in Table 4-6.

Table 4-6: Cable sizes and voltage drop across 150 m at a rated current output of 20 A

Rated Area [mm^2]	Impedance [Ω/km]	Current Rating [A]	Voltage drop [V]	% Loss
25	0.879	125	2.637	2.64%
35	0.639	156	1.917	1.92%
50	0.479	183	1.437	1.44%
70	0.339	223	1.017	1.02%
95	0.257	266	0.771	0.77%
120	0.213	301	0.639	0.64%

Based on the information contained in Table 4-6, a cable with a rated area of 25 mm^2 has a voltage drop within 5 % of the source voltage and will therefore not significantly influence the performance of the system. Five cables with a rated area of 25 mm^2 and a length of 150 m will therefore be installed to connect the TRU to the AJBs. The resistances of these cables will be taken into account in the calculation of the total resistance of the CP circuit along with the resistance of the cable connecting the tanks to the TRU.

The decision on the type of cable to be installed between the CJB and the TRU is dependent on the information contained in Table 4-7. The information contained in this table will be used in the decision on the size of cable to be installed to connect the CJB to the TRU.

Table 4-7: Cable sizes and voltage drop across 150 m at a rated current output of 100 A

Rated Area [mm^2]	Impedance [Ω/km]	Current Rating [A]	Voltage drop [V]	% Loss
25	0.879	125	13.185	13.19%
35	0.639	156	9.585	9.59%
50	0.479	183	7.185	7.19%
70	0.339	223	5.085	5.09%
95	0.257	266	3.855	3.86%
120	0.213	301	3.195	3.20%

The most suited cable for connecting the CJB to the TRU is a cable with a rated area of 70 mm2. The voltage drop across this type of cable over a distance of 150 m is close enough to 5 % of the maximum output of the TRU and will not significantly compromise the performance of the CP system. The resistance of this cable will contribute towards the total resistance of the CP circuit.

The resistance of the cables is made up out of two components. The first component of this resistance is made up of the five 25 mm^2 cables stretching 150 m each and serve as the

connection between the AJBs and the TRU. The second component of this resistance is made up of the 70 mm^2 cable stretching 150 m and serves as the connection between the CJB and the TRU. The resistance of the cables in the CP circuit is therefore:

$$R_{cables} = 0.051 + 0.026 = 0.077\ \Omega\,.$$

(4-18)

The total CP circuit resistance of the CP circuit is the sum of all resistive components within the system and can be calculated as follows:

$$R_T = R_A + R_C + R_{cables} = 0.75 + 0.0034 + 0.077 = 0.83\ \Omega\,.$$

(4-19)

4.2.8 Sizing of TRU

This section is used to determine the size and outputs of the TRU. It has to be kept in mind that the output voltage of the TRU has to be less than 100 V. The required voltage of the TRU in this case, is a direct result of Ohm's Law:

$$V_{TRU} = I_T \times R_T = 90\ \text{A} \times 0.83\ \Omega = 74.74\ \text{V}\,.$$

(4-20)

The value of the output voltage calculated in (4-20) is well below the maximum limit of 100 V and also allows for some extra capacity, should the need arise during the lifetime of the CP system. Based on the calculated voltage output and the required current, the output power of the TRU can be calculated:

$$P_{TRU} = V_{TRU} \times I_T = 75\ \text{V} \times 90\ \text{A} = 6.75\ \text{kW}.$$

(4-21)

In the case where the maximum voltage output of the TRU is required, the TRU must be able to deliver the required power to the system. For this reason the output power of the TRU is rated at maximum admissible current and voltage:

$$P_{max} = V_{max} \times I_{max} = 100\ \text{V} \times 100\ \text{A} = 10\ \text{kW}.$$

(4-22)

With the output power of the TRU as calculated in (4-22), the TRU would be able to deliver more current and voltage should the need arise during the lifetime of the CP system. The design framework that was used during the empirical design of the CP system for the protection of the small tank farm will form part of the general design framework that will be put in place for the design of CP systems in the petrochemical industry.

4.3 Underground pipeline network

There is four underground pipelines present in the plant that require cathodic protection. Two of the pipes are manufactured from carbon steel and include the storm water sewer (SWS) and oily water sewer (OWS) pipes respectively. The other two pipelines are manufactured from 304L stainless steel and comprise of the chemical conservation sewer (CCS) and rhodium conservation sewer (RCS).

The CP system to be used to protect the respective pipelines against corrosion is to be an ICCP system and the following criteria are to be met:

Criteria for protection: Instant off-potential : Upper limit: -950 mV
Lower limit: -2500 mV

Operating criteria for TRU : Output voltage < 50 V

4.3.1 Site survey

Some field work is required before the design of the CP system. The field work will include a current drain test that is performed on the pipeline network. The current drain test is to be used in the calculation of the current requirement that is required to provide sufficient protection to the pipeline.

The second set of tests will include a comprehensive soil resistivity measurement to be able to determine the resistivity of the soil in which the pipelines are installed and to recognise the best possible location(s) to install the anode ground bed(s).

Lastly, the resistance-to-earth of the pipeline network must be measured. This measurement will be used in the calculation of the entire resistance-to-earth of the system and in the sizing of the TRU to be installed.

4.3.1.1 Current drain test

The current drain test for this specific scenario was performed as follows:

A temporary anode ground bed system was set up comprising sets of earth spikes located at the proposed ground bed locations. These temporary ground beds were interconnected by means of 35 mm² cable and were connected to the positive terminal of the temporary transformer rectifier unit. A negative connection was made to the pipe network by means of 35 mm² cable. Current was passed from the ground bed system to the pipe network and the potential shift from the

natural state was measured at all available test points. The following potential measurement were taken from the available test points.

Table 4-8: Current drain test results

Test Point No.	As Found (Off) Potential [V]	On Potential [V]	Potential shift [V]
1	-0.31	-2.24	-1.93
3	-0.40	-2.35	-1.95
4	-0.37	-2.26	-1.89
6	-0.40	-2.80	-2.40
7	-0.32	-2.33	-2.01
9	-0.32	-2.22	-1.90
10	-0.36	-2.13	-1.77
11	-0.36	-2.08	-1.72
12	-0.35	-2.18	-1.83
14	-0.35	-2.03	-1.68
15	-0.44	-2.07	-1.63
19	-0.34	-2.35	-2.01
20	-0.33	-2.42	-2.09
21	-0.44	-2.57	-2.13
25	-0.40	-3.33	-2.93
28	-0.34	-2.34	-2.00
28	-0.40	-2.00	-1.60
31	-0.43	-3.70	-3.27
33	-0.48	-3.36	-2.88
36	-0.41	-2.56	-2.15
42	-0.49	-3.36	-2.87
43	-0.37	-3.53	-3.16
46	-0.44	-3.44	-3.00
47	-0.38	-3.34	-2.96
Averages	-0.38	-2.62	-2.24

The current drain test will be used to determine the total current that is required to efficiently polarise the underground pipeline network. In this instance it is recommended that a potential shift of -2000 mV is designed for due to the presence of stray currents. Based on the results contained in Table 4-8, an average potential shift of -2240 mV was achieved with an impressed current of 5 A. The potential shift obtained from the current drain test can be calculated as follows:

$$\frac{2240\ \text{mV}}{5\ \text{A}} = 448\ \text{mV/A}\,.$$

(4-23)

Designing for a potential shift of -2000 mV, the required current can be calculated:

$$I_S = \frac{2000\ \text{mV}}{448\ \text{mV/A}} = 4.46\ \text{A}\,.$$

(4-24)

Only 80 % of the underground pipeline network had been completed at the time of the current drain test and the required current calculated in (4-24) is only representative of 80 % of the network. The following calculation is made to account for the total required current to efficiently protect the entire underground pipeline network:

$$I_T = \frac{4.46\ \text{A}}{0.8} = 5.575\ \text{A} \approx 5.6\ \text{A}\,.$$

(4-25)

4.3.1.2 Soil resistivity measurements

The soil resistivity was measured on the northern, eastern and western sides of the plant. The Wenner 4 pin method was used whereby the resistance measured between the inner two pins represents the average resistance of hemisphere of soil of radius equal to the pin spacing. Measurements were taken at incremental pin spacing up to 30 m thereby determining the resistivity of the soil to a depth of 30m.

Table 4-9: Soil resistivity survey measurements

Position	North	East	West
Pin Spacing	Resistivity [Ωm]	Resistivity [Ωm]	Resistivity [Ωm]
2	57.40	72.00	62.50
4	54.00	53.80	51.20
6	44.90	38.10	39.50
8	36.20	32.20	37.30
10	32.00	32.70	34.50
12	38.20	37.70	36.30
14	47.10	40.50	42.10
16	33.90	45.10	45.80
18	44.40	43.20	42.80
20	43.10	46.40	44.60
22	41.50	49.00	45.90
24	46.50	48.40	43.80
26	48.90	48.30	47.30
28	48.70	44.30	42.70
30	41.40	47.40	48.30
Average	43.88	45.27	44.31

In order to simplify the calculation of the grounding resistance of anodes and anode ground beds, the average soil resistivity value will be used. An integer value is desired and therefore the following value will be used in calculations that include soil resistivity:

$$\rho = \frac{43.88 + 45.27 + 44.31}{3} = 44.49\ \Omega\text{m}\ \approx 45\ \Omega\text{m} \tag{4-26}$$

4.3.1.3 Measurement of pipeline resistance to remote earth

The pipe resistance to remote earth was measured by means of the “60-40 Rule”, whereby a four pole megger is used with C1 and P1 connected to the pipe network and P2 and C2 are connected to pins located 60 m and 100 m (40 m from the first pin) away from the pipe. The measured grounding resistance of the underground pipeline network is

$$R_C = 0.91\ \Omega\,. \tag{4-27}$$

4.3.2 Empirical design

The empirical design of the CP system for the protection of the underground pipeline network differs slightly from the empirical design performed on the CP system for the protection of the small tank farm. This section will be used to perform the empirical CP system design for the underground pipeline network based on the information contained in the preceding sections.

4.3.2.1 Surface area calculations

The surface area of the underground pipeline network will be calculated in this section. The available information regarding the geometry of the underground pipeline network is the outside diameter of the pipes along with the length of each pipe section. The surface area of the different pipe sections will be presented in Table 4-10.

The total surface area, S_A, that was calculated in Table 4-10 will be used to calculate the current density on the surface of the underground pipeline network:

$$J_s = \frac{I_T}{S_A} = \frac{5.6\ \text{A}}{891.04\ \text{m}^2} = 6.29\ \text{mA/m}^2\ \approx 6.3\ \text{mA/m}^2\,. \tag{4-28}$$

The current density that was calculated in (4-28) can be used as an indication of the state of the coating that is applied to the underground pipeline network. The current density is prove that the

coating was either poorly applied or damaged during the installation of the underground pipeline network.

Table 4-10: Underground pipeline network sizes and surface area

Outside diameter [in]	Outside diameter [mm]	Pipe section length [m]	Pipe surface area [m^2]
1	25.4	12.8	1.02
2	50.8	67.1	10.71
3	76.2	0.2	0.05
4	101.6	1078.6	344.27
6	152.4	710.9	340.36
10	254	26.6	21.23
12	304.8	33.8	32.37
14	355.6	6.5	7.26
16	406.4	30.8	39.32
20	508	34.1	54.42
24	609.6	20.9	40.03
	TOTALS:	2022.3	891.04

4.3.2.2 Anode ground bed design

Based on the layout of the underground pipeline network and the available space around the underground pipeline network, deep anode ground beds are preferred. The use of deep anode ground beds will keep stray current corrosion to surrounding structures to a minimum. The soil resistivity at a depth of up to 30 m is more favourable for anode ground bed installation compared to the soil resistivity closer to the surface. The fact that the grounding resistance of a deep ground bed is lower than its shallow counterparts further supports the use of a deep anode ground bed installation.

It is important to note that the deep anode ground bed(s) will be installed close to the underground pipeline network and will therefore not operate as a remote ground bed. The number of required ground beds will be dependent on the voltage cone of the ground bed.

The voltage cone of a deep anode ground bed is displayed in Figure 4-7. The voltage cone is used to determine the maximum length of the structure that can be protected by the deep anode ground bed. It can be seen from Figure 4-7 that the voltage cone crosses the desired protection potential at a distance of 15 m away from the anode ground bed. When two anode ground beds are installed, the combined gradient curve of the voltage cones will interact and allow for the protection of a greater distance.

In the case of the underground pipeline network five deep anode ground beds is recommended for efficient protection. Due to the layout of the underground pipeline network it is recommended that two deep ground beds are installed at the eastern part of the structure along with two ground bed at the western part of the structure. A single ground bed installed at the northern part of the structure will ensure a sufficient current distribution ensuring that the entire underground pipeline network is protected.

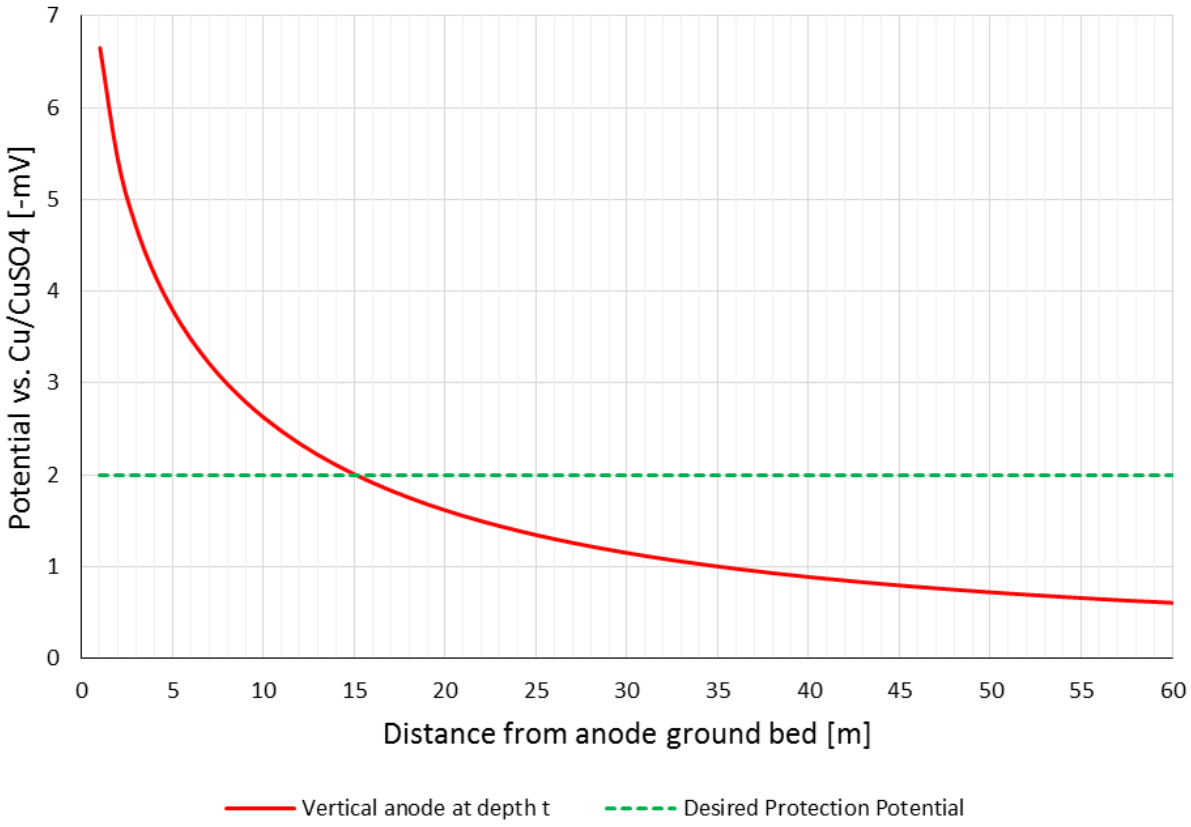

Figure 4-7: Voltage cone of deep ground bed

The grounding resistance of the anode ground beds is dependent on the dimensions of the anode ground bed and the number of anodes installed in the ground bed will not influence the grounding resistance. The soil resistivity is more favourable at a depth of 10 m from the surface of the earth and suits the installation of a ground bed. Deep anode ground beds with a total length of 20 m and a diameter of 0.165 will be installed. The grounding resistance of a single deep anode ground bed with the mentioned dimensions can be calculated as follows:

$$R_{GB} = \frac{\rho}{2\pi L}\ln\left(\frac{2L}{d}\sqrt{\frac{4t+3L}{4t+L}}\right) = \frac{45}{2\pi(20)}\ln\left(\frac{2(20)}{0.165}\sqrt{\frac{4(10)+3(20)}{4(10)+20}}\right) = 2.06\ \Omega\,.$$

(4-29)

The total resistance of the five anode ground beds installed in parallel can be calculated using the conventional method for resistances in parallel:

$$R_A = \frac{1}{2.06} + \frac{1}{2.06} + \frac{1}{2.06} + \frac{1}{2.06} + \frac{1}{2.06} = 0.412\ \Omega\,.$$

(4-30)

4.3.2.3 Total circuit resistance

It is necessary to calculate the theoretical grounding resistance of the pipeline to ensure that the average of the theoretical and measured resistances will be taken into account in the calculation of the size of the TRU. The calculation of the grounding resistance of the underground pipeline network is based on the assumption that the coating of the pipeline is in a good condition.

The resistance of the cathode is taken as an average value of the measured grounding resistance and the theoretical grounding resistance of the underground pipeline network. The theoretical grounding resistance of the underground pipeline network will be based on the condition of the protective coating applied to the surface of the pipeline. Assuming that the coating of the pipeline is in a very poor condition, based on the measured grounding resistance of the pipeline, the assumption is made that the conductance of the coating, G_n, is $4 \times 10^{-3}\ \mu\mathrm{S/m^2}$ in 10 Ωm soil. The theoretical resistance of the underground pipeline network can then be calculated as follows:

$$R_G = \frac{1}{G_n \times S_A} \times \frac{\rho}{10\ \Omega\mathrm{m}} = \frac{1}{4 \times 10^{-3} \times 891} \times \frac{60}{10} = 1.685\ \Omega\,.$$

(4-31)

As the theoretical and measured resistances of the underground pipeline are different, the average value of the measured grounding resistance and the theoretical grounding resistance will be used in the total circuit resistance for calculations to follow. This will not affect the results to follow but has to be kept in mind when evaluating the results.

$$R_C = \frac{0.91 + 1.685}{2} = 1.298\ \Omega\,.$$

(4-32)

The total circuit resistance is the sum of the grounding resistance of the anode ground beds, the grounding resistance of the cathode, i.e. the underground pipeline network, and the resistance of the cables used to complete the circuit. In this case the resistance of the cables is negligible when compared to the other resistances in the circuit. The total resistance of the circuit is thus:

$$R_T = R_A + R_C = 0.412 + 1.298 = 1.71\ \Omega\,.$$

(4-33)

4.3.2.4 Sizing of TRU

The calculation of the size of TRU needed is based on the total required current and the total resistance of the circuit. Using Ohm's Law, the required output voltage of the TRU can be calculated and subsequently the required power output of the TRU. The required output voltage of the TRU is a direct result from Ohm's Law:

$$V_{TRU} = I_T \times R_T = 5.6 \times 1.71 = 9.576\ \text{V} \approx 10\ \text{V}. \quad \textbf{(4-34)}$$

It is good practise to ensure that the size of the TRU that is installed will be able to handle the need for larger voltage outputs in the future. This is due to coating breakdown and added sources of stray current that may present a challenge during the lifetime of the CP system. Therefore is deemed good practice to make the voltage output of the TRU adjustable. In this case the voltage of the TRU will be adjustable to a maximum of 50 V. The possible current output of the TRU with a maximum voltage output is also a direct result from Ohm's Law:

$$I_{max} = \frac{V_{max}}{R_T} = \frac{50\ \text{V}}{1.71\ \Omega} = 29.24\ \text{A}. \quad \textbf{(4-35)}$$

Whenever the maximum current is supplied to the underground pipeline network at the maximum allowable voltage of the TRU the required power output of the TRU is:

$$P_{max} = V_{max} \times I_{max} = 50\ \text{V} \times 29.24\ \text{A} = 1.462\ \text{kW}.$$

The empirical design of the underground pipeline is now complete and the simulation of the CP system is the following step towards the verification of the design framework that was followed during the empirical design of the CP system.

4.4 Cost considerations during CP system design

During CP system design a couple cost considerations are required. These cost drivers are considered to identify the components within the CP system that will have a significant impact on the total cost of the CP system under consideration. Some of the signicant cost drivers have been discussed throughout the dissertation. The cost drivers that have not been discussed up to this point are covered in this section.

Cables are considered as one of the most significant cost drivers that can increase the total cost of a CP system. The size and length of the cables to be installed in a CP system will contribute significantly towards the total cost of a given system. Considerations to be kept in mind when

considering the cables to be installed include: the type of cables required, the total length of the cables, the number of required cables, and the size of cables to be installed. The cost of cables are dependent on the mentioned parameters and the cost of cabling can increase the total cost of a CP system considerably.

Other cost drivers to consider when designing CP systems include the cost and number of TRUs to be installed to protect a given structure. By limiting the number of TRUs to be installed the total cost of the CP system. With this in mind, keeping the number of AJBs and CJBs to a minimum, the cost of the CP system can also be reduced.

The last significant cost driver to keep in mind during CP system design is that of test points to be installed. Different types of test points are available for installation and the number of required test points will depend on the type of system installed and the surrounding environment. Nevertheless, the cost of test points must be kept in mind when designing CP systems to be cost effective.

4.5 Design framework

The design framework that is suggested for CP system design for the petrochemical industry is presented in Figure 4-8. The design framework is based on procedures found in international standards as well as in literature. The flow diagram of the design framework is used for the visual representation of the framework that was used to perform the empirical CP system design for the small tank farm as well as that of the underground pipeline network.

Any CP system design starts with a comprehensive site survey. The data to be obtained during the site survey have been discussed in detail in section 4.1. This information also forms part of the basic flow diagram of the design framework included in Figure 4-8. Depending on whether the CP system is to be designed for a new or existing structure, the required current demand to fully protect the structure is determined in different ways.

In the case of an existing structure it is possible to perform a current drain test in order to determine the required current for adequate protection of the tank. The same applies for measuring the resistance-to-earth of the structure and measuring the conductance of the structure. These are very important parameters to be used during the empirical design of the CP system.In the case of a new installation the abovementioned measurements are not always possible to perform and the theoretical calculations of required current, structure-to-earth resistance, and coating conductance must be performed. These steps are also included in the basic flow diagram.

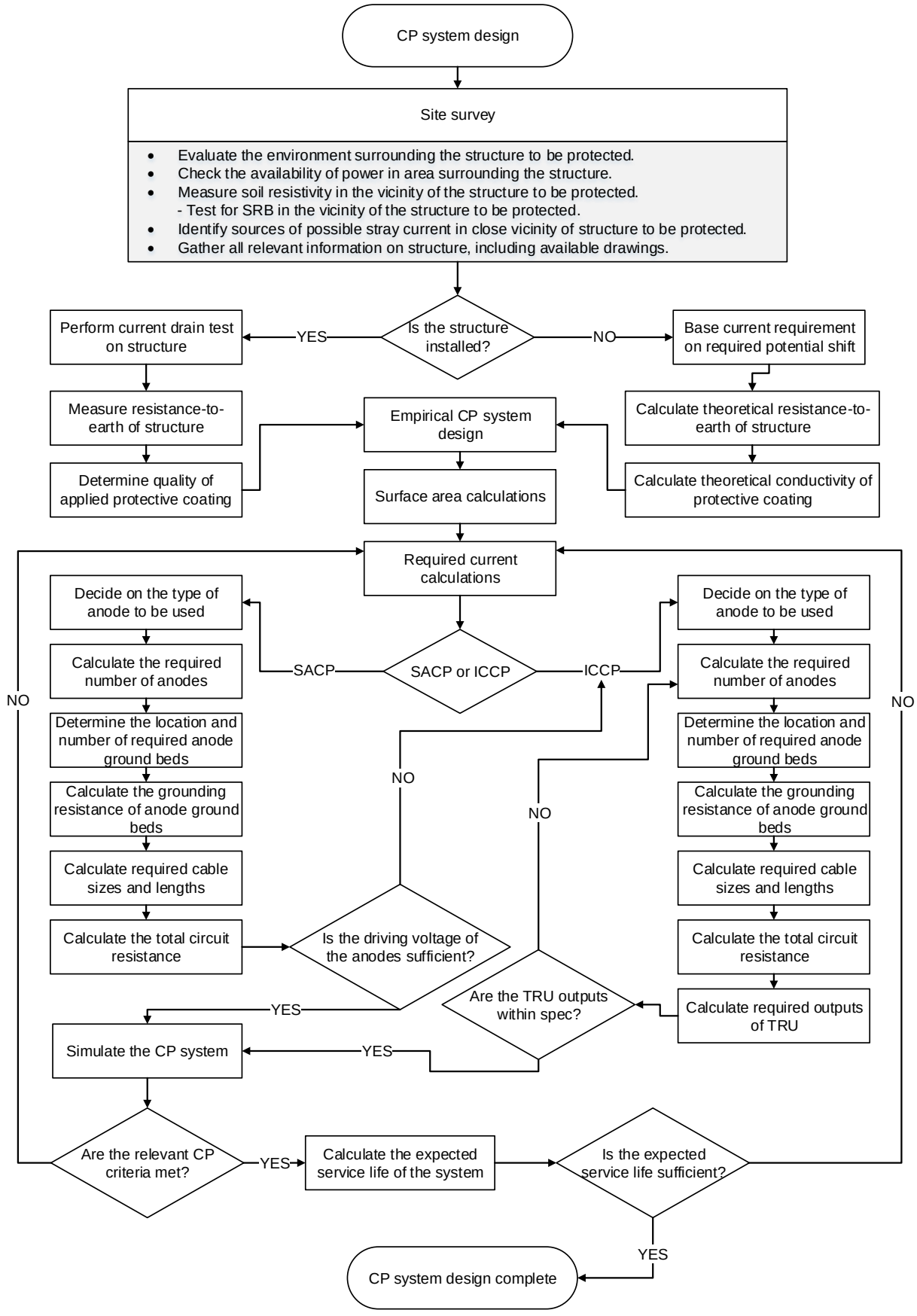

Figure 4-8: Flow diagram of design framework

The empirical CP system design comprise the use of empirical equations. The empirical calculations and the sequence of the calculations are clear from the information contained in the flow diagram presented in Figure 4-8.

It is very important to note that the flow diagram recommends that the empirically designed CP system is simulated with the aid of a computer software package. The results obtained from the simulation of the CP system are to be used to determine whether the system meets the relevant CP criteria required for the protection of the structure throughout its entire service life.

Two important questions are raised after the simulation of the CP system. If the answer to any of these two questions are no, the flow diagram enters an iterative process. This iterative process is also linked to the high flow diagram presented in Figure 1-3 that was used to discuss the research methodology. Once the relevant CP criteria have been met and it has been established that the CP system will protect the structure for the expected service life, the design of the CP system is concluded.

Chapter 4 was used to cover the empirical CP system design of a small tank farm and an underground pipeline network. The purpose of this chapter was to identify and use a design framework based on international standards and literature. The equations that is generally associated with CP system design have been identified and aided in the forming of the general design framework. The simulation of the two CP systems designed in this chapter is included Chapter 5. The verification of the proposed CP system design framework is included and discussed in Chapter 5.

5

CHAPTER

DESIGN FRAMEWORK VERIFICATION

This chapter is dedicated to the verification of the design framework that was established in Chapter 4. The main focus of this chapter falls on the polarisation of the surface of the mentioned structures and the overall performance of the CP systems. The design framework is verified using the appropriate CP criteria in terms of the performance of the CP systems based on the design framework. The polarisation results used for verification purposes are obtained from simulations performed in BEASY™ Corrosion and CP.

5.1 Small tank farm

The empirical design of the CP system for the protection of the small tank farm will be evaluated in the sections to follow. The evaluation of the CP system will comprise the visualisation of the potential on the outside surface of the tanks as well as the current distribution on the outside surface of the tanks as generated from the simulations. The empirical design of the CP system is implemented in the simulation software package in order to evaluate the overall performance of the CP system in terms of the level of protection offered. The CP criteria is used to verify that the CP system that was empirically designed sufficiently polarises the metal to an acceptable value.

In the case of the level of protection not being satisfactory or unacceptable, the design will be altered until the criteria is met. The alteration to the design will be discussed in greater detail and reasons will be supplied for the difference in performance if any are present.

5.1.1 Geometry of small tank farm

The geometry of the small tank farm is presented in this section. The geometry of the tank farm is important for the visualisation of the performance of the system as well as for the evaluation of the CP system. Some of the information regarding the geometry of the tank farm have already been disclosed in the previous chapter and the detail to follow will be used to supplement that. The geometry of the tanks and the depth of the tanks in the soil are displayed in Figure 5-1.

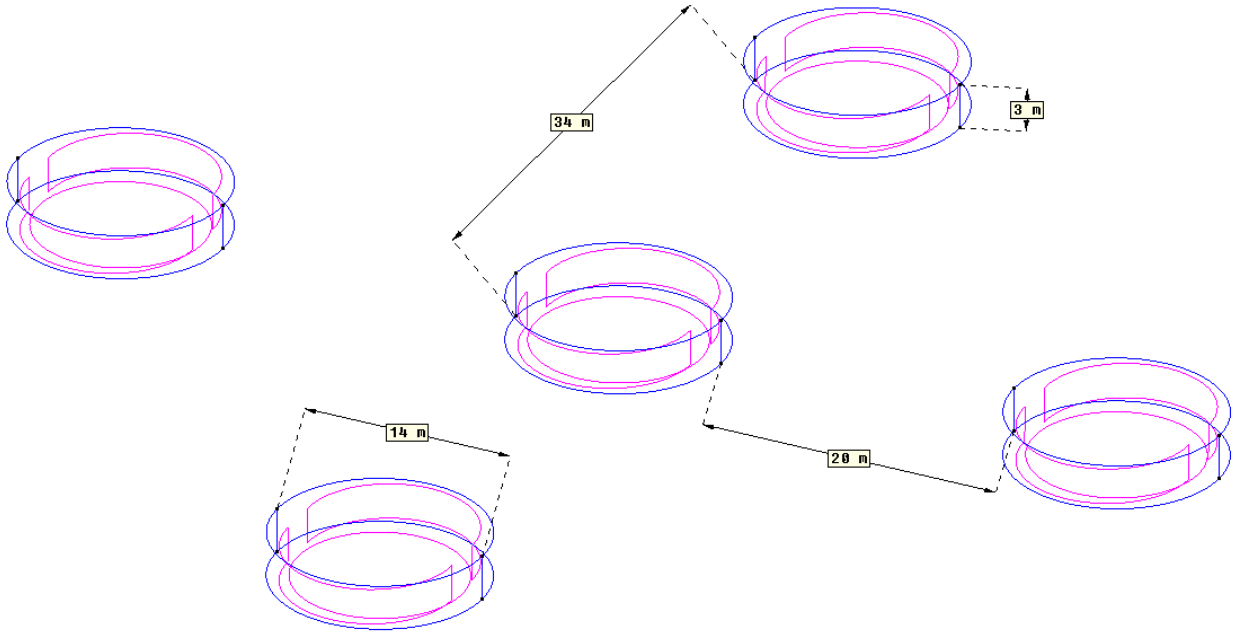

Figure 5-1: Geometry and layout of small tank farm

In this case all the tanks are at an equal spacing and the dimensions displayed in the above figure are applicable to all the tanks. The visual representation of the geometry of the tanks will be used to indicate the location of the anodes with respect to the tanks as determined in Chapter 4. The geometry and general arrangement of the anodes with respect to the tanks are displayed in Figure 5-2.

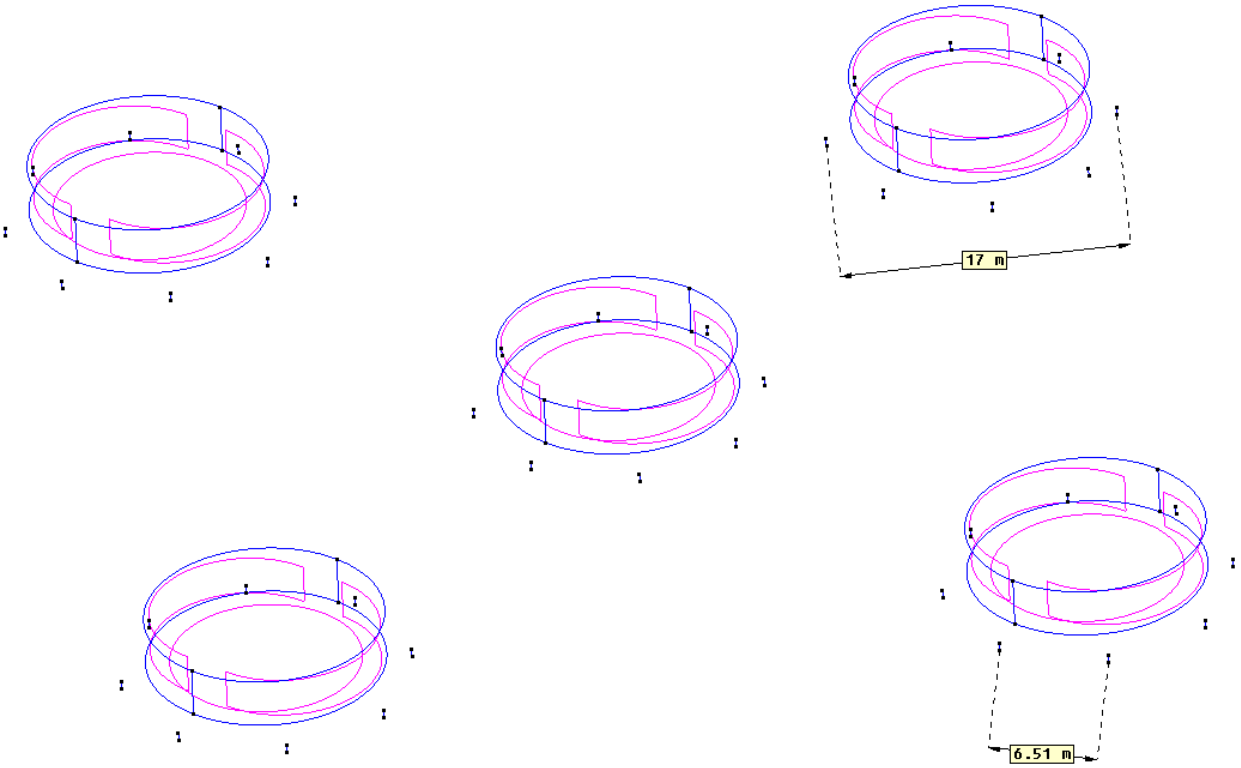

Figure 5-2: Geometry of anodes with respect to the tanks

The anodes are buried at a depth of 3.5 m measured from the surface of the earth. The layout of the anodes is used to display the position of the anodes with respect to the tanks as specified in the empirical design of the CP system.

The geometry will now be used to implement the CP system as designed in Chapter 4. Using the CP solver of the BEASY™ Corrosion and CP software package the boundary conditions and current requirement will be defined in order to evaluate the performance of the CP system.

5.1.2 Definition of boundary conditions

The boundary conditions to be defined are very important for the accuracy and validity of the results obtained from the simulations. It is stated that the boundary confining the electrolyte area must be 20 times the size of the structure or larger for the results to be accurate. The default boundary conditions on the surfaces representing the box containing the electrolyte are a normal flux density of zero.

The other important boundary conditions to be defined include that of the material from which the tanks and the anodes are manufactured respectively. The boundary conditions regarding the tanks and anodes are defined by means of the respective polarisation curves. The polarisation curve for the tank material has already been defined in Figure 4-2. The polarisation curve presented in Figure 5-3 is anodic of nature and represents the boundary conditions of the MMO anodes.

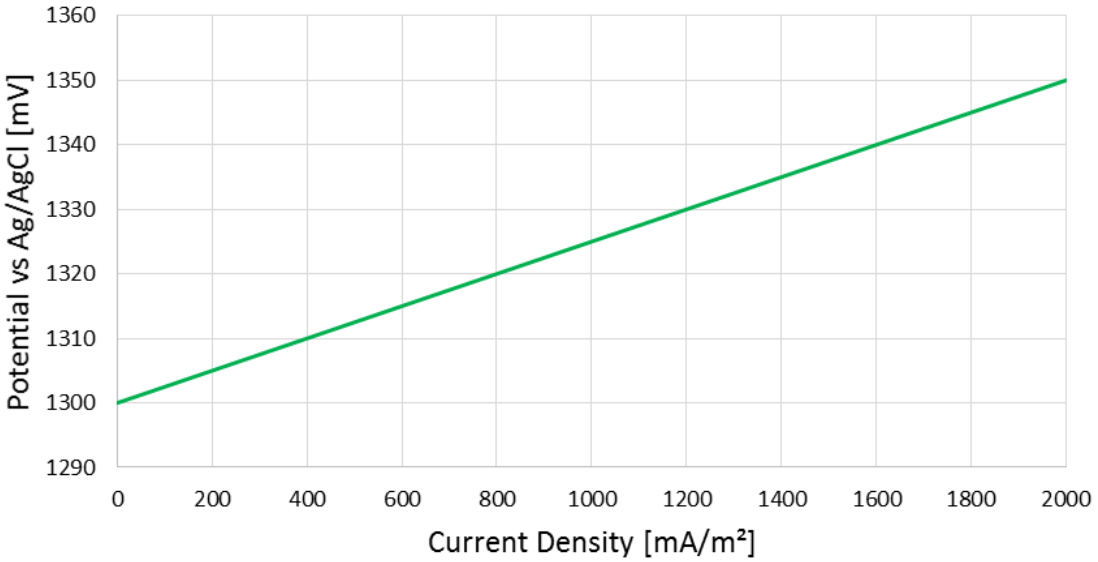

Figure 5-3: Polarisation curve for MMO anodes

5.1.3 Implementing system requirements

The required current and voltage output of the TRU must be defined within the BEASY™ CP Wizard along with the connections between the anode ground beds and the tanks. This section will be used to discuss the interaction between the different components within the CP circuit. The BEASY™ CP Wizard allows for the definition of the resistance of the cables interconnecting the anodes and tanks and is therefore implemented within the simulation.

The CP system layout with respect to the anodes, tanks (cathodes), and the TRU within the CP "circuit" are displayed in Figure 5-4. Also included within the CP circuit is the resistance of the cables that are used to interconnect the different components within the CP system. The resistance of the cables interconnecting the different components can affect the performance of the system and are therefore included for the purpose of thoroughness.

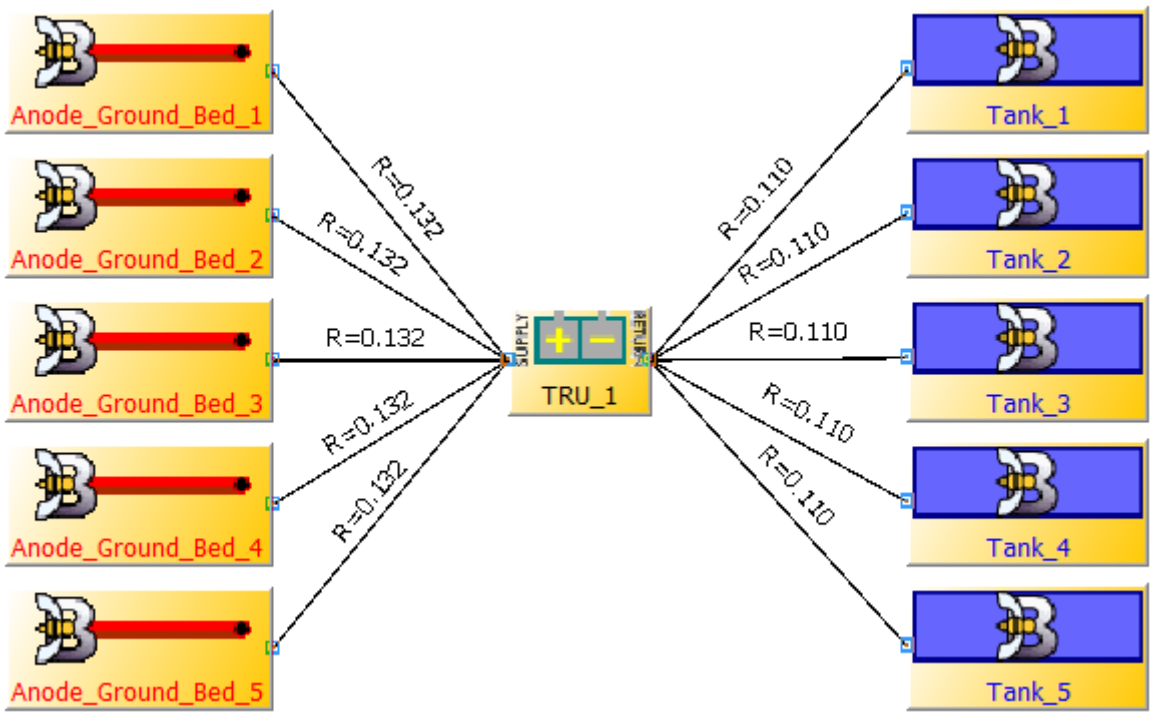

Figure 5-4: CP circuit layout of CP system for small tank farm

Important parameters to be declared within the BEASY™ CP Wizard are that of the output current and voltage of the TRU respectively. The wizard that is used as solver allows for the definition of the TRU either in terms of the target output voltage or the target output current. In this case the target output voltage of the TRU is defined. By defining the target output voltage of the TRU, the current output of the TRU will be limited to the value defined in Figure 5-5. The definition of the output voltage and current of the TRU are displayed in Figure 5-5.

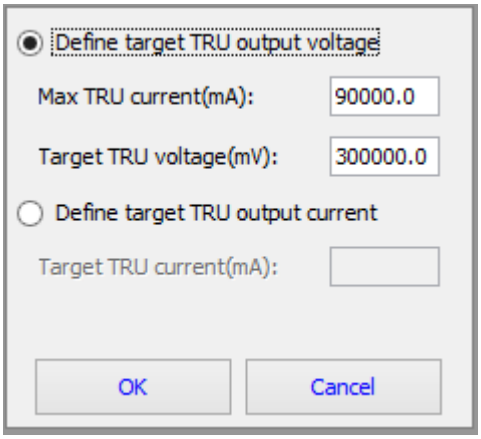

Figure 5-5: Defining voltage and current output of TRU in small tank farm

It is noted from Figure 5-5 that the target output voltage of the TRU is different from that calculated in (4-34) . The output voltage as displayed in Figure 5-5 is attributed to the fact that only the anodes were defined within the simulation. For simulation purposes, the columns in which the anodes are to be installed have been excluded.

Using the same approach as that used in Chapter 4 and calculating the grounding resistance of a single anode as installed in the simulation is calculated in (5-1).

$$R_v = \frac{\rho}{2\pi L}\ln\left(\frac{2L}{d}\times\sqrt{\frac{4t+3L}{4t+L}}\right) = \frac{100}{2\pi(0.5)}\ln\left(\frac{2(0.5)}{0.025}\times\sqrt{\frac{4(3.5)+3(0.5)}{4(3.5)+0.5}}\right) = 118.47\ \Omega\,.$$

(5-1)

The resistance of 8 anodes installed in order to protect a single tank in the small tank farm is thus calculated as 8 resistances in parallel with the value as calculated in (5-1). The 8 anodes that are installed around the single tank will therefore be referred to as a single ground bed. The calculation is presented in (5-2).

$$R_{GB1} = \left[\frac{8}{118.47}\right]^{-1} = 14.81\ \Omega\,.$$

(5-2)

As the individual ground beds surrounding each tank are connected in parallel, the total grounding resistance of the anodes is calculated in (5-3).

$$R_A = \left[\frac{5}{14.81}\right]^{-1} = 2.96\ \Omega\,.$$

(5-3)

This grounding resistance value will be verified using the post simulation report that is created by the BEASY™ CP Wizard as soon as the simulation is completed.

5.1.4 Simulated results

The simulated results obtained from using the BEASY™ CP Wizard are discussed in this section. The first result to be discussed is that of the level of polarisation experienced by the metal surfaces within the small tank farm. The simulated potential distribution on the collective surface area of the tanks are displayed in Figure 5-6.

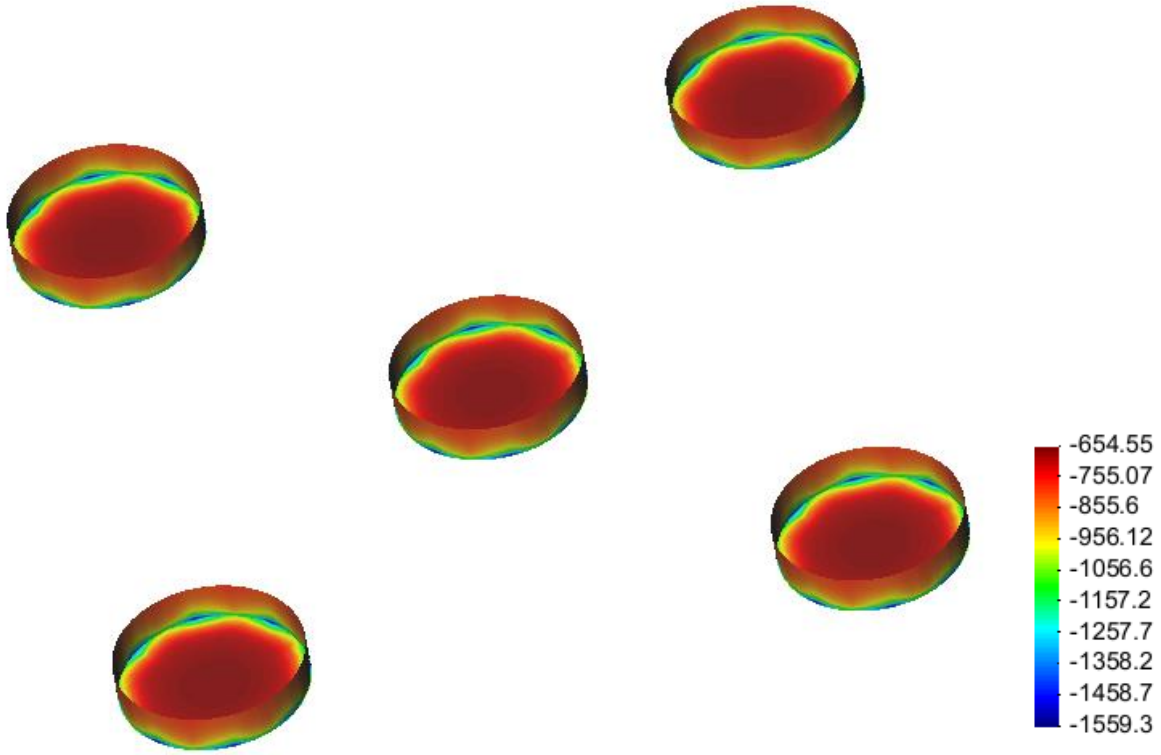

Figure 5-6: Simulated potential on tank surfaces in small tank farm with potential in mV against an Ag/AgCl RE

From the potential distribution on the tank surfaces presented in Figure 5-6 it is visible that the level of protection provided by the CP system is insufficient. Important to notice at this point is that the potential on certain areas on the tank surfaces are more negative than found on other areas on the surfaces. This is an import observation to be made at this point as the placement of the anodes with respect to the tanks is expected to be responsible for this phenomenon.

In order to explain the potential distribution on the tank surfaces it is necessary to investigate the polarisation curve of the material used in the CP simulation. The polarisation curve resulting from the CP simulation is displayed in Figure 5-7.

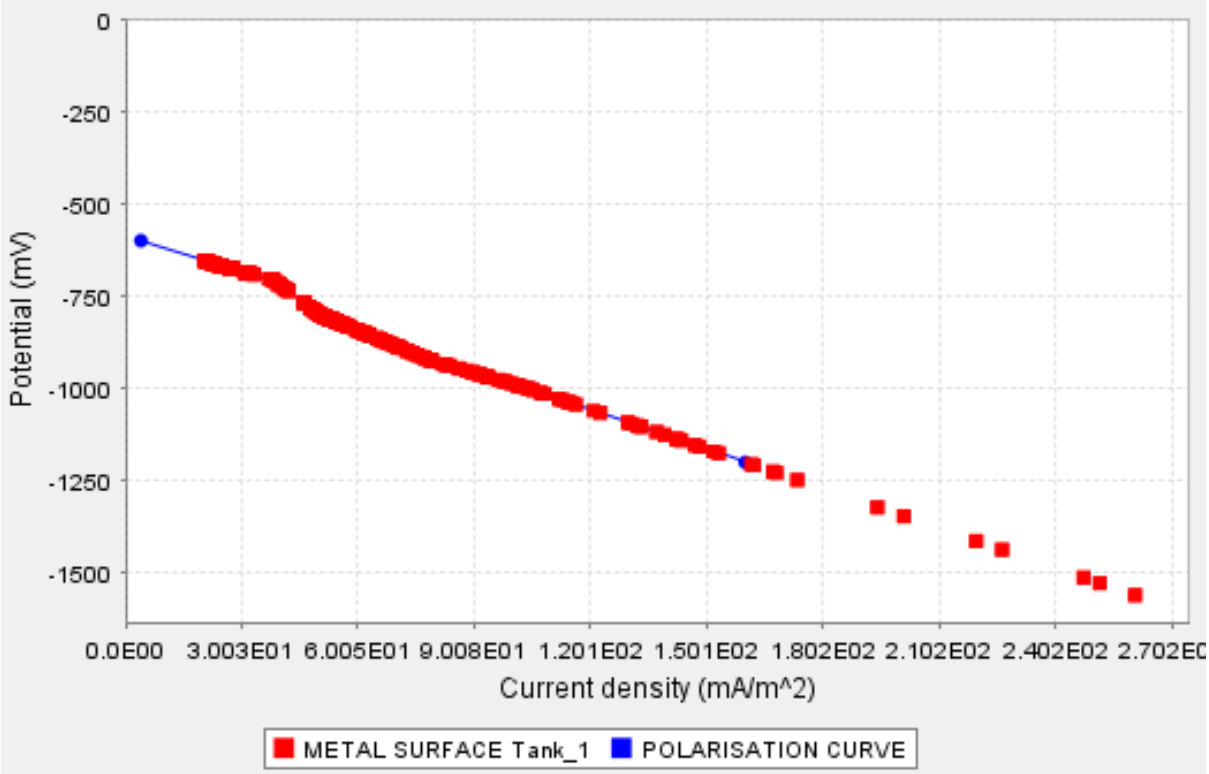

Figure 5-7: Polarisation curve of tank material after completion of simulation

The polarisation curve displayed in Figure 5-7 is very important when evaluating the potential distribution on the surface of the tanks. More importantly, it will also be used in evaluating the current density on the surface of the structures and finding the link between potential and current distribution. The potential distribution along with the current distribution on the tank bottoms will now be evaluated by taking a closer look at these parameters on a single tank bottom.

The potential distribution on the tank bottom of one of the tanks found in the small tank farm is displayed in Figure 5-8. The potential is thus measured at a depth of 3 m which is where the tank bottoms are situated in the small tank farm. The colour bar that is displayed in Figure 5-8 displays the potential measured vs a $Cu/CuSO_4$ reference electrode. The voltage and current outputs of the TRU is the same as that found in Figure 5-5. The anodes in this case is installed at depths of 3.5 m and 1.5 m from the outside diameter of the tanks.

The position of the anodes with respect to the tanks is evident from the potential distribution found in Figure 5-8. The colour bar to the right of the surface in the figure represents the potential [mV] at the specific areas. The dark blue areas are the areas closest to the anodes and therefore have the most negative potential compared to the rest of the surface. Using the applicable CP criteria, -850 mV with CP applied criterion or polarised potential of -850 mV criterion, it is evident that the level of protection is not sufficient. In order to understand the potential distribution on the tank

bottoms the current distribution and the strength of the electric field in certain areas require further investigation. The current density distribution on the tank bottom is presented in Figure 5-9.

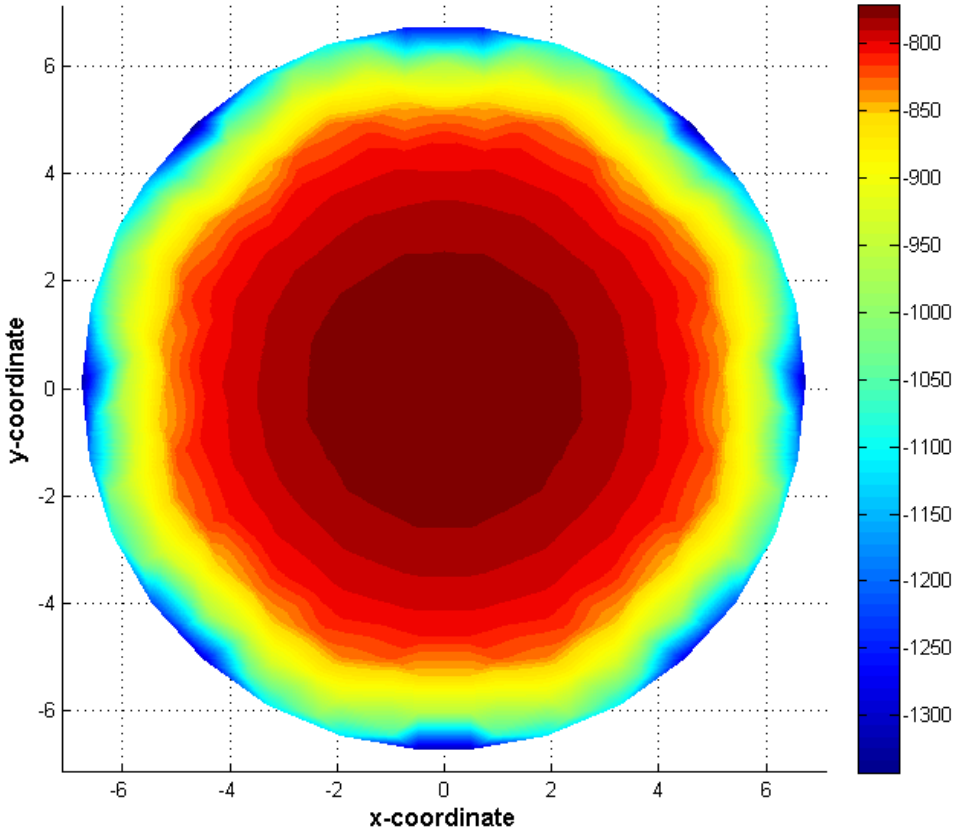

Figure 5-8: Potential distribution on tank bottom with anodes installed at a depth of 3.5 m against CSE

From the potential and current distribution on the tank surfaces, displayed in Figure 5-8 and Figure 5-9 respectively, it is evident that current density is directly proportional to potential. The colour bar found in Figure 5-9 is used to describe the current density at a given point on the tank bottom with the unit being mA/m^2. This is confirmed when investigating the polarisation curve used in the simulations. By ensuring a certain current distribution is reached on a surface the desired potential, and indirectly polarisation, is reached for efficient protection against corrosion.

Although the required current is supplied to the exposed areas of the tank surfaces, the required current distribution for effective protection is not reached on all the areas. This is a very important concept to keep in mind when designing CP systems for a given application. By evaluating the electric field strength on the tank bottoms, it may be possible to better describe the current distribution found in Figure 5-9. A top view of the 3-D electric field strength on the tank bottom is displayed in Figure 5-10. The strength of the electric field at specific areas on the tank bottom is used to explain the current distribution on the tank bottom.

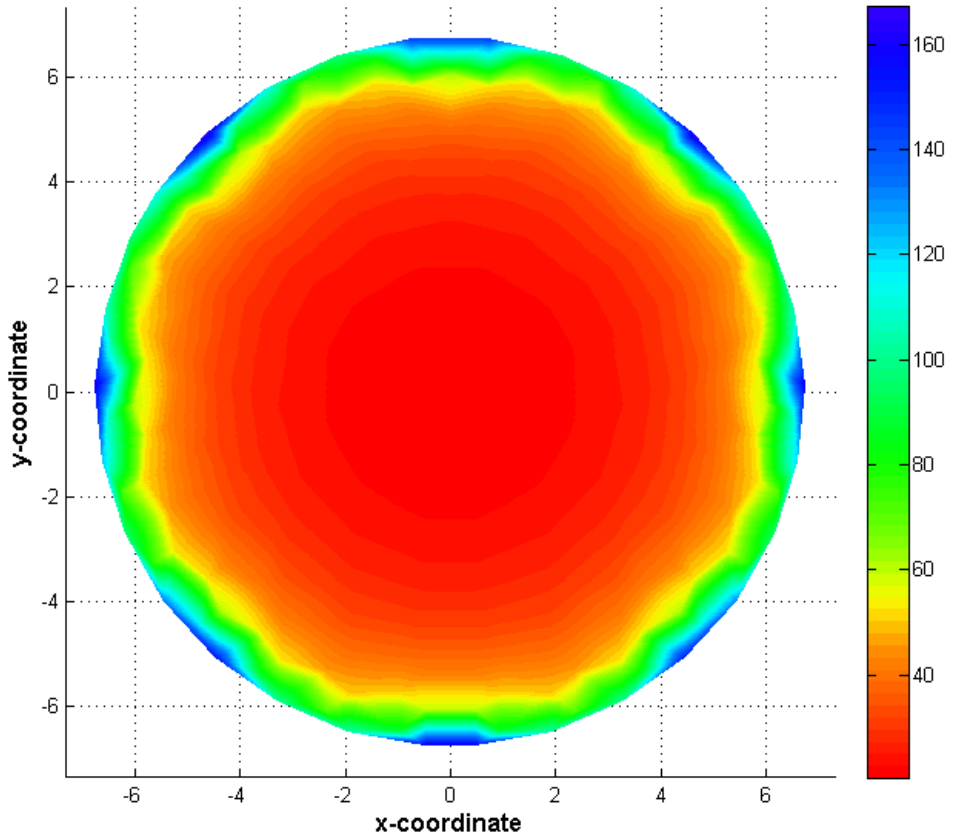

Figure 5-9: Current distribution on tank bottom with anodes installed at a depth of 3.5m

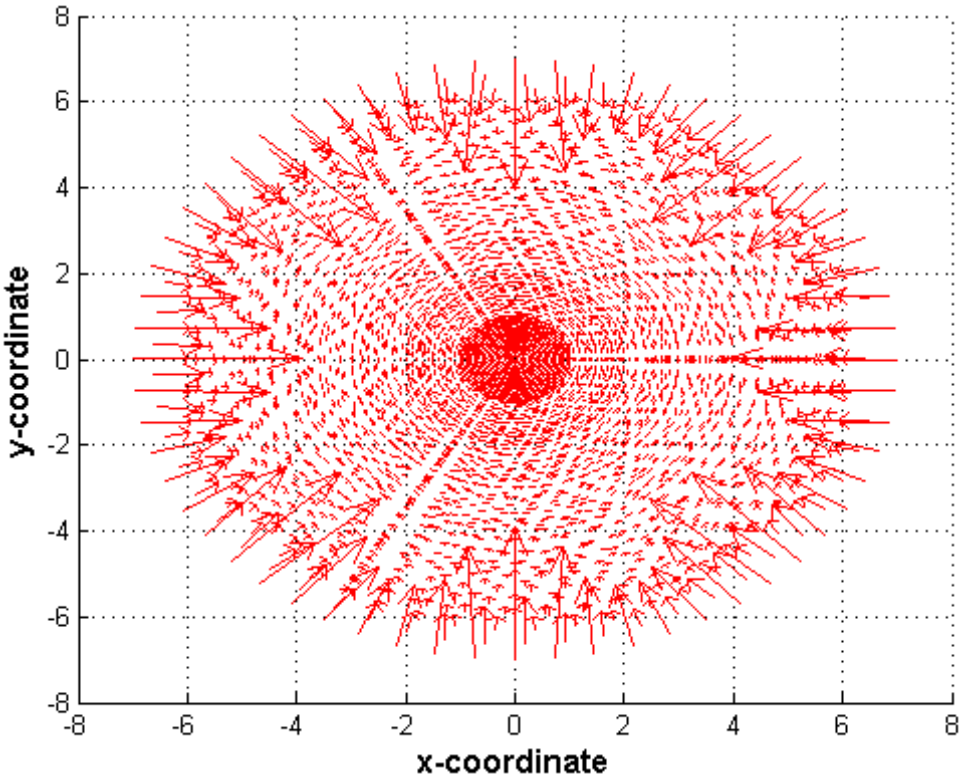

Figure 5-10: Top view of electric field strength on tank bottom with anodes installed at a depth of 3.5 m

From the top view of the electric field strength on the tank bottom displayed in Figure 5-10, the current distribution on the tank bottom can be explained. Taking a closer look at the following coordinates will explain the current distribution phenomenon: (-7; 0), (-5; 5), (0; 7), (5; 5), (7; 0), (5; -5), (0; -7), and (-5; -5). At these coordinates evidence of the electric field strength being at its highest exist. This is derived from the length of the arrows, representing vectors, found at these coordinates compared to the rest of the arrows in the plot. Compared to the current distribution on the tank bottom, these areas also represent the areas with the highest current density.

Whenever these areas are compared to the location of the anodes with respect to the tanks, these areas also correlate. The placement of the anodes with respect to the structure to be protected is thus a very important parameter to consider whenever CP systems are designed. To prove this point, the same CP system is simulated with the only difference being the depth at which the anodes are installed. For this simulation the anodes were installed at a depth of 13.5 m below the surface of the earth. The potential distribution on the tank bottom with the anodes installed at a depth of 13.5 m is displayed in Figure 5-11.

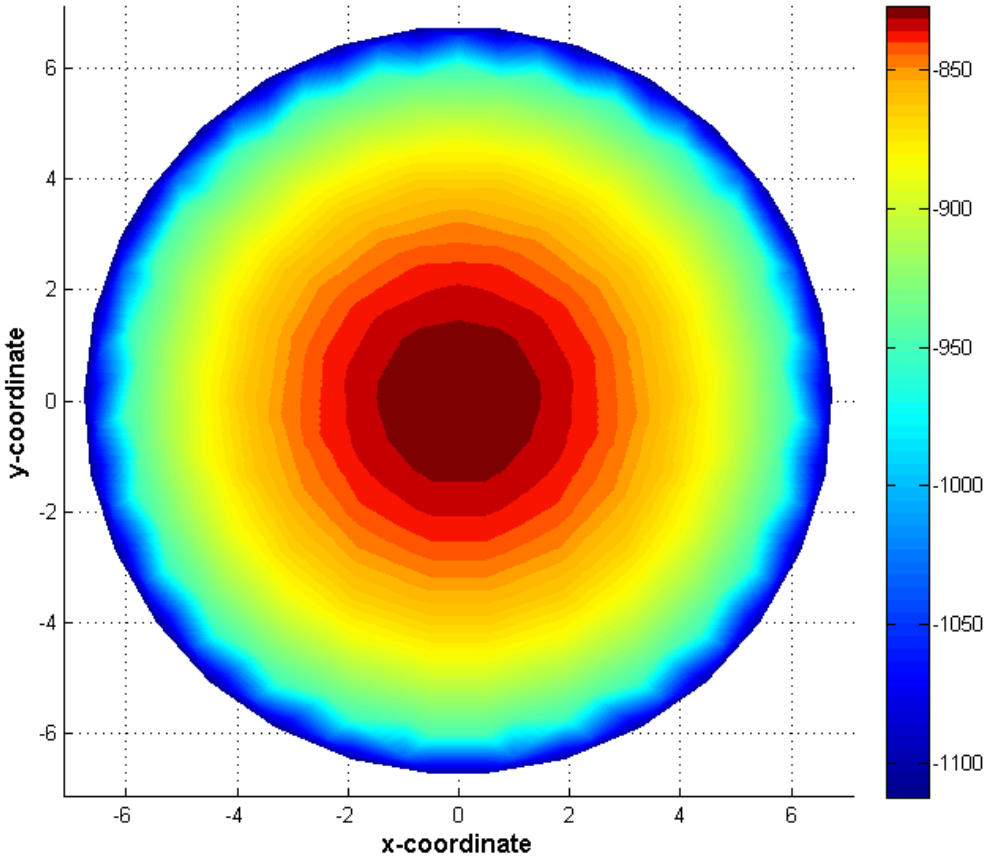

Figure 5-11: Potential distribution on tank bottom with anodes installed at a depth of 13.5 m against CSE

Comparing the potential distribution on the tank bottom found in Figure 5-11 to the potential distribution displayed in Figure 5-8 two observations are made. Firstly, the potential distribution

presented in Figure 5-11 is more uniform than the potential distribution presented in Figure 5-8. The second observation of importance is that a bigger area of the tank bottom is protected with the anodes installed at a depth of 13.5 m compared to the anodes installed at a depth of 3.5 m. From the previous discussion regarding the proportionality regarding potential and current distribution, it is expected that a better current distribution will be present on the tank bottom with the anodes installed at a depth of 13.5 m. The current distribution on the tank bottom with the anodes installed at a depth of 13.5 m is displayed in Figure 5-12.

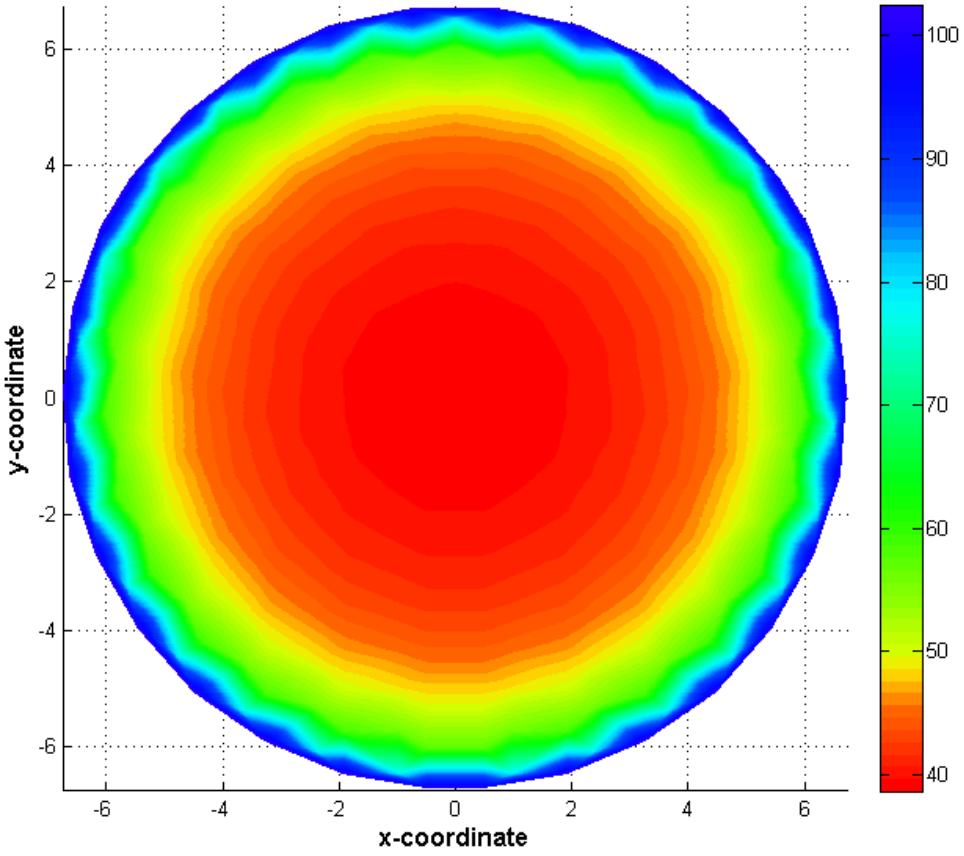

Figure 5-12: Current distribution on tank bottom with anodes installed at a depth of 13.5m

Although the current distribution on the tank bottom presented in Figure 5-12 does not ensure that the whole surface is sufficiently polarised, a more uniform current distribution is present when compared to Figure 5-9. It is expected that the electric field strength on the tank bottom will be more uniform than was the case in Figure 5-10. Due to the location of the anodes with respect to the tanks the electric field is expected to distribute more uniformly through the electrolyte to the surface of the tanks. The electric field strength distribution is presented in Figure 5-13.

Comparing the top view of the electric field strength on the tank bottom with anodes installed at a depth of 13.5 m, Figure 5-13, to that found in Figure 5-10, interesting observations are made. The

first observation to be made is that of the general shape of the electric field distribution. The overall shape of the distribution found in Figure 5-13 is more uniform than that found in Figure 5-10. Secondly, the electric field strength displayed in Figure 5-13 is more uniform on the outer edges when compared to the distribution found in Figure 5-10.

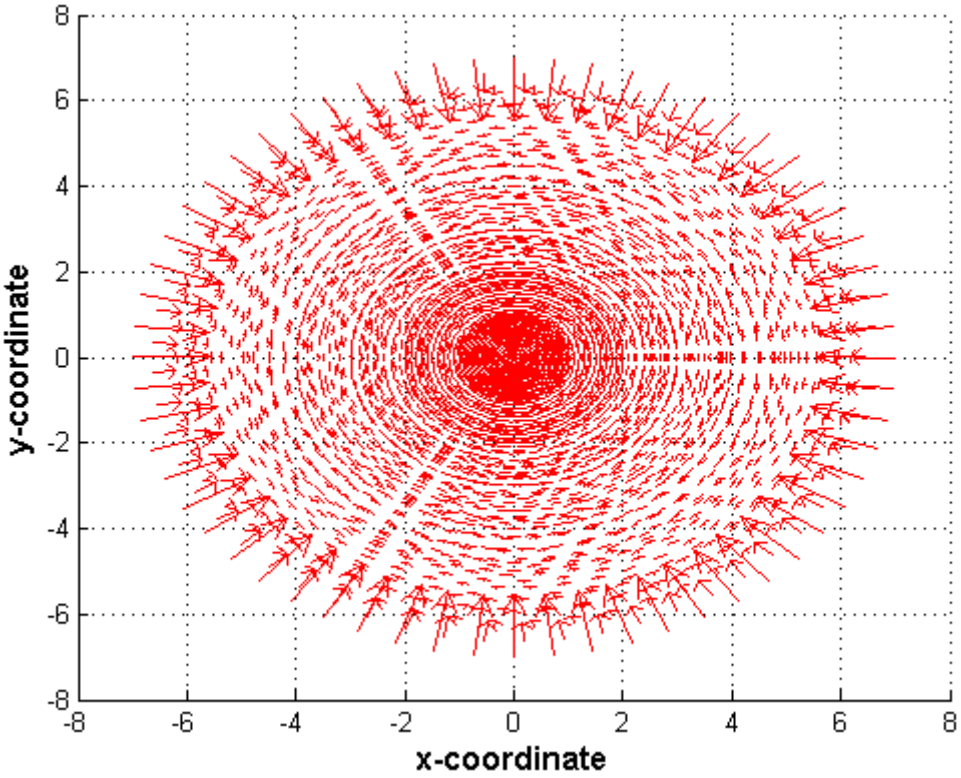

Figure 5-13: Top view of electric field strength on tank bottom with anodes installed at a depth of 13.5 m

At this point in the verification process the empirical design of the CP system has been verified to the point that the required current and voltage applied to the structures suggest that the structures is protected at certain areas. The placement of the anodes proves to be essential in reaching the ultimate uniform current distribution required to fully protect the entire structure and satisfying the applicable CP criteria. To verify that it is able to sufficiently protect the structures with the anodes installed at a depth of 13.5 m, a small adjustment is made to the current output of the TRU. The current output of the TRU is increased to 95 A with the result of this current increase discussed in the paragraphs that follow.

The potential distribution on the tank bottom with the current output of the TRU increased to 95 A and the anodes still installed at a depth of 13.5 m is displayed in Figure 5-14. With this small increase in the output current of the TRU it is evident that the potential distribution present on the surface of the tank bottom is very close to the desired potential distribution for the full protection of the tank bottom surface. This statement is based on the potential on the surface of the tank

bottom being either close to or over the -850 mV (CSE) limit as declared by the applicable CP criteria. The reason for the more uniform and desired potential distribution on the surface of the tank bottom is expected to be a better and more uniform current distribution on the areas of interest.

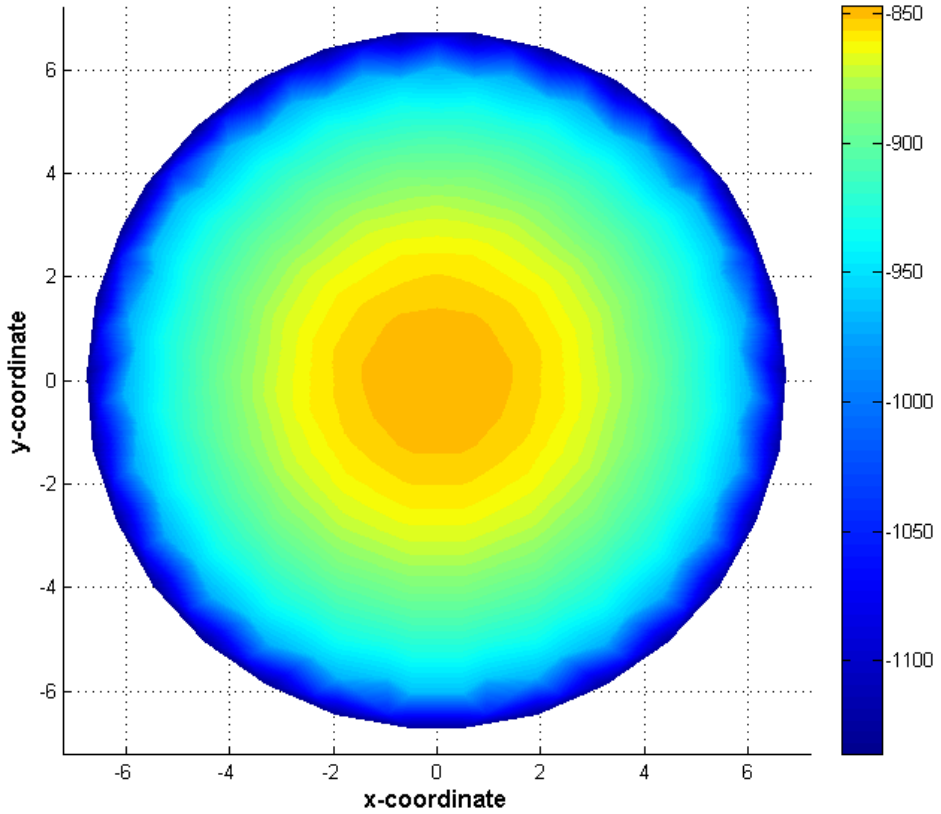

Figure 5-14: Potential distribution on tank bottom with TRU current output at 95 A against CSE

The current distribution of the setup, with the output current of the TRU equal to 95 A, and the anodes installed at a depth of 13.5 m, is displayed in Figure 5-15. When a closer look is taken at the current distribution, it can be seen that the current distribution is either over or close to 50 mA/m^2. This was the current density used in the empirical design of the CP system to calculate the required current for the protection of the total surface area of the tanks situated in the small tank farm.

With the setup used throughout the simulation of the CP system designed for the protection of the tanks in the small tank farm, it was proven that the design framework was successfully used in designing the CP system. Concluding remarks regarding the verification of the CP system design framework follows in the next paragraph.

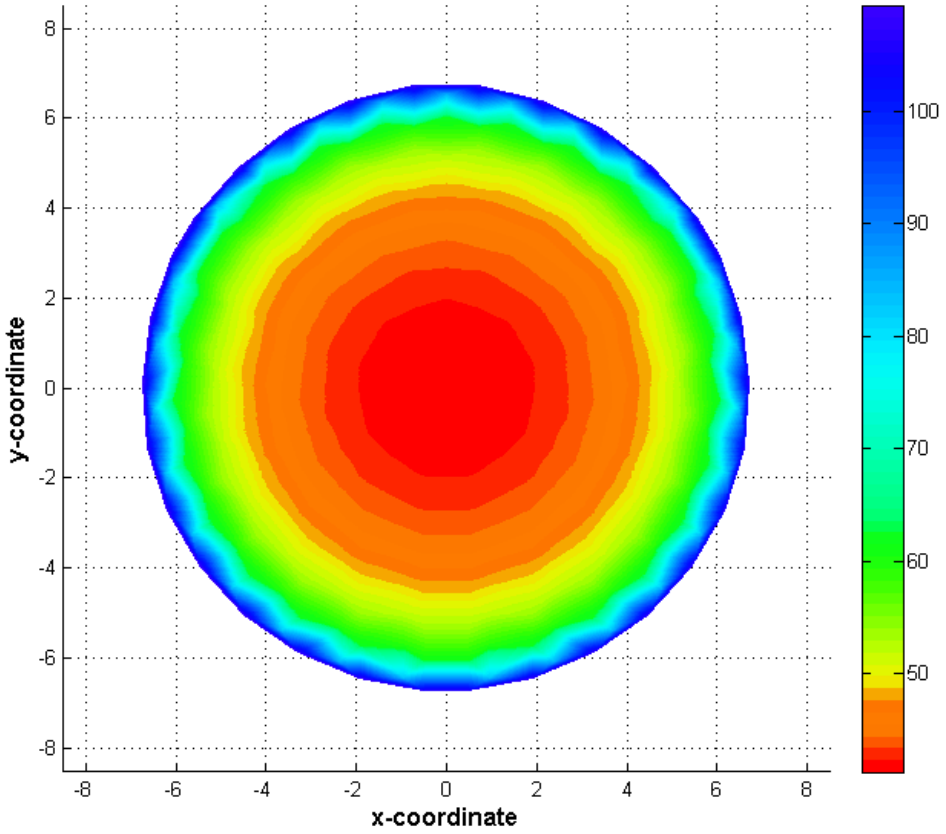

Figure 5-15: Current distribution on tank bottom with TRU current output at 95 A

5.1.5 Small tank farm summary

The empirical design of the CP system, and more importantly, the CP system design framework have been verified in terms of required current and output voltage of the TRU. This is two of the most important parameters, along with the grounding resistance of the anodes to be installed, to emerge from the empirical design of CP systems. As the CP circuit is dependent on Ohm's Law, the empirically calculated grounding resistance of the anodes is also verified within these simulations. The verification process regarding the grounding resistance of the anodes can be found in Appendix F.

Some very important parameters came to the fore during the verification process. One parameter that is paramount in the effectiveness of a given CP system is the location of the anodes with respect to the structure to be protected. It is important to keep in mind that the type of ground bed to be installed along with the orientation of the anodes may influence the location of the anodes.

For this CP system installation the only possible anode locations were in close proximity to the tanks which were installed around the circumference of the tanks. From the results presented in the preceding section it was evident that the area of influence surrounding the anodes installed at a depth of 3.5 m only affected the areas in very close proximity to the anodes. From this result

it is evident that the area of influence surrounding the anodes is a very important parameter when considering anode ground bed designs for a given application.

The area of influence surrounding an anode ground bed will be influence by non-uniform soil resistivity and by the specific soil resistivity in the immediate vicinity of the anode ground bed. Due to this phenomenon it is difficult to design CP systems to provide “perfect” protection to a given structure and adjustments to the current and voltage output of the TRU will be required during commissioning of the system.

5.2 Underground pipeline network

The empirical design of the CP system for the protection of the underground pipeline network will be evaluated in the sections to follow. The evaluation of the CP system will comprise the visualisation of the potential on the outside surface of the tanks as well as the current distribution on the outside surface of the tanks as generated from the simulations. The empirical design of the CP system is implemented in the simulation software package in order to evaluate the overall performance of the CP system in terms of the level of protection offered. The CP criteria is used to verify that the CP system that was empirically designed sufficiently polarises the metal to an acceptable value.

It is important to note that the underground pipeline network has a very complex layout with the network of pipelines crossing one another at various points underground. The layout of the underground pipeline network will be displayed in the section to follow. Another important aspect to note is that the only the pipelines installed underground are of interest for simulation purposes and only the potentials of the underground pipelines are considered in the discussions to follow.

5.2.1 Geometry of underground pipeline network

The geometry of the underground pipeline is discussed in this section. It is considered impractical to include all the dimensions of the pipelines within the underground network and therefore only two dimensions of the underground pipeline network are displayed. These dimensions will provide the reader with the necessary perspective to be able to get a better idea of the layout of the system.

The anode ground beds installed for the protection of the underground pipeline network are also displayed in the general layout of the underground pipeline network. The anode ground beds are indicated with labels in order to provide the reader with as much as possible information regarding

the layout and geometry of the underground pipeline network. The geometry and general arrangement of the underground pipeline network are displayed in Figure 5-16.

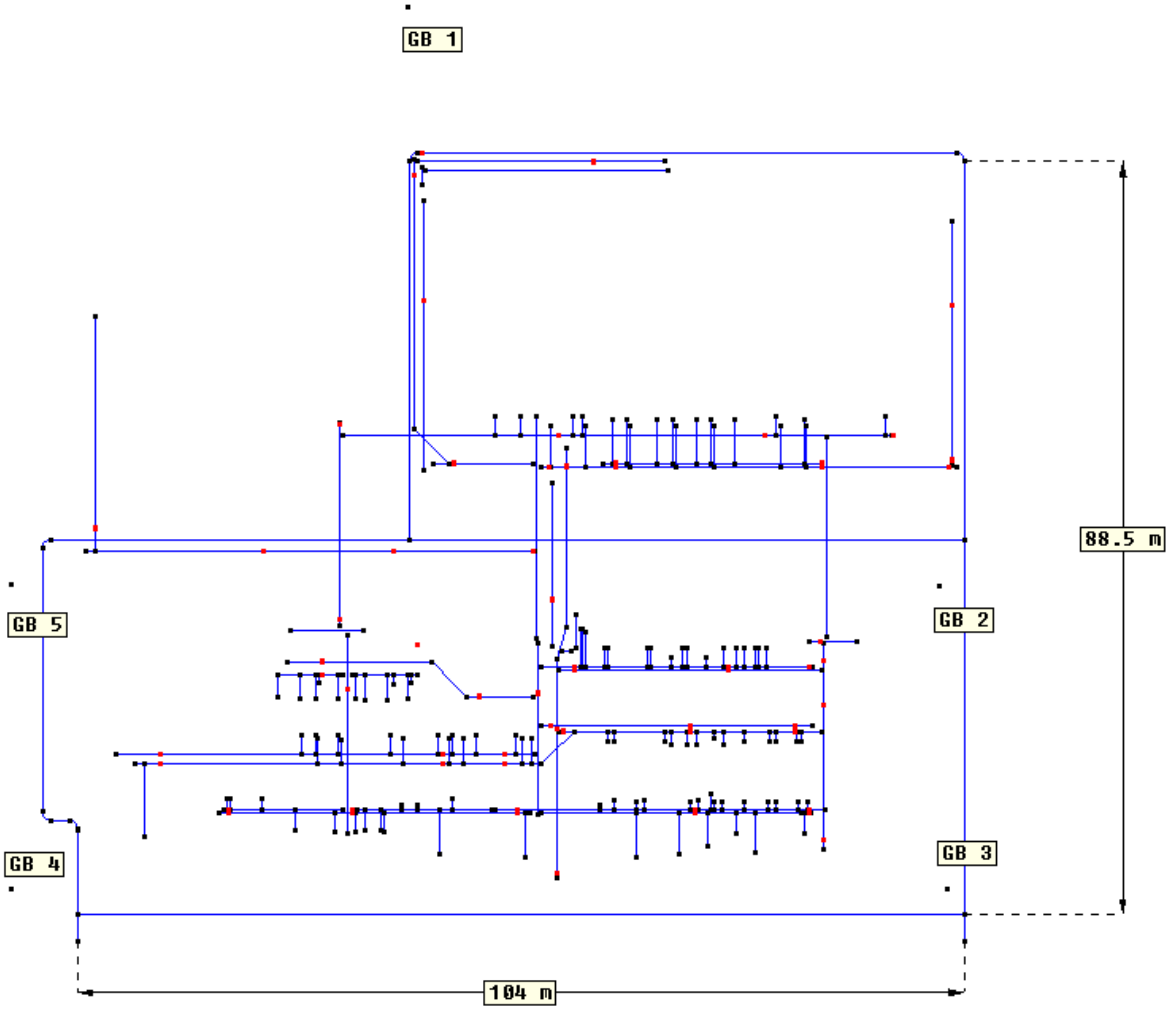

Figure 5-16: Geometry and general arrangement of the underground pipeline network

The most important information contained in Figure 5-16 is the location of the anode ground beds with respect to the underground pipelines. The definition of the boundary conditions and the implementation of the system requirements for simulation purposes are to follow in the following sections respectively.

5.2.2 Definition of boundary conditions

The boundary conditions to be defined are very important for the accuracy and validity of the results obtained from the simulations. It is stated that the boundary confining the electrolyte area must be 20 times the size of the structure or larger for the results to be accurate. The default boundary conditions on the surfaces representing the box containing the electrolyte are a normal flux density of zero. For the simulation of the CP system for the underground pipeline network, a

multi-layered zone have been defined. The values of the soil resistivity used in the different layers are the same as that found Table 4-9.

The boundary conditions concerning the underground pipeline network are obtained from the current drain test as found in Table 4-8. The polarisation curve for the underground pipeline network is made up from the average values found in Table 4-8.

5.2.3 Implementation of system requirements

The required current and voltage output of the TRU must be defined within the BEASY™ CP Wizard along with the connections between the anode ground beds and the tanks. This section will be used to discuss the interaction between the different components within the CP circuit. The BEASY™ CP Wizard allows for the definition of the resistance of the cables interconnecting the anodes and tanks and is therefore implemented within the simulation.

The CP system layout with respect to the anodes, tanks (cathodes), and the TRU within the CP "circuit" is displayed in Figure 5-17. Also included within the CP circuit is the resistance of the cables that is used to interconnect the different components within the CP system. The resistance of the cables interconnecting the different components can affect the performance of the system and are therefore included for the purpose of thoroughness.

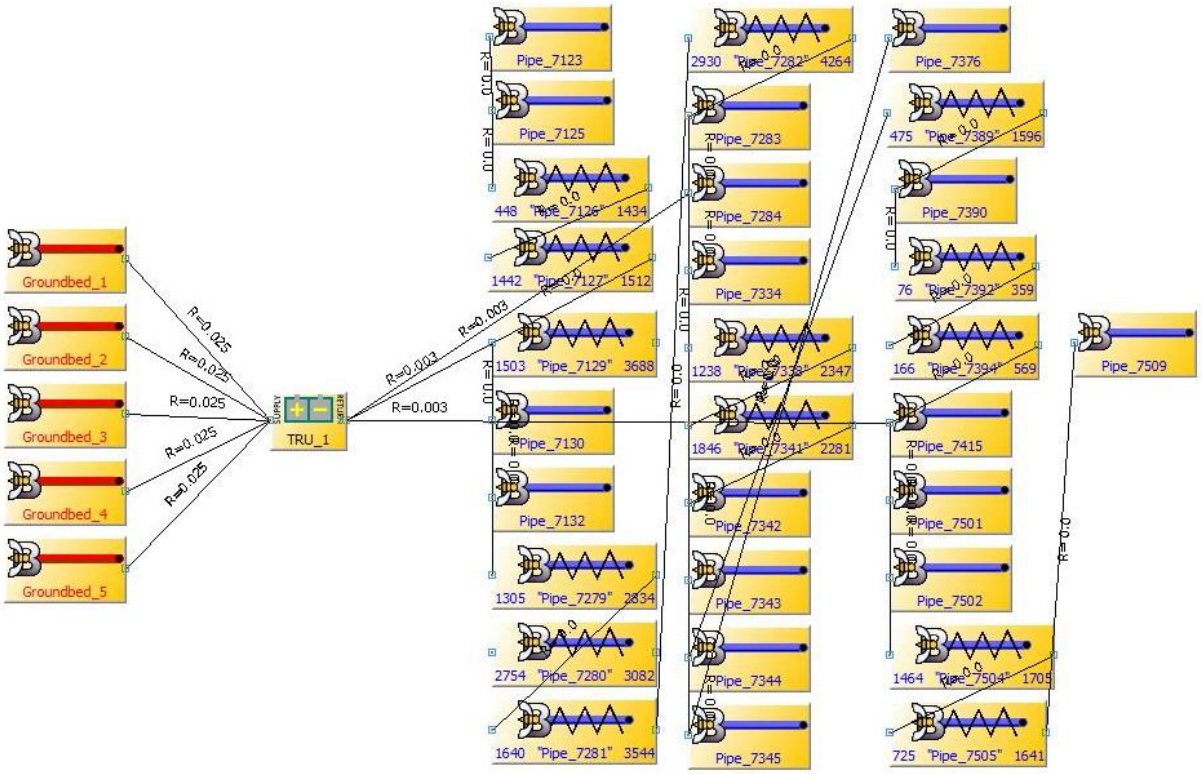

Figure 5-17: CP circuit layout of CP system for underground pipeline network

The following important parameters to be declared within the BEASY™ CP Wizard are that of the output current and voltage of the TRU respectively. The wizard that is used as solver allows for the definition of the TRU either in terms of the target output voltage or the target output current. In this case the target output voltage of the TRU is defined and limiting the output current of the TRU by defining the maximum output current of the TRU. The definition of the output voltage and current of the TRU are displayed in Figure 5-18.

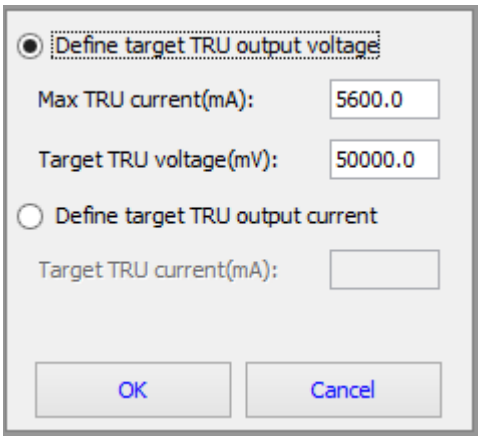

Figure 5-18: Defining voltage and current output of TRU of underground pipeline network

The definition of the soil resistivity for simulation purposes is based on the measured soil resistivity presented in Table 4-9. A multi-layered electrolyte definition was used to simulate the soil resistivity at the varying depths. This is very important to keep in mind when analysing the simulated results as the soil resistivity is kept uniform throughout these various layers depending on the assigned values for the varying depths.

5.2.4 Simulated results

It is important to note that two sets of simulated results are generated for the underground pipeline network. The first set of simulated results to be generated is based on the initial parameters of the pipeline, i.e. the parameters of the pipeline at the start of its service life. This set of simulated results is used for verifying the design of the CP system in terms of the relevant CP criteria. In the preceding paragraphs, this set of results is referred to as the new underground pipeline installation.

At the time of the actual potential measurements taken for validation purposes, the underground pipeline had been in service for approximately 15 years. The actual potential measurements are compared to the simulated results generated in this section and the detailed discussion follows in Chapter 6. For reference, the underground pipeline that has been in service for 15 years will hereafter be referred to as the aging underground pipeline network installation.

The simulated results obtained from using the BEASY™ CP Wizard are discussed in this section. The first result to be discussed is that of the level of polarisation experienced by the metal surfaces that form part of the underground pipeline network. The simulated potential distribution on the collective surface area of the pipelines is displayed in Figure 5-19.

The results presented in Figure 5-20 are seen to satisfy the CP criteria as the potential on the entire structure is below -0.850 V, indicated by the dashed green line. These results were obtained through the use of the CP system design framework formulated in Chapter 4. At this point in time it appears that the design framework satisfies the addresses the problem statement and provides a proven solution. The next set of results to be discussed will be used for the validation of the CP system design framework.

The graphical representation of the simulated polarised potentials on the new underground pipeline network are presented in the form of a line graph in Figure 5-20. This graphical representation of the ON-potentials is made up of the ON-potentials measured at the locations where the test points are installed in reality for test purposes. The graphical representation of the mentioned data is made up out of the data contained in
Table 5-1. These simulation results are essential to the validation of the CP system design framework and will be discussed in greater detail in Chapter 6.

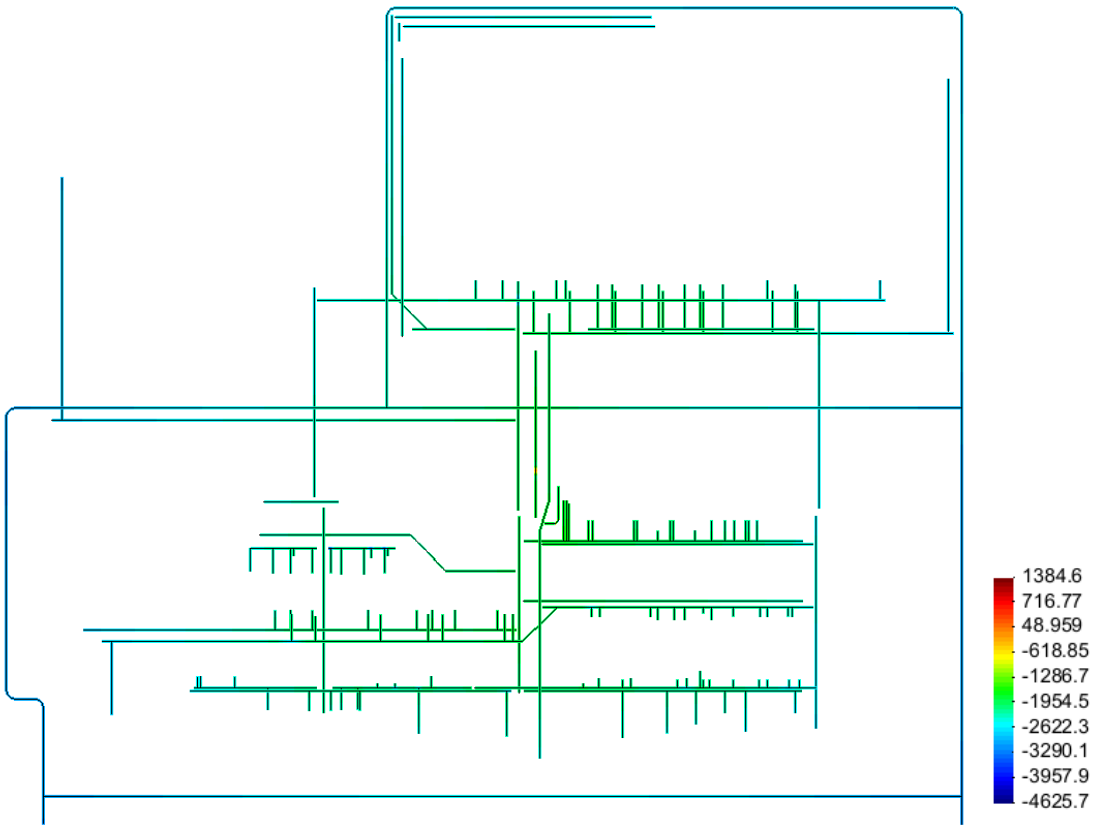

Figure 5-19: Potential distribution on new underground pipeline network installation

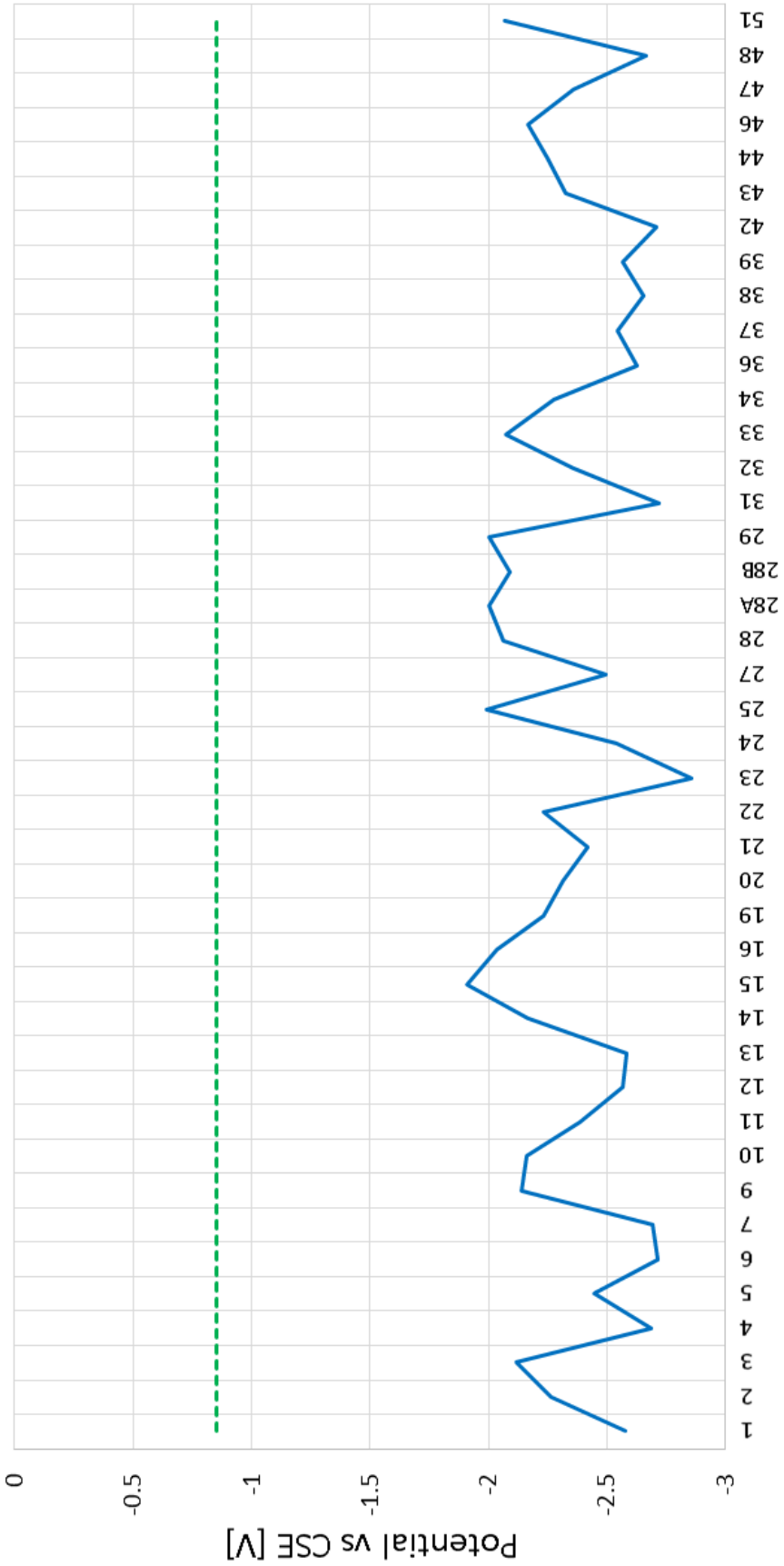

Figure 5-20: Graphical representation of simulated polarised potentials of new underground pipeline network

Table 5-1: Simulated polarised potentials on new underground pipeline network installation

Test point No.	Pipe connected to:	On-Potential [V]	Pipe connected to:	On-Potential [V]
1	7132	-2.575	7344	-2.543
2	7130	-2.263	7344	-2.235
3	7284	-2.119	7344	-2.148
4	7284	-2.689	7345	-2.225
5	7284	-2.444	7345	-2.458
6	7282	-2.716		
7	7342	-2.692	7283	-2.702
9	7283	-2.141	7342	-2.083
10	7343	-2.163		-2.157
11	7343	-2.385	7383	-2.389
12	7282	-2.567		
13	7281	-2.584	7340	-2.472
14	7340	-2.167	7281	-2.214
15	7340	-1.909	7281	-1.950
16	7281	-2.037	7341	-2.175
19	7129	-2.233		
20	7341	-2.314	7123	-2.314
21	7126	-2.418		
22	7505	-2.230		
23	7415	-2.855		
24	7415	-2.541		
25	7415	-1.991	7389	-1.986
27	7501	-2.495		
28	7501	-2.063	7283	-2.005
28A	7396	-2.003		
28B	7281	-2.090	7342	-1.974
29	7504	-2.001		
31	7334	-2.718	7338	-2.715
32	7334	-2.360	7376	-2.099
33	7334	-2.076	7376	-2.359
34	7390	-2.276		
36	7126	-2.626		
37	7394	-2.547		
38	7509	-2.653	7392	-2.784
39	7125	-2.569	7392	-2.565
42	7338	-2.709		
43	7415	-2.327		
44	7280	-2.250		
46	7125	-2.167	7394	-2.172
47	7125	-2.360		
48	7125	-2.664		
51	7334	-2.068	7504	-2.143

The second result to be discussed is that of the level of polarisation experienced by the metal surfaces that form part of the underground pipeline network after 15 years of service life. The simulated potential distribution on the collective surface area of the pipelines are displayed in Figure 5-21.

The graphical representation of the simulated polarised potentials on the aging underground pipeline network are presented as a line graph in Figure 5-22. This graphical representation of the ON-potentials is made up of the ON-potentials measured at the locations where the test points are installed in reality for test purposes. The graphical representation of the mentioned data is made up out of the data contained in Table 5-2. These simulation results are essential to the validation of the CP system design framework and will be discussed in greater detail in Chapter 6.

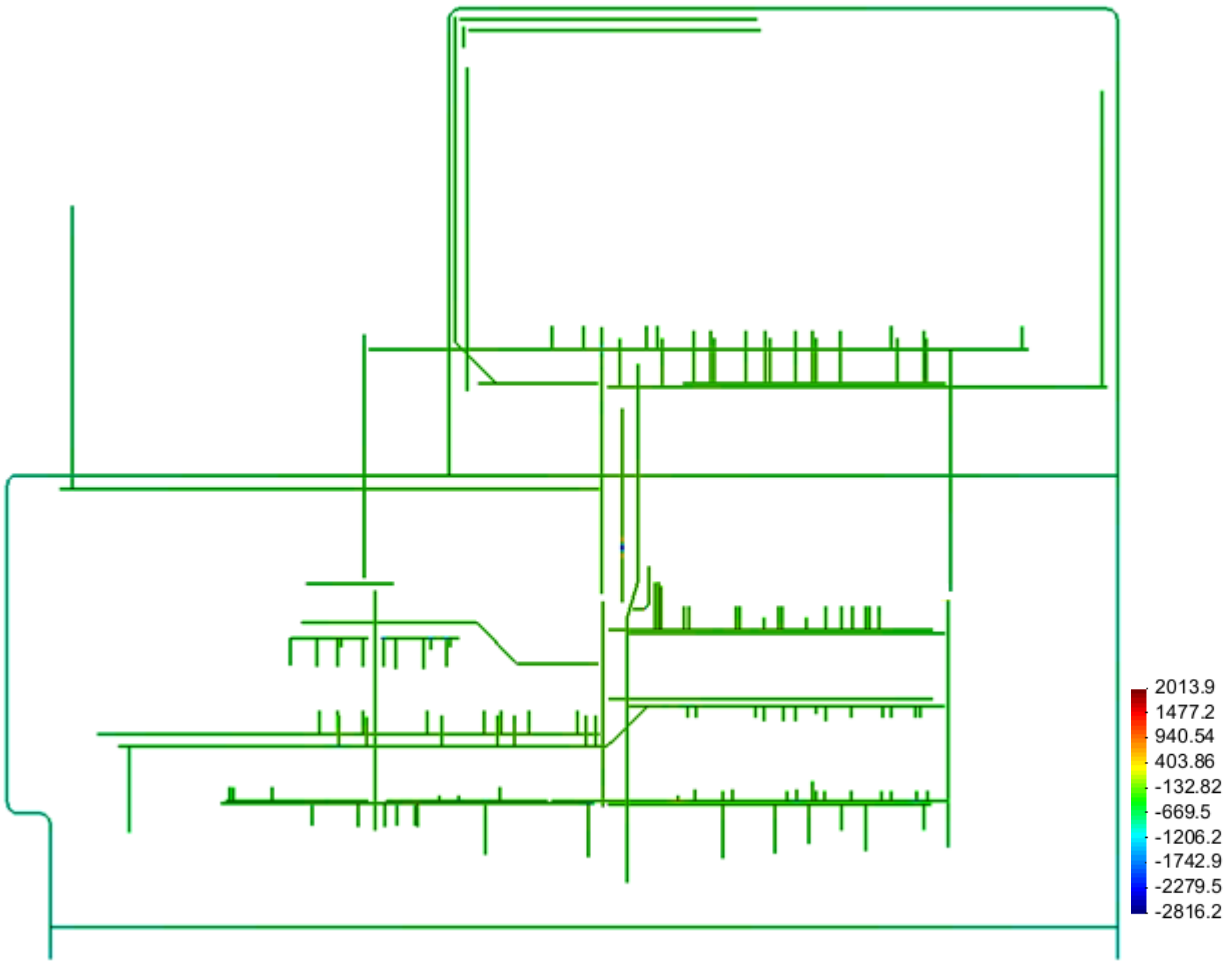

Figure 5-21: Potential distribution on aging underground pipeline network installation

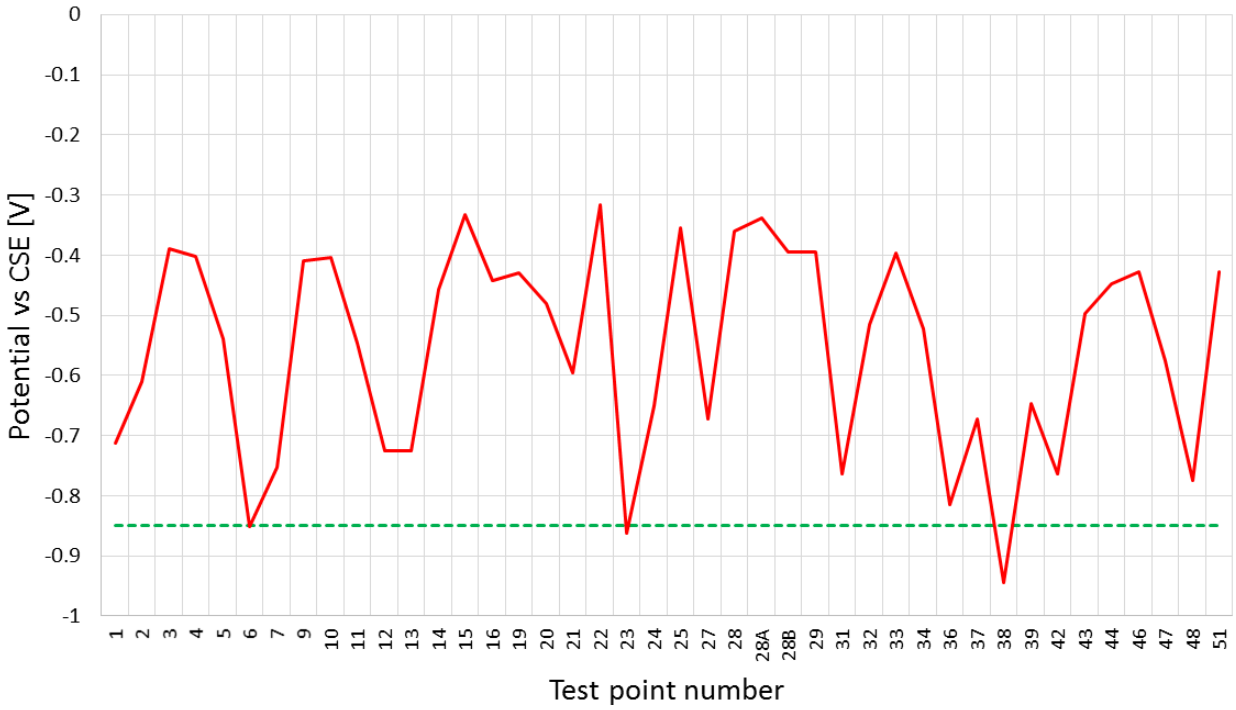

Figure 5-22: Graphical representation of simulated polarised potentials of aging underground pipeline network

The results presented in Figure 5-22 are seen to not satisfy the CP criteria as the potential on most parts of the structure is above -0.850 mV, indicated by the dashed green line. These results were obtained through the use of the CP system design framework formulated in Chapter 4 and incorporating the coating breakdown factor on the polarisation curve of the underground pipeline network. The accuracy of the CP system design framework will be evaluated against the actual potential measurements taken from the available test points on the underground pipeline network. It is important to note that the coating breakdown factor incorporated into the simulation results were taken for a period of 15 years. This time frame was taken as the underground pipeline network was in service for 15 years at the time of the actual measurements.

Table 5-2: Simulated polarised potentials on aging underground pipeline network installation

Test point No.	Pipe connected to:	On-Potential [V]	Pipe connected to:	On-Potential [V]
1	7132	-0.712	7344	-0.611
2	7130	-0.640	7344	-0.444
3	7284	-0.320	7344	-0.390
4	7284	-0.402	7345	-0.385
5	7284	-0.522	7345	-0.539
6	7282	-0.852		
7	7342	-0.750	7283	-0.752
9	7283	-0.409	7342	-0.364
10	7343	-0.403		-0.401
11	7343	-0.546	7383	-0.547
12	7282	-0.725		
13	7281	-0.726	7340	-0.625
14	7340	-0.409	7281	-0.457
15	7340	-0.302	7281	-0.332
16	7281	-0.362	7341	-0.442
19	7129	-0.430		
20	7341	-0.480	7123	-0.468
21	7126	-0.595		
22	7505	-0.316		
23	7415	-0.862		
24	7415	-0.651		
25	7415	-0.355	7389	-0.324
27	7501	-0.672		
28	7501	-0.360	7283	-0.319
28A	7396	-0.338		
28B	7281	-0.396	7342	-0.394
29	7504	-0.395		
31	7334	-0.759	7338	-0.763
32	7334	-0.488	7376	-0.516
33	7334	-0.376	7376	-0397
34	7390	-0.523		
36	7126	-0.814		
37	7394	-0.673		
38	7509	-0.725	7392	-0.944
39	7125	-0.646	7392	-0.635
42	7338	-0.763		
43	7415	-0.497		
44	7280	-0.447		
46	7125	-0.428	7394	-0.432
47	7125	-0.576		
48	7125	-0.775		
51	7334	-0.358	7504	-0.428

Chapter 5 verified the CP system design framework, developed in Chapter 4, with the aid of simulation results. The simulation results served as verification for the design framework and will be supported with measured results obtained from the actual underground pipeline network in the Chapter 6. The CP system design framework have successfully been verified as both the CP system designs discussed in Chapter 5 have met the relevant CP criteria. The validation of the CP system design framework comprise the comparison of the simulated results generated in Chapter 5 to the actual potential measurements obtained from the available test points on the underground pipeline network after being in service for 15 years.

6

CHAPTER

DESIGN FRAMEWORK VALIDATION

This chapter addresses the validation of the CP system design framework as proposed in this dissertation. The results obtained from the simulations performed during the verification of the design framework are compared to practical results obtained from the actual underground pipeline network. The results were taken from all the available test points installed on the underground pipeline network and compared to the relevant areas of interest obtained from the simulations.

6.1 Background

During the construction of the underground pipeline network, various test points have been installed on the pipeline at strategic locations. Reference electrodes (RE) have also been installed in close proximity to the connections between the underground pipeline and the respective test points. The test points are used to measure the potential of the underground pipeline with respect to the RE. These values are then used in conjunction with the relevant CP criteria to assess the performance of the CP system. The values of interest for the validation of the CP system design framework include the on-potentials with CP applied, the instant off-potentials, and the grounding resistance of the respective anode ground beds.

6.2 Measured results

The on-potential measurements with CP applied were taken at all available test points. In many locations the test points are connected to two of the respective pipelines under CP. The on-potentials at the available test points were measured using a digital multi-meter and the measurements were documented. The on-potentials of the underground pipeline as measured at the available test points including the connections to the respective underground pipelines are presented in Table 6-1. The graphical representation of the measured results presented in Table 6-1 is displayed in Figure 6-1.

Table 6-1: Measured ON-potentials at available test points on underground pipeline network

Test point No.	Pipe connected to:	On-Potential	Pipe connected to:	On-Potential
1	7132	-0.903	7344	-0.903
2	7130	-0.631	7344	-0.631
3	7284	-0.074	7344	-0.074
4	7284	-0.608	7345	-0.608
5	7284	-0.658	7345.	-0.658
6	7282	-0.719		
7	7342	-1.288	7283	-1.288
9	7283	-0.944	7242	-0.944
10	7343	-0.594		-0.594
11	7343	-0.741	7383	-0.743
12	7282	-0.981		
13	7281	-1.055	7340	-1.051
14	7340	-0.589	7281	-0.587
15	7340	-0.679	7281	-0.679
16	7281	-0.287	7341	-0.129
19	7129	-0.701		
20	7341	-0.851	7123	-0.851
21	7126	-0.421		
22	7505	-0.348		
23	7415	-1.747		
24	7415	-1.317		
25	7415	-0.283	7389	-0.283
27	7501	-0.601		
28	7501	-0.1	7283	-0.1
28A	7396	-0.148		
28B	7281	-0.55	7342	-0.55
29	7504	-0.199		
31	7334	-1.737	7338	-1.737
32	7334	-1.234	7376	-1.237
33	7334	-0.852	7376	-0.854
34	7390	-0.871		
36	7126	-0.96		
37	7394	-0.878		
38	7509	-0.88	7392	-0.88
39	7125	-0.678	7392	-0.678
42	7338	-1.126		
43	7415	-1.217		
44	7280	-0.841		
46	7125	-1.101	7394	-0.829
47	7125	-0.979		
48	7125	-0.917		
51	7334	-0.847	7504	-0.845
52	7503	-0.618		

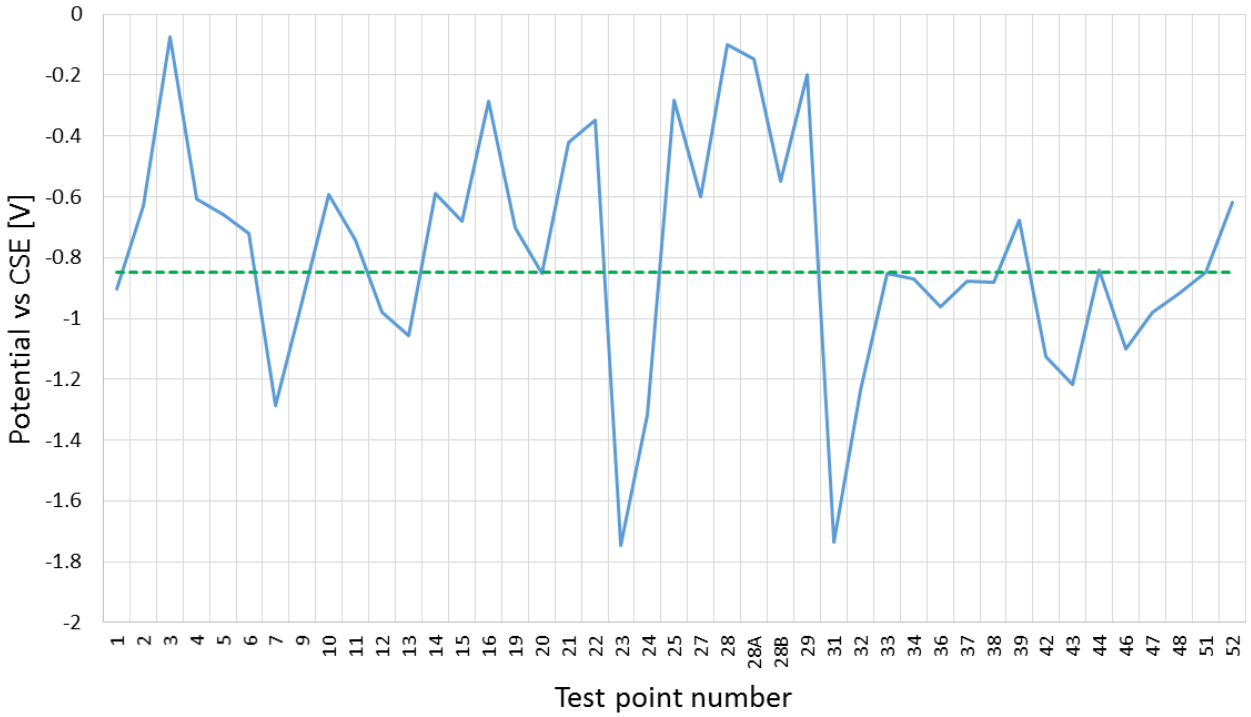

Figure 6-1: Graphical representation of measured ON-potentials at available test points

It is important to note that the CP system connected to the underground pipeline network has been in service for approximately 15 years at the time of the measurements. It can be seen from the measured results presented in Table 6-1 that the system does not provide sufficient protection to the entire underground pipeline network. The level of protection provided by the CP system is influenced by various parameters with the most notable being coating breakdown and anode consumption.

The level of polarisation experienced by the underground pipeline network due to the application of CP can be determined by measuring the ON-potential of the structure followed by the instant OFF-potential. The instant OFF-potential is measured at the moment the TRU is switched off. The measured ON- and instant OFF-potentials of the underground pipeline network at selected test points are presented in Table 6-2. The polarisation results presented in Table 6-2 are essential in ensuring that the underground pipeline network experiences cathodic protection.

The polarisation results presented in Table 6-2 will also be used in the discussion concerning the comparison between the measured ON-potentials obtained from the underground pipeline network and the simulated results of the underground pipeline network. This discussion is deemed paramount to the validation of the CP system design framework.

Table 6-2: Measured ON- and instant OFF-potentials on underground pipeline network

Test point No.	ON-Potential	Instant OFF-Potential
1	-0.917	-0.829
3	-0.086	-0.064
6	-0.728	-0.655
12	-0.984	-0.79
16	-0.144	-0.122
20	-0.873	-0.796
32	-1.21	-0.77
33	-0.875	-0.749
34	-0.887	-0.799

The potential measurements that are presented in Table 6-2 are important for validating the CP system design framework. The instant OFF-potential, often referred to as the polarised potential, is used to eliminate any voltage drops that may be present in measurements taken while the CP system is on. The simulated results are free of any voltage drops and are referred to as polarised potentials. The measurements used for validation purposes must therefore also be free of any voltage drops. The instant OFF-potentials presented in Table 6-2 are used in the preceding paragraph to determine the accuracy of the simulated results compared to the measured results.

6.3 Comparison of results

This section is dedicated to discuss the comparison between the measured potentials at the available test points installed on the underground pipeline network and the simulated potentials at the corresponding test points. The graphical comparison of the measured ON-potentials and simulated polarised potentials at the available test points on the underground pipeline network is presented in Figure 6-2. The actual measurements are represented by the blue line in Figure 6-2 and the simulated results are presented by the red line in Figure 6-2.

From the graphical comparison of the simulated polarised potentials and the actual measured ON-potentials measured at the available test points on the underground pipeline network it is evident that a certain difference between the results are present. This is a very important observation to be made as this comparison is based on a CP system in service for close to 15 years. The simulated polarised potentials are based on all the information gathered from the site survey presented in the CP system design framework and allowing for coating breakdown over a service life of 15 years.

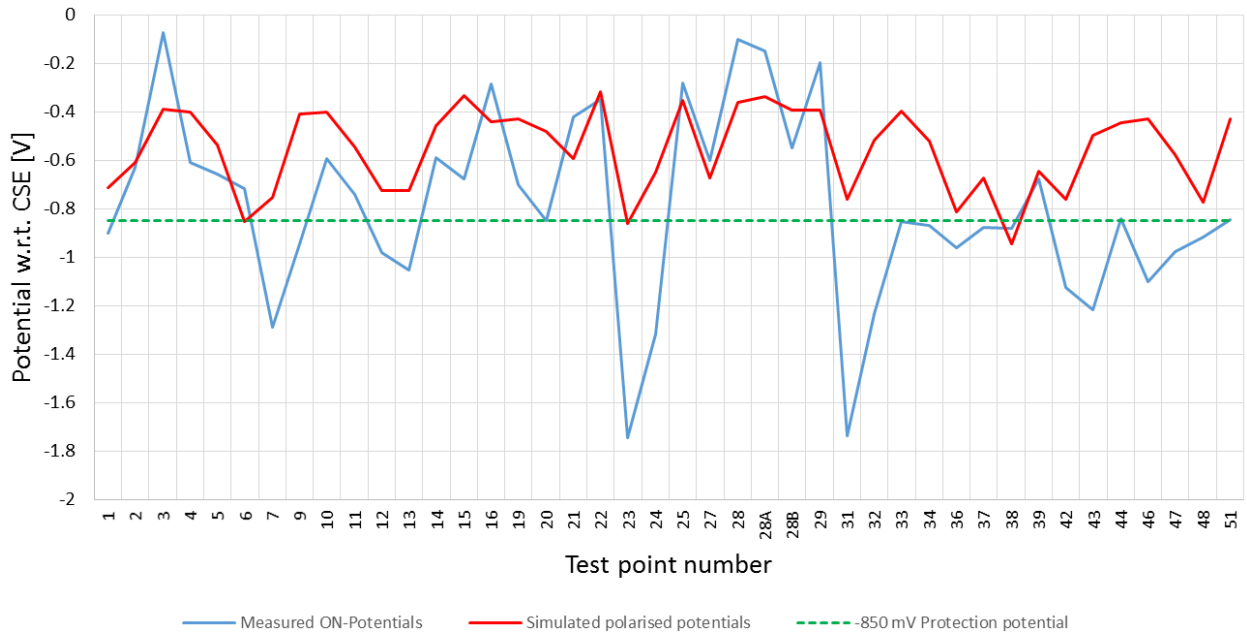

Figure 6-2: Comparison of measured and simulated potentials at available test points

From the comparison between the measured ON-potentials and the simulated polarised potentials presented in Figure 6-2 it is evident that deviations exist between the two sets of results. It is important to note that the measured ON-potentials are compared to the simulated polarised potentials. A difference in the results is expected due to a measured voltage drop in the ON-potentials. The error between the measured ON-potentials and the simulated polarised potentials is presented in Figure 6-3.

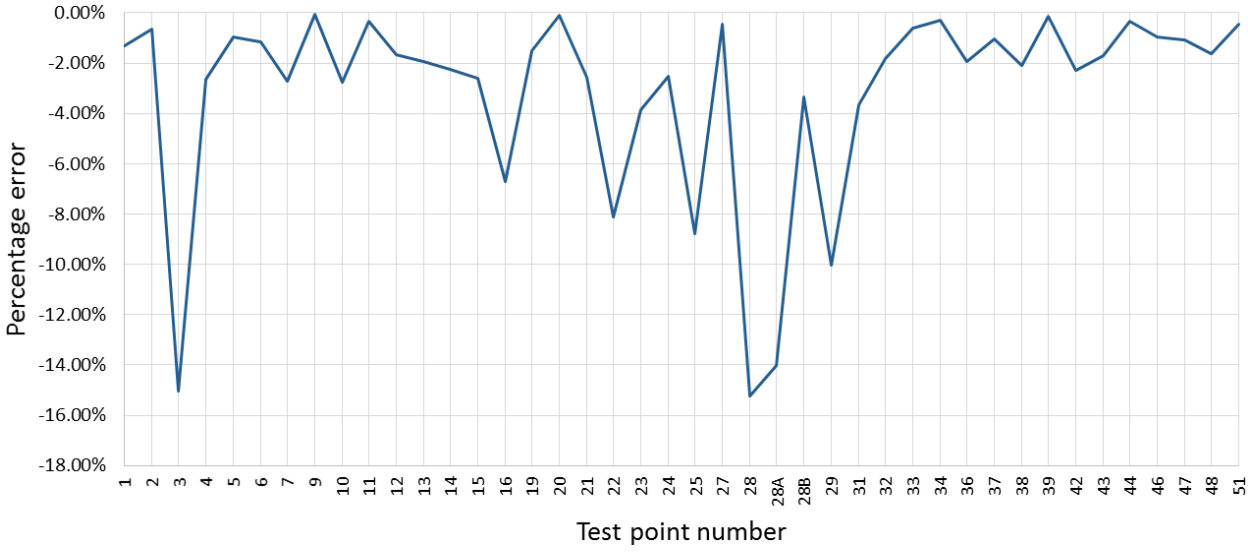

Figure 6-3: Percentage error between measured ON-potentials and simulated polarised potentials

From the graph presented in Figure 6-3 it is evident that a certain error between the measured ON-potentials and the simulated polarised potentials exist. Large deviations between the sets of results are evident at certain test points. It is noted that a possible reason for the large deviations between the two sets of results is that a certain voltage drop was measured in the measured ON-

potentials of the underground pipeline network. The average percentage error between the measured ON-potentials and the simulated polarised potentials was calculated to be -2.95%.

By using the instant OFF-potentials at the test points presented in Table 6-2, the error between the two sets of results can be evaluated more realistically. A graphical comparison between the simulated polarised potentials and the measured instant OFF-potentials are presented for specific test points in Figure 6-4.

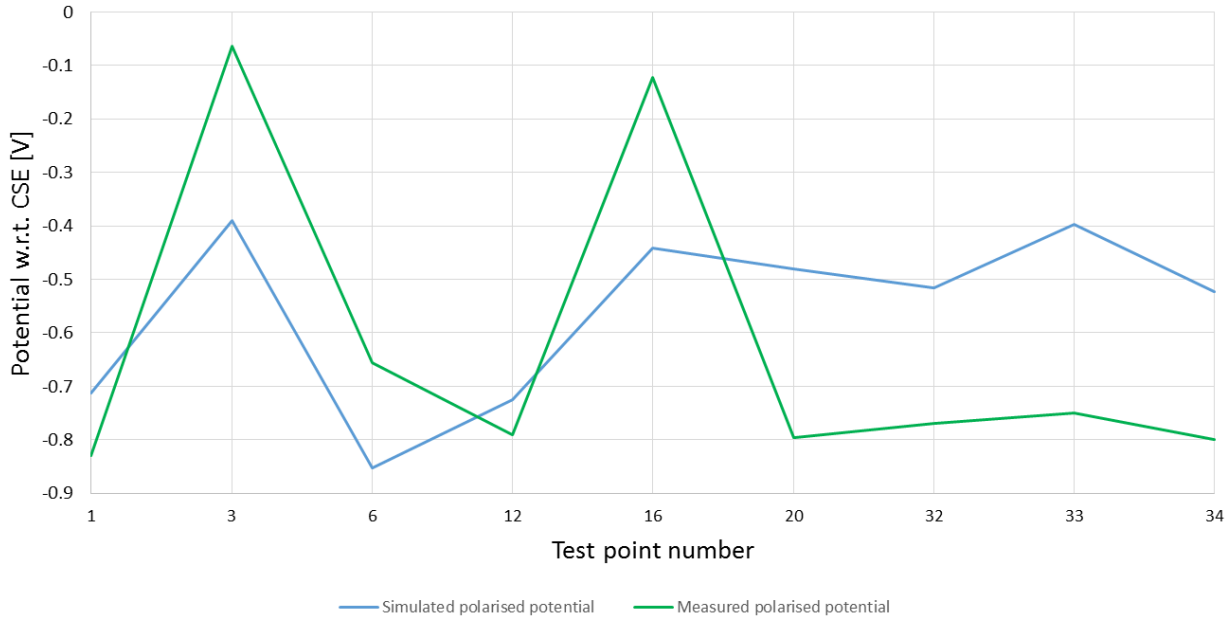

Figure 6-4: Graphical comparison of simulated polarised potential and measured instant OFF-potential

It is evident from the graphical comparison of results presented in Figure 6-4 that a difference between the measured and simulated results is still present. The percentage error between the measured instant OFF-potential and the simulated polarised potentials is presented in Figure 6-5.

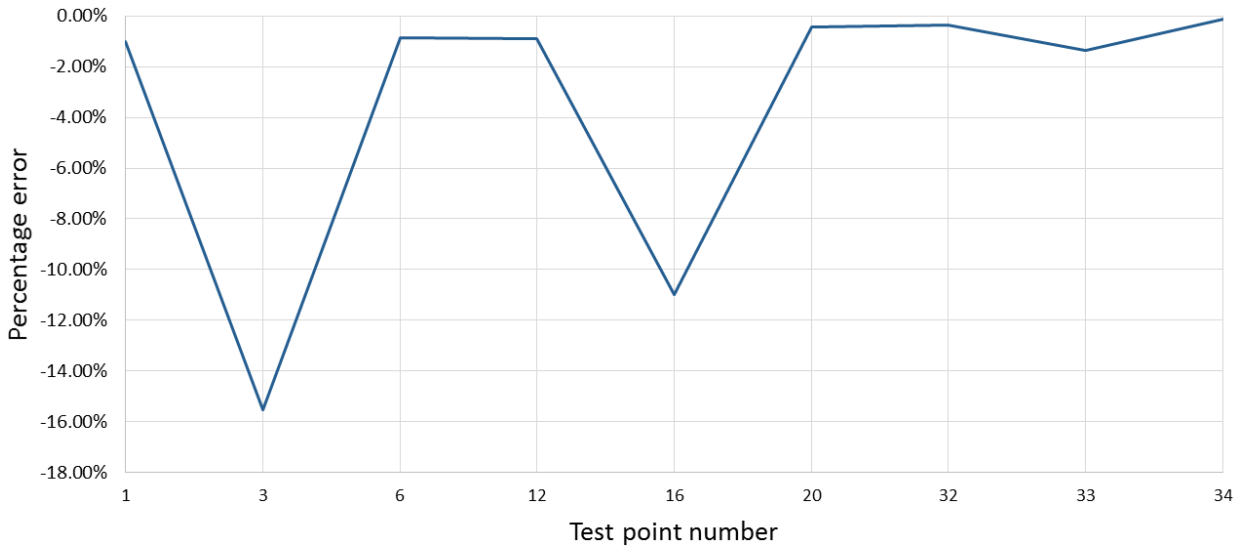

Figure 6-5: Percentage error between measured instant OFF-potentials and simulated polarised potentials

From the graph presented in Figure 6-5 it is evident that a certain error between the measured instant OFF-potentials and the simulated polarised potentials is still present. Large deviations between the sets of results are still evident at test points 3 and 16 respectively. These large deviations are areas of concern as possible voltage drops in the measured potentials have been ruled out. The average percentage error between the measured ON-potentials and the simulated polarised potentials was calculated to be -2.79%. Although voltage drops influenced the accuracy of the measured potentials, the outliers at test points 3 and 16 make it difficult to conclude the reasons for the large error between the results.

The average error has decreased compared to the percentage error results presented in Figure 6-3. The outliers in the results (test points 3, 28, and 28A) however influence the average error between the two sets of results. By removing these results from the statistic calculations, the average error between the results is close to -2%. Reasons for the outliers can be attributed to a couple of circumstances.

The first important observation to be made is that the operating temperatures of the pipelines in the underground pipeline network have not been taken into account in the simulated results. The operating temperatures of the pipelines can have a major impact on the performance of the CP system as it influences the electrical conductivity of the pipeline material. This in turn will influence the current distribution on the surface of the pipeline and directly influence the potential distribution on the pipeline.

Stray currents are known to influence the potential of structures under CP. The absence of cross bonds on certain sections of pipeline will cause these sections to experience high levels of stray current corrosion due to the sections of pipeline being disconnected from the CP source. The current being induced by the anodes of the CP system can cause stray current corrosion on areas of the underground pipeline as sections of the pipeline are no longer connected to the source. As the condition of the cross bonds between the pipelines is unknown, the probability that stray currents are responsible for specific outliers is high.

Due to the fact that the underground pipeline network has experienced insufficient levels of CP for an extended period of time the possibility exists that coating holidays have developed with time. These coating holidays will cause areas on the underground pipeline network that experiences high rates of corrosion due to coating damage and bare metallic areas that are exposed to the surrounding electrolyte. The current density required to prevent corrosion at these areas will increase significantly compared to the rest of the structure. If the output voltage of the CP system is not increased these areas will experience high rates of corrosion and is referred to

as localised corrosion cells. The probability that localised corrosion cells are present at areas on the underground pipeline network cannot be disregarded.

When comparing the actual potential measurements to the simulated potentials it has to be kept in mind that the soil resistivity was kept uniform at the varying depths at which it was defined. The uniform soil resistivity used in the simulations will affect the matching of the results as the actual soil resistivity distribution is not uniform. The comparison of the actual and simulated potentials revealed that the soil resistivity distribution could affect the values of the measured potentials.

The initial CP system design was based on an average soil resistivity value of 45 Ωm. The average value used in the empirical design of the CP system does not give a true reflection of the soil resistivity distribution but is used to simplify the empirical calculations. It is evident from the results that varying soil resistivity contributes to the deviation between the measured and simulated potentials.

The comparison of the different results as found in Figure 6-2 suggests that the CP system design framework can successfully be implemented for CP system design. The design framework was also successfully used to evaluate the CP system after 15 years of its service life and the average accuracy of the generated results was within 3% of the actual measured potentials. For this reason the CP system design framework developed throughout this dissertation is successfully validated through comparison of the results as found in Figure 6-2.

Chapter 6 validated the CP system design framework, developed in Chapter 4, with the aid of simulation results. The comparison between the simulated and measured potentials revealed that the CP system design framework can be successfully implemented and even used to evaluate the performance of CP systems at certain service life intervals. The largest deviations between the measured and simulated potentials can be attributed to various factors and were explained in detail. The possibilities suggest that future work is required to determine the exact cause of these deviations but for the purpose of validating the CP system design framework the results are satisfactory.

7

CHAPTER

CONCLUSIONS AND RECOMMENDATIONS

This chapter is dedicated to concluding the research covered in the dissertation. The chapter will also make certain recommendations regarding the use of the CP system design framework for designing CP systems for the petrochemical industry. The conclusions and recommendations made in this chapter are of high important for successfully implementing the CP system design framework in the petrochemical industry.

7.1 Conclusions

The design framework developed throughout this dissertation can be successfully utilised for designing a wide variety of CP systems for the petrochemical industry. The design framework was verified with the aid of a simulation software package that simulated the performance of two respective CP systems. The first CP system was designed to protect five tanks situated in a small tank farm. This CP system was only verified with the use of BEASY™ CP and Corrosion and the results confirmed that the CP system design framework contains some shortcomings.

The shortcomings of the CP system design framework identified from the simulated results obtained for the tanks in the small tank farm confirmed that the electrical field strength surrounding structures protected by a CP system is paramount to the efficiency of the system. This conclusion is based on the fact that the initial depth of the anodes installed for the protection of the tanks had to be altered in order to provide a more uniform current distribution on the surface of the tanks. The calculation of the electric field strength surrounding a given structure cannot be calculated with the use of the CP system design framework and can only be determined with the aid of the simulation software package.

An underground pipeline network was also used to verify and validate the CP system design framework. The CP system utilised for the protection of the underground pipeline network was also designed with the aid of the CP system design framework established throughout this dissertation. In the first instance the CP system design for the underground pipeline network was based on the conditions that the underground pipeline network is entirely new. From the resulting

simulation results the level of protection provided by the CP system proved to be sufficient and served as further proof that the design framework is adequate for designing new CP systems.

The actual measured results available for the validation of the CP system design framework comprised the potential measurements of the underground pipeline network. The underground pipeline network had been in service for 15 years at the time these potential measurements were taken. This necessitated another set of simulation results to be generated for the underground pipeline network which represented the 15 year old underground pipeline network. The simulated results for the underground pipeline network after 15 years in service were compared to the actual measurements taken from the available test points on the underground pipeline network.

In order to generate the simulated results of the underground pipeline network after a service life of 15 years, it was necessary to take into account the coating breakdown factor of the underground pipeline network. The CP system design framework initially didn't allow for the coating breakdown factor to be included in the calculations of current requirements as it only focused on new installations. From the results obtained it became evident that the inclusion of the coating breakdown factor in the CP system design framework is very important for ensuring that a given CP system provides adequate protection through the entire expected service life of a structure. Therefore the coating breakdown factor was included in the CP system design framework for verifying whether a CP system will protect a given structure for the entire expected service life of the structure.

Validation of the CP system design framework revealed that a wide array of factors can have an influence on the performance of a CP system. Factors such as stray currents, non-uniform soil resistivity, electrical continuity of the structure, coating holidays, and faulty reference electrodes can all compromise the integrity of the CP system. The CP system design framework does not allow for all these factors to be taken into account during the initial design of a given CP system. It is almost impossible to incorporate all of the abovementioned factors into the CP system design framework as it will complicate the calculations in such a way that it will be impossible to use the CP system design framework in general. This statement is supported by the fact that each CP system is dependent on its surrounding environment and the characteristics of each underground structure are unique under operating conditions.

Although the CP system design framework can be successfully utilised to design CP systems for various underground structures up to the end of its service life, the monitoring of the system and structure after the installation of the CP system is of utmost importance.

7.2 Recommendations

The design framework was successfully implemented for the empirical design of CP systems for the protection of tanks situated in a small tank farm as well as an underground pipeline network. The verification of the CP system design framework indicated that the design framework has certain limitations in terms of determining the electrical field strength on the entire surface of the structure to be protected. This limitation was identified using the simulation software package which indicated that the depth at which the anodes were initially installed at for the protection of the tanks in the small tank farm did not provide a uniform current distribution on the tank surfaces. By adjusting the depth of the anodes, the current distribution on the tank surfaces have improved and the tank surfaces were sufficiently polarised to satisfy the CP criteria.

It is recommended that future work is performed on determining the influence that the use of an average soil resistivity value during the empirical design of a CP system has on the overall performance of the system. This recommendation is based on the fact that every CP system requires that some adjustments are made to the voltage and current outputs of the TRU. Other factors contributing to the required adjustments must also be identified and the effects of these factors must be incorporated in the CP system design framework presented in this dissertation.

Future work that is also recommended on the CP system design framework include finding the relationship between the electric field strength on the protected surface and the location of the anodes with respect to the structure. The current emitted by the different anodes installed in a single anode ground bed should also be investigated in cases where the soil resistivity is not uniform. During the empirical design of both the CP systems discussed in this dissertation the assumption was made that the soil resistivity is uniform. Investigations into how this assumption influences the results obtained from the empirical design, especially the resistance-to-earth of the anode ground beds are also recommended.

7.3 Closure

The CP system design framework developed for designing CP systems for the petrochemical industry was based on a proper understanding of the operating principles of CP systems. The literature covered in this dissertation was used as foundation for the development of the CP system design framework. The literature background was successfully implemented to evaluate the CP system design framework through verification and validation processes.

The CP system design framework was successfully validated which is proof that the framework can be utilised for designing CP systems for tank farms, underground pipelines, and plant areas.

The problem statement has been addressed successfully by the CP system design framework which can be successfully implemented to design CP systems for the petrochemical industry in South Africa.

REFERENCES

[1] J. E. Ramirez and C. D. Taylor, “Preventing Corrosion Failures,” *Advanced Materials & Processes,* vol. 172, no. 8, pp. 15-17, 2014.

[2] L. T. Popoola, A. S. Grema, G. K. Latinwo, B. Gutti and A. S. Balogun, “Corrosion problems during oil and gas production and its mitigation,” *International Journal of Industrial Chemistry,* vol. 35, no. 4, 2013.

[3] K. R. Larsen, “Wanted: Corrosion Professionals,” *Materials Performance,* vol. 46, no. 12, pp. 26-29, 2007.

[4] J. R. Davis, Corrosion: Understanding the basics, 1 ed., vol. 1, ASM International, 2000.

[5] H. D. Holler, “The electrical nature of corrosion and cathodic protection,” *Electrical Engineering,* vol. 71, no. 4, pp. 367-373, 1952.

[6] R. Nave, “Corrosion as an Electrochemical Process,” [Online]. Available: http://hyperphysics.phy-astr.gsu.edu/hbase/chemical/corrosion.html. [Accessed May 2014].

[7] W. von Baeckmann, W. Schwenk and W. Prinz, Handbook of Cathodic Corrosion Protection, 3rd ed., Gulf Professional Publishing, 1997.

[8] A. W. Peabody, Peabody's control of pipeline corrosion, 2nd ed., NACE International, 2001.

[9] P. E. Francis, “Cathodic Protection in Practise,” [Online]. Available: http://www.npl.co.uk/upload/pdf/cathodic protection in practise. [Accessed March 2014].

[10] R. E. Colson and N. J. Moriber, “Corrosion Control,” *Civil Engineering,* vol. 67, no. 3, pp. 58-59, 1997.

[11] W. F. Smith and J. Hashemi, Foundations of Materials Science and Engineering, 4th ed., McGraw-Hill, 2006.

[12] F. E. Kulman, “Corrosion Control of Underground Power Cables in New York,” *Transactions of the American Institute of Electrical Engineers, Power apparatus and systems, Part III,* vol. 73, no. 1, pp. 745-760, 1954.

[13] J. C. Kotz, P. M. Treichel and J. R. Townsend, Chemistry and chemical reactivity, 7th ed., Thomson Brookes/Cole, 2006.

[14] M. O. Durham and R. A. Durham, “Consequences and standards from using CP systems to prevent corrosion,” *IEEE Industry Applications Magazine,* vol. 11, no. 1, pp. 41-47, 2005.

[15] L. B. Hobgen, K. A. Spencer and P. W. Heselgrave, “Cathodic Protection,” *Proceedings of the IEE - Part A: Power Engineering,* vol. 11, no. 1, pp. 307-315, 1957.

[16] D. A. Jones, Principles and prevention of corrosion, 2nd ed., Prentice-Hall, 1996.

[17] R. A. Corbett, “Cathodic protection as an equivalent circuit,” *IEEE Transactions on industry applications,* Vols. IA-21, no. 6, pp. 1533-1537, 1985.

[18] P. R. Roberge, Corrosion Engineering, 1st ed., McGraw-Hill, 2008.

[19] M. Mohitpour, H. Golshan and A. Murray, Pipeline design and construction: A practical approach, 3rd ed., ASME Press, 2007.

[20] AUCSC, “Appalachian Underground Corrosion Short Course: Advanced course notes,” [Online]. Available: https://aucsc.com/. [Accessed June 2014].

[21] C. Lee, R. Jacob, P. Morgan and R. Weatherhead, “International Experiences with Cathodic Protection of Offshore Pipelines and Flowlines, TWI Report 17562/1/07,” 2007.

[22] Corrosionpedia, “Corrosionpedia,” [Online]. Available: http://www.corrosionpedia.com. [Accessed July 2014].

[23] H. D. Dwight, “Calculation of resistances to ground,” *Transactions of the American Institute of Electrical Engineers,* pp. 1319-1328, 1937.

[24] F. Müller Filho, L. Pereira Da Silva, A. Baria and A. Miocque, “Cathodic Protection: Conventional shallow groundbed vs deep groundbed anodes,” *Materials Performance,* vol. 39, no. 10, pp. 22-25, 2000.

[25] R. P. Nagar, “Remoteness of impressed current anode groundbeds,” *Corrosion,* vol. 67, no. 1, pp. 025001-1-025001-8, 2011.

[26] ISO 15589-1:2003(E), “Petroleum and natural gas industries - Cathodic protection of pipeline transportation systems - Part 1: On-land pipelines,” International Standard, 2003.

[27] Det Norske Veritas, “Recommended Practice DNV-RP-B401 - Cathodic Protection Design,” 2010.

[28] NACE International, “Standard Practice: Control of external corrosion on underground or submerged metallic piping systems,” NACE International, 2007.

[29] L. A. Bash, “Robert J. Kuhn's -0.85 V, CSE, cathodic protection criterion for buried coated steel pipelines is scientifically sound,” in *Corrosion*, 2006.

[30] R. M. Park, “A guide to understanding reference electrode readings,” *Materials Performance,* vol. 48, no. 9, pp. 32-36, 2009.

[31] Pipeline Maintenance Limited, “Mixed Metal Anodes Data Sheet MMAN01 Rev 01”.

[32] R. A. Corbett, “Cathodic protection of a nuclear fuel facility,” *Materials Performance,* vol. 28, no. 6, pp. 24-27, 1989.

[33] German Cathodic Protection, The experts with worldwide experiance in cathodic corrosion protection, Essen: German Cathodic protection, 2013.

[34] M. E. Parker and E. G. Peattie, Pipe Line Corrosion and Cathodic Protection, 3 ed., vol. 1, Gulf Publising Company, 1988.

[35] O. Bekker, “Cathodic Protection from a hazardous viewpoint,” [Online]. Available: http://www.flp.co.za. [Accessed May 2014].

[36] F. L. LaQue, “What can management expect from a corrosion engineer?,” *Materials Pefromance,* vol. 25, no. 9, pp. 82-84, 1985.

[37] R. Cleveland Corp, “What is cathodic protection?,” [Online]. Available: http://www.rcleveland.net/services/cathodic-protection. [Accessed April 2014].

[38] R. N. Tuttle, “Corrosion in oil and gas production,” *Journal of Petroleum Technology,* vol. 39, pp. 756-762, 1987.

A

ANNEXURE

SOIL RESISTIVITY

This annexure is used to provide supplementing information on soil resistivity along with information on the measurement techniques used to measure soil resistivity. Soil characteristics and the relation between soil corrosiveness and soil resistivity are also presented in this annexure.

A.1 Specific soil resistivity measurement

Different procedures can be used to determine the specific soil resistivity of an area. Under aerobic conditions, the resistance of the electrolyte determines the rate of the corrosion of the structure. Thus, it is an important parameter regarding the size of the anode ground bed to be installed, along with the output voltage of the DC source to be used. As not all of the procedures are known to deliver the same results, the procedure regarded as the most accurate is the Wenner 4-pin method.

A.1.1 Soil box method

Although this method of soil resistivity testing is not as accurate for soil as it is for fluid, it can give an idea of the value of the soil resistivity in a specific area. The difference in resistance value of the sample and that of the resistivity at the actual site is due to variations in natural conditions. The variations in natural conditions include: moisture content of soil, compaction of the soil, as well as the particle size of the soil etc [15]. The soil box method requires the sample of soil to be tested, to be properly compacted and the box should be fully filled with the sample. This is necessary to ensure proper contact to the electrodes within the box and that no bubbles and empty space are present in the sample.

The soil box is constructed from plastic in a rectangular shape with metal end plates. Potential terminals, to permit for voltage drop measurements, are also installed in the box. A normal 4-terminal earth resistance meter is used to measure the specific resistivity of the sample. This method is in accordance with Wenner's 4-electrode method, which is to be discussed later on.

The value of the resistance measured by the earth resistance is multiplied by the form factor of the box in which the sample is placed. The form factor of the box is determined by the dimensions of the box, along with the distance between the potential terminals installed in the box. The value of the form factor is presented in cm and is also indicated on the side of the soil in most cases. The value of the specific soil resistivity of the soil sample is presented in Ω-cm.

A.1.2 Wenner 4-electrode method

This method is also referred to as the 4-electrode method. The method makes use of four electrodes that is placed in the soil of the area of which the soil resistivity is to be measured. The 4-electrodes used in this method comprise two current electrodes, along with two voltage probes. The four electrodes are placed in a straight line at equal distances apart, with the two outer electrodes being the current electrodes, and the inner two electrodes being the voltage electrodes.

The layout of the electrodes and the measuring equipment that is used to conduct a specific soil resistivity measurement using the Wenner method is displayed in Figure A-1. The electrodes used in this measurement are spaced at an equal distance, d, from one another. The voltage source in the layout is adjustable. Modern measuring equipment that comprises an ammeter, voltmeter, as well as a voltage source, is available in the form of 4-electrode earth resistance meters. The mentioned electrodes are connected to these meters by means of electrode cables.

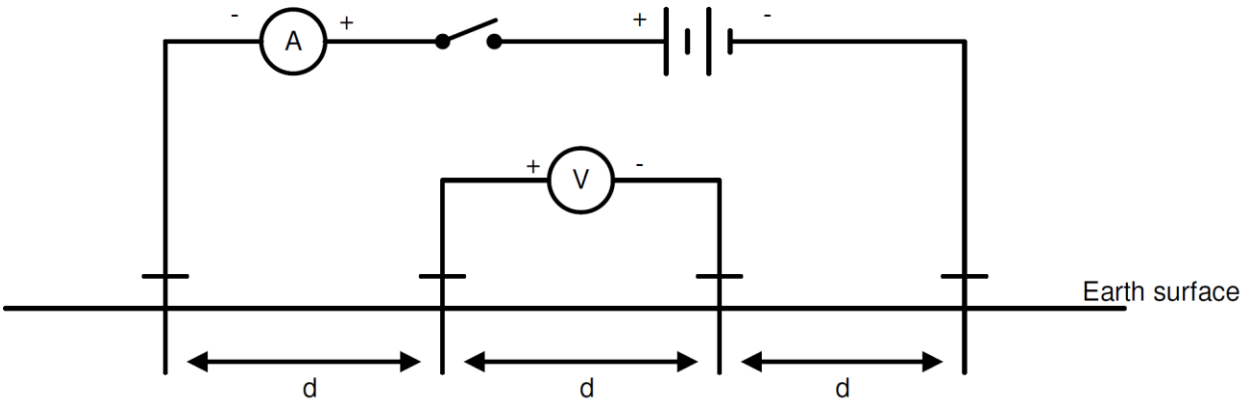

Figure A-1: Layout of electrodes and measuring equipment in Wenner method **[15]**

The specific soil resistivity, ρ, is calculated from the Wenner method using the following equation:

$$\rho = 2\pi d\left(\frac{V}{I}\right) \quad \textbf{(A-1)}$$

where d represents the distance between the electrodes, U the reading on the voltmeter, and I the reading on the ammeter. The approximate depth of the survey is calculated by use of (A-1).

$$d_{depth} = \frac{3d}{2} \tag{A-2}$$

A.1.3 Schlumberger method

The Schlumberger method is almost identical to the Wenner method, the only difference being the distance between the respective electrodes. The spacing between the current and potential electrodes is increased in this method and is no longer equal. The spacing between the current and voltage electrodes are equal, but not equal to the spacing between the potential electrodes, as displayed in Figure A-2.

The equations that are used to calculate the specific soil resistivity and approximate depth of the survey are respectively:

$$\rho = \pi A\left(\frac{U}{I}\right)\left(\frac{B}{A} + \frac{B^2}{A^2}\right) \tag{A-3}$$

$$d_{depth} = \frac{A + 2B}{2} \tag{A-4}$$

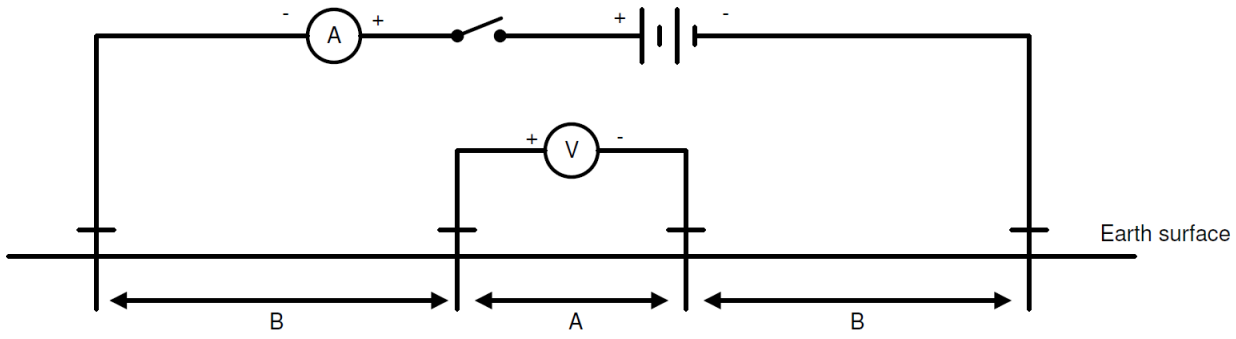

Figure A-2: Layout of electrodes and measuring equipment in Schlumberger method

From the three methods that were discussed, it is believed that the Wenner method delivers the most accurate results. It is therefore the most preferred method to be used whenever specific soil resistivity surveys are conducted.

The corrosiveness of the electrolyte can be coupled to the acidity of the electrolyte in which a structure is to be submerged. The table to follow will contain a list of different electrolyte pH values along with the corrosiveness rating for the respective pH values. The more acidic the nature of

the electrolyte, the more corrosive it would be with respect to steel and copper structures. The results in the table are based on an on–site survey performed at a nuclear fuel facility that required cathodic protection. Although the survey was specifically performed for investigation purposes on a specific location, any site can be investigated in the same manner [32].

Table A-1: Soil characteristics as a factor for corrosiveness to underground steel and copper piping **[32]**

Electrolyte Acidity (pH)	Rating	Corrosiveness
below 4.5	Extremely acid	Extremely
4.5 - 5.0	Very strongly acid	
5.1 - 5.5	Strongly acid	
5.6 - 6.0	Medium acid	Mildly
6.1 - 6.5	Slightly acid	
6.6 - 7.3	Neutral	
7.4 - 7.8	Mildly alkaline	
7.9 - 8.4	Moderately alkaline	
8.5 - 9.0	Strongly alkaline	Non
above 9.1	Very strongly alkaline	

The resistivity of a given electrolyte can also be used as a measure to determine the corrosiveness of the electrolyte. Table A-2 presents the corrosiveness of soil based on the soil resistivity.

Table A-2: Soil corrosiveness based on the resistivity of the electrolyte **[32]**

Soil resistivity [Ω-cm]	Soil corrosiveness
0 to 2000	Very corrosive
2000 to 5000	Corrosive
5000 to 10000	Moderately corrosive
10000 to 25000	Mildly corrosive
25000 to 50000	Relatively less corrosive
above 50000	Progressively non-corrosive

B

ANNEXURE

RESISTANCE-TO-EARTH OF ANODES

This annexure contains two tables used to supplement the calculation of resistance-to-earth of anodes. The tables presented in this annexure can be used as reference to calculate the resistance-to-earth values of various shapes of anodes as well as the voltage cone associated with the different shaped anodes.

Table B-1: Calculation formulas for simple anodes (anode voltage $U_0 = IR$) [7]

Line	Anode shape	Anode arrangement	Grounding resistance	Remarks	Voltage cone
1	Hemisphere, radius r_0, diameter d	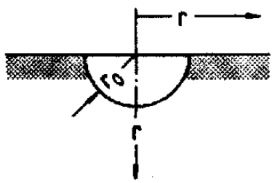	$R = \frac{\rho}{\pi d}$	Spherical field	$U_r = U_0 \frac{r_0}{r} = \frac{I\rho}{2\pi r}$
2	Circular plate, diameter d, radius r_0	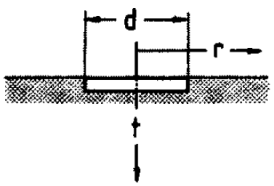	$R = \frac{\rho}{2d}$	Surface Depth	$U_r = \frac{2}{\pi} U_0 \arcsin\left(\frac{r_0}{r}\right)$ $U_t = \frac{2}{\pi} U_0 \arctan\left(\frac{r_0}{t}\right)$
3	Rod anode, length l, diameter d	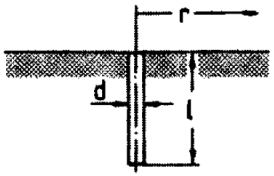	$R = \frac{\rho}{2\pi l} \ln\frac{4l}{d}$	$l \gg d$	$U_r = \frac{I\rho}{2\pi l} \ln\left(\frac{l+\sqrt{l^2+r^2}}{r}\right)$
4	Horizontal anode, length l, diameter d	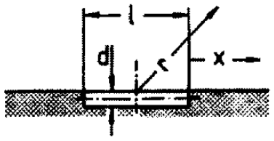	$R = \frac{\rho}{\pi l} \ln\frac{2l}{d}$	$l \gg d$	$U_r = \frac{I\rho}{\pi l} \ln\left(\frac{l}{2r} + \sqrt{1+\left(\frac{l}{2r}\right)^2}\right) \approx \frac{I\rho}{2\pi r}$ $U_x = \frac{I\rho}{2\pi l} \ln\left(\frac{2x+l}{2x-l}\right) \approx \frac{I\rho}{2\pi x}$ [the approximation holds for $(r, x) \gg l$]
5	Sphere, diameter d, depth below surface t	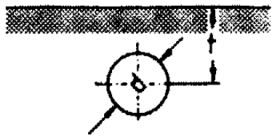	$R = \frac{\rho}{2\pi}\left(\frac{1}{d} + \frac{1}{4t}\right)$	$t \gg d$	$U_r = \frac{I\rho}{2\pi\sqrt{t^2+r^2}}$

Table B-2: Calculation formulas for simple anodes (anode voltage $U_0 = IR$) Continued [7]

Line	Anode shape	Anode arrangement	Grounding resistance	Remarks	Voltage cone
6	Ring-shaped ground, band width b, radius r_0	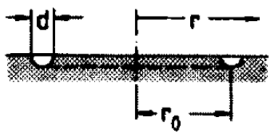	$R = \frac{\rho}{2\pi^2 r_0} \ln\left(\frac{16 r_0}{d}\right)$	$d = \frac{b}{2}$	$U_r = \frac{I\rho}{\pi^2 (r_0 + r)} F\left(\frac{2\sqrt{r_0 r}}{r_0 + r}\right)^a$
7	Vertical anode, length l, diameter d, depth below surface t	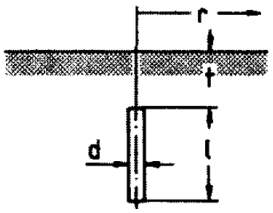	$R = \frac{\rho}{2\pi l} \ln\left(\frac{2l}{d}\sqrt{\frac{4t+3l}{4t+l}}\right)$	$t \gg d$ $d \ll l$	$U_r = \frac{I\rho}{2\pi l} \ln\left(\frac{t+l+\sqrt{r^2+(t+l)^2}}{t+\sqrt{r^2+t^2}}\right)$
8	Vertical anode		$R = \frac{\rho}{2\pi l} \ln\left(\frac{2l}{d}\right)$	$t \gg l$	$U_r = \frac{I\rho}{2\pi l} \ln \frac{\sqrt{t^2+r^2+\left(\frac{l}{2}\right)^2}+\frac{l}{2}}{\sqrt{t^2+r^2+\left(\frac{l}{2}\right)^2}-\frac{l}{2}}$
9	Horizontal anode, length l, diameter d, depth below surface t	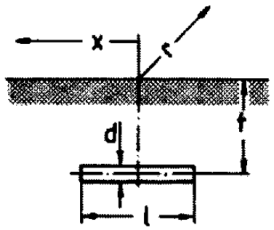	$R = \frac{\rho}{2\pi l} \ln\left(\frac{l^2}{td}\right)$	$d \ll l$ $t \ll l$	$U_x = \frac{I\rho}{2\pi l} \ln \frac{\sqrt{t^2+\left(x+\frac{l}{2}\right)^2}+x+\frac{l}{2}}{\sqrt{t^2+\left(x-\frac{l}{2}\right)^2}+x-\frac{l}{2}}$
10	Horizontal anode		$R = \frac{\rho}{2\pi l} \ln\left(\frac{2l}{d}\right)$	$t \gg l$	

C

ANNEXURE

BASIC THERMODYNAMICS OF CORROSION

This annexure provides supplementing information on the basic thermodynamics of corrosion. This topic has been addressed briefly in Chapter 2 along with corrosion kinetics. The information contained in this annexure provides detailed information regarding the thermodynamics of corrosion and this information is to be used in conjunction with Chapter 2 should more information be required.

C.1 Basic thermodynamics

The energy associated with the reactions discussed in the preceding section needs to be known in order to assess the severity of the corrosion taking place. To calculate the energy associated with the corrosion process, the basic thermodynamics of the corrosion process needs to be addressed. The paragraphs to follow will be used to address the basic thermodynamics associated with corrosion and how it can be used to assess the corrosion process.

The driving force for the transport of all particles is a change in the electrochemical potential $\tilde{\mu}_i$ which is related to the partial molar free enthalpy μ_i and the electric potential φ as follows:

$$\tilde{\mu}_i = \mu_i + z_i \mathcal{F} \varphi,$$

(C-1)

and z_i is the charge number and $\mathcal{F}$ is the Faraday constant. For a homogeneous conductor and in the migration direction:

$$\vec{w}_i = -B \nabla \tilde{\mu}_i = B\left(-\nabla\tilde{\mu}_i + z_i \mathcal{F} \vec{E}\right),$$

(C-2)

where $\vec{w}_i$ is the velocity in the migration direction, B is the mobility, and $\vec{E}$ is the electric field strength in the migration direction. The factor $B = D/RT$ and contains the diffusion coefficient D, the gas constant R, and the absolute temperature T.

Equation (C-2) includes a diffusion and a migration term. Correspondingly, (C-2) gives the first diffusion law for $z_i = 0$ and Ohm's Law for $\nabla \mu_i = 0$. The transfer across a phase boundary is presented by the following:

$$w_i = B(\Delta\mu_i + z_i \mathcal{F} \Delta\varphi).$$

(C-3)

If $w_i = 0$, the equilibrium is given by:

$$0 = \Delta\tilde{\mu}_i^* = \Delta\mu_i^* + z_i \mathcal{F} \Delta\varphi^*,$$

(C-4)

where $\tilde{\mu}_i^*$ is the electrochemical potential in thermodynamic equilibrium, μ_i^* is the partial molar free enthalpy in thermodynamic equilibrium, and φ^* the electric potential in thermodynamic equilibrium.

To supplement the discussion regarding basic thermodynamics, it is necessary to define the potential-determining reaction of the reference electrode. The potential-determining reaction of the standard hydrogen electrode is presented as follows:

$$2H^+ + 2e^- = 2H \rightarrow H_2.$$

(C-5)

By applying (C-4) to the reactions in (2-1) and (C-5) lead to the Nernst potential equation:

$$-U^* = \Delta\varphi^* - \Delta\varphi_B = -\frac{\Delta\mu_i^* - \Delta\mu_B}{z_i \mathcal{F}} = -\frac{\Delta G}{z_i \mathcal{F}},$$

(C-6)

where U^* is the voltage in thermodynamic equilibrium, φ_B the electrical potential of the reference electrode, μ_B the partial molar free enthalpy of the reference electrode, and ΔG the free reaction enthalpy of the chemical reaction

$$Me + zH^+ \rightarrow Me^{z+} + \frac{z}{2} H_2.$$

(C-7)

The reaction in (C-7) corresponds to adding the electrochemical half-reactions found in (2-1) and (C-5). The negative sign of U^* in (C-6) accounts for the fact that all $\Delta\varphi$ contain potential differences in the reaction direction of (C-7) in the cell H_2/electrolyte/metal and ΔG is appropriately defined [7]. Due to the concentration dependence of μ_i it follows that:

$$\mu_i = \mu_i^0 + RT \ln\left(\frac{c_i}{mol\ L^{-1}}\right),$$

(C-8)

where μ_i is the partial molar free enthalpy, ${\mu_i}^0$ the partial molar free enthalpy under standard conditions, R the gas constant, T the absolute temperature, and c_i is the concentration of the material per molar of liquid. Considering the standard state of the hydrogen electrode with a variable metal ion concentration, $c(Me^{z+})$, the equilibrium potential against the standard hydrogen electrode is:

$$U_H{}^* = \frac{\Delta G}{z\mathcal{F}} = \frac{\Delta G^0}{z\mathcal{F}} + \frac{RT}{z\mathcal{F}} \ln\left[c\frac{(Me^{z+})}{mol\ L^{-1}}\right] = U_H{}^0 + \frac{RT}{z\mathcal{F}} \ln\left[c\frac{(Me^{z+})}{mol\ L^{-1}}\right],$$

(C-9)

where $U_H{}^\circ$ is the potential measured against the standard hydrogen electrode in thermodynamic equilibrium, ΔG is the free enthalpy of the formation, ΔG^0 is the free enthalpy of the formation under standard conditions. The factor $RT/\mathcal{F}$ is $26\ \mathrm{mV}$ at $25\ ℃$, and $U_H{}^0$ the potential measured against the standard hydrogen electrode under standard conditions. In the same way, a potential equilibrium can be derived for a simple redox reaction:

$$U_H{}^* = U_H{}^o + \frac{RT}{z\mathcal{F}} \ln\left(\frac{c_{Ox}}{c_{Red}}\right),$$

(C-10)

where c_{Ox} is the concentration of the oxidising agents in the reaction, and c_{Red} is the concentration of the reducing agents in the reaction. More often than not, redox reactions are rather complicated. For a general redox reaction, with components X_i and their coefficients n_i written as

$$\sum_i n_i X_i = e^-,$$

(C-11)

the relation can be derived [7]:

$$U_H{}^* = U^o - \frac{RT}{z\mathcal{F}} \sum_i n_i ln\left[\frac{c(X_i)}{mol\ L^{-1}}\right].$$

(C-12)

By using the basic thermodynamic equations that were derived in the preceding section along with a table containing the standard potentials for given reactions, Pourbaix diagrams can be drawn. The standard potentials presented in Table C-1 are used when drawing Pourbaix diagrams for the cases where electrochemical redox reactions occur. The value of these standard potentials are measured against the standard hydrogen electrode as reference.

Table C-1: Standard potentials for electrochemical redox reactions

Chemical reaction	$U_H{}^o$ @ 25℃ [mV]
$2H^+ + 2e^- \leftrightarrow H_2$	0.00
$O_2 + 2H_2O + 4e^- \leftrightarrow 4OH^-$	+400
$O_2 + 4H^+ + 4e^- \leftrightarrow 2H_2O$	+1230
$Cl_2 + 2e^- \leftrightarrow 2Cl^-$	+1360
$Cr^{2+} + e^- \leftrightarrow Cr^+$	-410
$Cu^{2+} + e^- \leftrightarrow Cu^+$	+160
$Fe^{2+} + 2e^- \leftrightarrow Fe$	-447
$Fe^{3+} + e^- \leftrightarrow Fe^{2+}$	+770

A simplified Pourbaix diagram for iron in an aqueous solution (H_2O) is displayed in Figure C-1. Pourbaix diagrams are often utilised for showing conditions of solution oxidising power (potential) and acidity or alkalinity for the various possible phases that are stable in an aqueous electrochemical system [16]. Potential is presented on the vertical axis of the diagram and pH on the horizontal axis of the Pourbaix diagram. Strong oxidising agents tend to occur at the top of the diagram, while strong reducing agents occur at the bottom of the diagram.

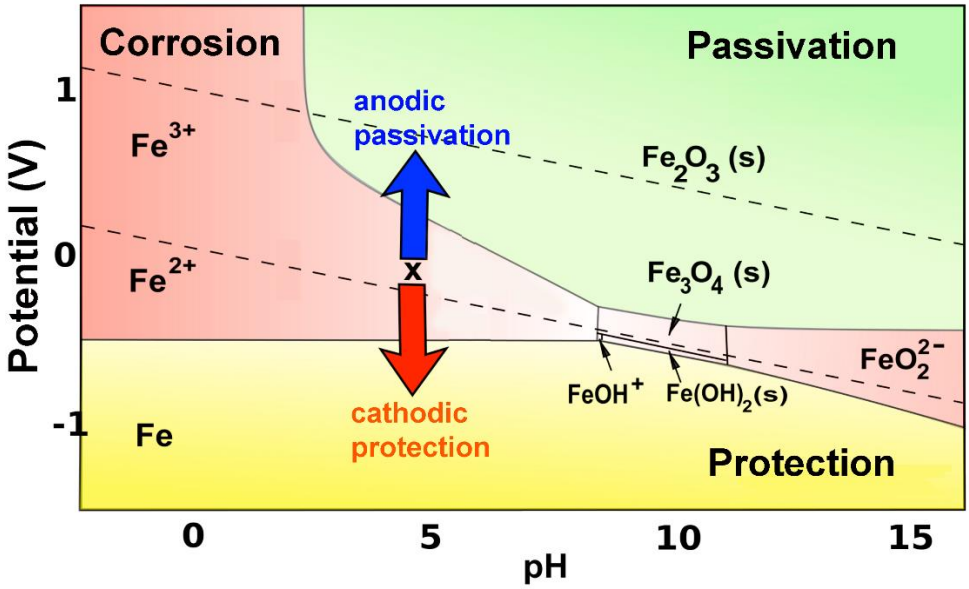

Figure C-1: Simplified Pourbaix diagram for iron in an aqueous solution

The boundary lines on the Pourbaix diagram dividing the areas of stability for different phases are derived from the Nernst equation [16]. The different boundary lines are described as follows:

- The vertical lines separate the species that are in acid/alkali equilibrium
- The non-vertical lines separate the species which are at redox equilibrium. The non-vertical lines can be categorised as follows:

(xiv) Horizontal lines – used to separate the redox equilibrium species that do not include hydrogen or hydroxide ions.

(xv) Diagonal lines – used to separate the redox equilibrium species that include hydrogen or hydroxide ions.

- The dashed lines in the diagram are used to enclose the practical region of stability of the aqueous solution to oxidation or reduction. In the regions that fall outside the dashed lines, the solution breaks down and not the metal.

The use of Pourbaix diagrams does come with certain limitations. No predictions in terms of corrosion rates can be made with these diagrams. This is due to the relatively low temperatures present in electrolytes where corrosion may occur. Thermodynamics are more efficient at higher temperatures, and therefore corrosion kinetics are more effective in determining corrosion rates. The electrochemical kinetics of corrosion will be addressed in terms of corrosion rates. Ultimately, the aim is to successfully mitigate corrosion and rapidly slow down the rate of corrosion. In order to successfully mitigate corrosion and understanding how it is achieved, electrochemical polarisation is addressed from first principles.

D

ANNEXURE

ANODES

D.1 Sacrificial anodes

There exist a few requirements for a material, in this case a metal or an alloy, to be classified as a sacrificial anode. By recalling some information from a previous section, the most determining factor for a metal to qualify as a sacrificial anode is its natural potential. The potential between the anode and the structure being protected must be large enough to prevent the formation of anode-cathode cells on the protected structure. Another application may require the potential to be large enough to overcome already formed anode-cathode cells on a corroding structure. This is required to stop the corrosion process from causing further damage to the already corroded structure.

Sufficient electrical energy current is required from the material from which the anode is manufactured. Sufficient current from the material is needed to permit a reasonably long lifetime to the anode, without the need for unreasonable amounts of anode material. In its installed capacity, the anode is generally expected to last for about 15 years.

It is also expected from the material from which sacrificial anodes are manufactured to have good efficiency. This means that a high percentage of the electrical energy content of the material should be available for useful CP current output [18]. The amount of energy consumed by the material during self-corrosion must be relatively small compared to the energy available for useful CP current output. Materials best fitted to be used as sacrificial anodes shall be discussed.

D.1.1 Sacrificial anode materials

- Iron

Iron is known to be the oldest form of material used as sacrificial anodes, generally used to protect the copper cladding on wooden ships from the early 19th century [7]. Iron anodes are still in use today and implemented to protect structures manufactured from materials with a relatively positive protection potential.

- Zinc

Zinc was also used for the protection of metals in seawater in the early 19th century. The problem with the zinc used in that era, was that the material was not pure enough, which meant that the zinc became passive. The zinc used as anode material has a high purity to prevent passivation from occurring. Although zinc anodes have a low driving voltage, in the range of about 0.2 V, it is the mostly used anodes for the external protection of vessels in seawater. Zinc anodes, in the form of bracelets, are also used to protect pipelines in seawater. In oil drilling and mining environments, zinc anodes are preferred as sacrificial anodes for the internal protection of tanks.

In fresh water applications, where zinc tends to passivate, the use of zinc anodes are very limited. The same applies in soils where the resistivity of the soil is relatively high. The zinc anodes, whenever installed in soils, have to be surrounded with bedding materials as backfill. The backfill will be used to reduce the passivation of the zinc, and will effectively lower the grounding resistance.

- Aluminium

Pure aluminium cannot be used as an anode material due to its easy passivation. For this reason, aluminium alloys are rather used as sacrificial anodes. The alloying elements in the aluminium alloys are responsible for the preventing the formation of surface films on the sacrificial anode.

The alloying elements commonly employed in these aluminium alloys include zinc and manganese. The long term activity of the aluminium alloy is ensured by further adding metals such as cadmium, gallium, indium, mercury, and thallium to the alloy. The mentioned elements are referred to as lattice expanders. Lattice contractors are also added to the alloy. The lattice contractors are added to optimize the current yield from the anode. Lattice contractors added to the alloys include manganese, silicon, and titanium. The various aluminium alloys behave very differently as anodes [7].

The natural potential of the aluminium anodes consisting of various alloys lie between -0.75 V and -1.3 V. Mercury containing anodes are seldom used due to the toxicity of mercury salts, in spite of the high current yield associated with these anodes. Therefore aluminium anodes containing zinc and indium as the activators are preferred. These alloys have a rest potential of about -0.8 V, but have a rather low polarisability. These anodes are preferentially used in offshore applications due to the low polarisability of the anodes. The polarisability of aluminium anodes are known to vary from one anode to another [7].

The rate of self-corrosion and the dependence on loading and medium of aluminium alloys fluctuates. These fluctuations are dependent on the alloy type and the fluctuations are always greater than that found in zinc anodes. Because of the different compositions of alloys, the anode material can display different behaviour in different regions of the anode. Anodes manufactured from aluminium alloys are primarily used in offshore applications. The low weight property of these anodes is particularly favourable in view of a service time of 20 – 30 years.

- Magnesium

Magnesium has the highest driving voltage of all the materials already discussed, in the region between -1.3 to -1.7 V. Another advantage that magnesium has over zinc and aluminium alloys is that magnesium is considerably less passivatable. These properties, along with the fact that magnesium anodes have high current content; make magnesium a very suitable material to use as sacrificial anodes. The only drawback with the use of magnesium as sacrificial anodes is that magnesium is prone to self-corrosion of considerable extent. Therefore the current content made available by pure magnesium is much less than the theoretical current content of the pure magnesium [7].

Magnesium anodes are also known to contain other elements other than pure magnesium and the manufactured anodes usually consist of alloys. Elements found in these alloys include aluminium, zinc, and manganese. Other elements are known to promote self-corrosion of magnesium if added to magnesium alloys. These elements include nickel, iron, and copper.

Magnesium anodes are used in applications where the driving voltage from either zinc or aluminium anodes is insufficient. Magnesium consist of a higher driving voltage and is also the preferred anode in applications where the danger of passivation exists. Magnesium anodes are especially preferred in cases of higher resistivity of the electrolyte and higher protection current densities [7]. Magnesium anodes can be used in stagnant freshwater and objects to be protected include the following: steel-water structures, ballast tanks, boilers and drinking water tanks.

D.1.2 Forms of sacrificial anodes

Sacrificial anodes are available in various shapes and sizes. The form of the sacrificial anode to be used will mainly depend on the application as well as the type and the size of the structure to be protected. The available forms of sacrificial anodes have been determined by a range of specifications, drawn up through the history of sacrificial anodes. These specifications were drawn up to put certain standards in place regarding safety and quality assurance. The different forms of anodes with some applications are to be briefly discussed.

- Rod anodes

Rod anodes are made available as lengths with a core wire. Rod anodes are either cast or extruded. The main applications of rod anodes include the following: protecting objects buried in soil, and the internal protection of storage tanks. Whenever individual anodes are to be used, an individual anode can be up to 1.5 m long. The weight of rod anodes is dependent on the size of the anode along with the alloy from which the anode is manufactured.

- Plates and compact anodes

Plates and compact anodes are generally used for the external protection of ships, the protection of steel-water structures, and for the internal protection of large storage tanks [7]. Plates and compact anodes are not commonly used in soils because of the large grounding resistance between the anodes and the soil.

In cases where the flow resistance of the anode should be as low as possible, plate anodes are readily installed. Flow resistance are rather important when considering the external protection of ships. These anodes have a teardrop-shaped contour. Compact anodes are manufactured in cross-sectional shapes that include the following: square, rectangular, and round. Compact anodes can be fixed by either bolting or welding the iron tube, cast into the anode, to the structure to be protected.

- Anodes for tanks

Tank anodes are elongated, with a round iron core running through them [7]. Cross-sections associated with anodes for tanks include the following: half round, almost rectangular, trapezoidal, and occasionally triangular. The iron core running through the anode is welded to fasteners in order to fix the anode to the structure to be protected. Anodes for tanks are generally found in lengths between 1.0 and 1.2 m, excluding the supports. In cases where internal tank protection is required, the anodes are fixed to the tank by bolts. This is necessary as in some cases welding and brazing is prohibited due to the danger of an explosion occurring.

- Offshore anodes

Offshore anodes are found in the same shapes as that discussed in anodes for tanks. Offshore anodes are much larger in size and weighs much more than anodes for tanks. Offshore anodes in the form of bracelets are fitted to offshore pipelines. These anodes are fixed under stress around the pipeline and then welded.

- Special forms

Special forms of sacrificial anodes are referred to as the anodes which are generally used to protect smaller containers such as boilers, heat exchangers, and condensers. These types of anodes can take on many forms and can be fixed to the structure to be protected by either bolting or welding. The anodes specified as special forms are predominantly manufactured from magnesium and the weight of these anodes lies between 0.1 and 1 kg.

Two forms of sacrificial anodes are displayed in Figure D-1. The anode displayed in Figure D-1 (a) is a representation of a ribbon anode. Ribbon anodes are manufactured in various shapes and sizes, and from a variety of magnesium and zinc alloys. The anode displayed in Figure D-1 (b) is a representation of a semi-cylindrical bracelet anode. Bracelet anodes are also available in multi-segmented forms and mainly implemented for the protection of offshore pipelines. Bracelet anodes are generally manufactured from various aluminium and zinc alloys respectively.

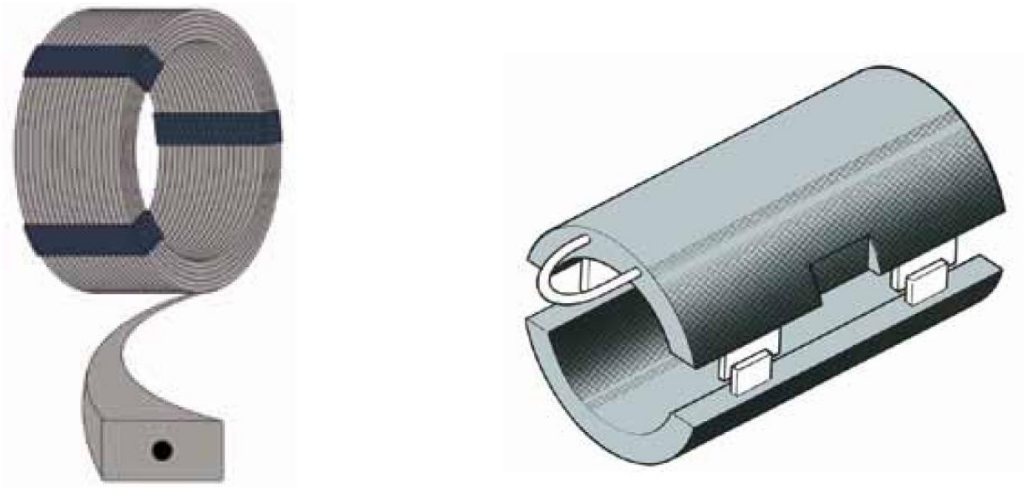

(a) **(b)**

Figure D-1: Forms of sacrificial anodes

Some form of selection guide for sacrificial anodes is included in Table D-1 This guideline is used to provide the reader with information regarding the type of anodes generally used in range of applications. Sacrificial anodes readily available on the market are listed against all possible applications in which sacrificial anode CP can be used. An “X” in Table D-1 indicates the anode to be used for a specific application.

Table D-1: Selection guide for sacrificial anodes **[33]**

	ANODES												
Application	**Mg pre-packed backfill**	**Fresh water Mg**	**Hull Mg**	**Hull Al**	**Hull Zn**	**Offshore Al**	**Offshore Zn**	**Tank Al**	**Tank Zn**	**Ribbon zinc**	**Ribbon magnesium**	**Bracelet aluminium**	**Bracelet zinc**
Onshore pipeline	X									X	X		
Offshore pipeline												X	X
Casing external	X									X	X		
Casing internal										X	X		
Tanks internal		X						X	X				
Sluices		X	X			X	X						
Offshore structures/shipping				X	X	X	X						
Internal protection		X	X	X	X	X	X	X	X				
Water well riser pipes		X								X	X		

D.2 Impressed current anodes

Impressed current anodes can deliver a much higher current supply than sacrificial anodes. The current supply is highest whenever anodic redox reactions are running in parallel. Impressed current anodes are known to have a more positive potential than the object they are connected to in order to provide protection. Materials from which impressed current anodes are manufactured from need as low solubility as possible. Caution should also be taken not to damage the material through impact, abrasion or vibration. Lastly, these materials should have high conductivity and must be capable of handling heavy current loads.

Two types of impressed current anodes are currently manufactured. The first type of impressed current anodes consists of anodically stable noble metals. One example of an anodically stable noble metal is platinum. The other type of impressed current anodes is manufactured from anodically passivatable materials that form conducting oxide films on their surfaces [69]. In both the aforementioned types of anodes, the theoretically possible potential at which anodic corrosion occurs, are higher than the potential at which anodic redox reactions occur.

The materials that can be used to manufacture impressed current anodes are relatively limited in practice. The materials most often used in the manufacturing process of impressed current anodes include: graphite, magnetite, high-silicon iron with various additions, and lead-silver

alloys. Coated anodes of so-called valve metals are also available. All of the mentioned metals used in the manufacturing of these anodes have stable passive films at very positive potentials. The passive films are not electron conducting, e.g., titanium, niobium, tantalum, and tungsten. The best known in this group are the platinised titanium anodes [7].

D.2.1 Impressed current anode materials

- Solid anodes

The most common solid anode to have been used, seldom used presently, is scrap iron. Forms of scrap iron that have been used as anodes include: old steel girders, pipes, and railway lines. The anodic dissolution of iron, through the formation of Fe(II) compounds, takes place with almost 100% current efficiency [7]. It is known that 1 kg of iron has the capacity to deliver about 960 Ah. The weight loss of iron under loading conditions is comparatively high. Whenever scrap iron is used as impressed current anodes, large amounts of scrap iron is required to be able to provide a practical service life to the system.

Other types of solid anodes shall be discussed briefly, considering the type of material used in the manufacturing and other important properties. The properties to be briefly mentioned will include: resistivity, anode consumption, anode current density, applications, advantages and disadvantages, where applicable.

Magnetite can also be used in the form of solid anodes. The defect structure that magnetite consist of, allows for electron conductivity. Pure magnetite is known to have a resistivity between 5.2×10^{-3} Ω m and 10×10^{-3} Ω m. From an anode current density in the region of 90 A m^{-2} to 100 A m^{-2}, the consumption rate of magnetite anodes is calculated to be 1.5 g $A^{-1}a^{-1}$. Although the consumption rate of magnetite anodes increases with the anode current density, it is still very low. Soils and aqueous environments, including seawater, are common electrolytes in which magnetite anodes can be used. Furthermore, magnetite anodes can endure high voltages, with the disadvantages of brittleness, casting difficulty, and relatively high electrical resistance.

As an anode material, graphite has a few advantages. These include that the material is relatively inexpensive, and that gaseous products are formed by the anodic reactions. The electron conductivity, which is around 200 to 700 S cm^{-1}, is also considered an advantage. The disadvantages of graphite include: mechanical weakness and high current densities raises the consumption rate of the anode. The typical consumption rate of graphite in soil amounts to about 1.5 kg $A^{-1}a^{-1}$. This consumption rate is based on a current density of 20 A m^{-2}. The consumption

rate of graphite anodes decreases in electrolytes where the graphite carbon is prohibited from reacting with oxygen.

Table D-2: Choosing the correct magnetite impressed current anodes **[33]**

Magnetite impressed current anodes		
Type	**Surrounding electrolyte**	**Applications**
MA-U	Neutral soil and water without chlorine and sulphate content	Shallow and deep ground beds
MA-CS	Chlorine and/or sulphate containing soil or stagnant water	Shallow and deep ground beds
MA-SEA	Flowing seawater or brackish water	Platforms, jetties, and harbours
MA-CHAIN-1	Chlorine containing soil or stagnant water	Open- and closed hole deep ground beds and water tanks
MA-CHAIN-2	Chlorine containing soil or stagnant water	Open- and closed hole deep ground beds and water tanks

High-silicon iron, an alloy containing 14% silicon and 1% carbon, is another form of solid anode used in ICCP systems. The performance of high-silicon anodes is dependent on the elements present in the alloy. These elements are responsible for forming surface films on the anode, which restricts the anodic dissolution of iron. Taken as an average, the loading capacity of high-silicon anodes is between 10 and 50 A m^{-2}. The average loading capacity value, along with certain service conditions, are needed to ensure that the consumption rate is kept below 0.25 kg $A^{-1}a^{-1}$. The low loss rate that high-silicon anodes comprise, allows these anodes to be buried directly in soil. The disadvantage associated with this, is that an outlet must be provided through which the evolved gasses surrounding the anode can evaporate. Failing to install this outlet, will lead to an increase in the anode resistance.

Lead-silver alloys are another form of solid anode that is regularly used. Various lead-silver alloys, containing various amounts of lead and silver, are available on the market. These anodes are primarily used in seawater and in the presence of electrolytes containing strong chlorides. The applications associated with lead-silver anodes include: protection of ships, and the protection of steel-water structures. The insensitiveness to mechanical stresses makes these anodes desirable for the mentioned applications. The average loading capacities and the anode consumption rate of these anodes are dependent on the composition of the alloy used during manufacturing. The average loading capacity of these anodes ranges between 50 to 350 A m^{-2}. The anode consumption rate of the respective alloys ranges from 45 to 80 g A^{-1}.

Lead anodes containing platinum pins are the last type of solid anodes to be commonly implemented as impressed current anodes. Literature covering these types of anodes is often

contradicting, regarding the consumption rate and the performance of these anodes. The consumption rate and lifetime of this type of anodes are dependent on the time that the platinum pins remain in the anode. The time these platinum pins remain in the material are in return dependent on the electrolyte and varies with each installation. Anodes containing lead are best fitted to be installed in chloride-rich electrolytes. Formability is considered an advantage in lead containing materials. Disadvantages of lead containing anodes include the high density of the material from which it is manufactured along with the low anode current density [7].

Solid anodes, of the substrates discussed above, are known to have a much higher consumption rate than that of the anodes manufactured from the substrates that are to follow.

- Noble metals

Noble metals and valve metals coated with noble metals are to be discussed. Noble metals are used to achieve high anode current densities along with long anode lifetimes. The most common noble metal used in impressed current anodes is platinum. Reasons why platinum is preferred in anode manufacturing includes: platinum has a high conductivity along with a rather low consumption rate. Platinum is a very expensive noble metal and are therefore not used to manufacture pure platinum anodes. Cladding or electroplating is generally used to coat a substrate, less expensive than platinum, with a thin layer of platinum. The coating of the substrate extends the effective anode surface area, which improves the overall performance of the anode. Titanium, niobium, and tantalum are the most common substrates to be coated with a thin layer of platinum [33].

This type of anodes is more desirable than other types, because the surfaces of these anodes are anodically stable. In their installed capacities, in suitable conditions, these anodes are able to deliver current densities of up to 10^4 Am^{-2} [7]. Under the same favourable conditions, these anodes have a practically unlimited driving voltage. Furthermore, the consumption rate of these anodes is very low and can be in the range of only a few milligrams per ampere per year. The aforementioned properties apply chiefly at low current densities in seawater where there is good dispersion of the hypo-chlorous acid that is formed [7]. In cases where these anodes are to be implemented in electrolytes with poor conductivity, the consumption rate of the platinum increases slightly.

The driving potential of the different substrates, namely titanium, niobium, and tantalum, coated with is dependent on the electrolyte surrounding the anode in its installed capacity. Titanium has a driving potential limit of 12 V. It is therefore required to use the valve metals like niobium and

tantalum, which has a driving voltage of up to 100 V in favourable conditions. Whenever niobium and tantalum are platinised, anodes of this type, have almost no limitations.

- Metal oxide-coated valve metals

Metal oxide-coated valve metals are more commonly referred to as mixed metal oxide anodes. This type of anodes is manufactured by applying a mixture of oxides as a coating to a high purity titanium substrate. Another substrate generally used in this type of anodes is niobium. The mixture of oxides used in the coating typically comprise cobalt, nickel, and lithium ferrites. The aforementioned ferrites are used in the substrate coatings due to their low consumption rates. Once again, the consumption rate of these anodes is dependent on the electrolyte and the surrounding conditions. When installed in seawater, the consumption rate of these anodes is given as 10^{-3} g $A^{-1}a^{-1}$. The consumption rate of these anodes in freshwater is given as 6×10^{-3} g $A^{-1}a^{-1}$ [7].

An advantage that these anodes hold over platinised titanium anodes is that mixed metal oxide anodes are very abrasion resistant. Also, the polarisation resistance of these anodes is also very low, which results in the voltage variations at the surface of these anodes being very small. Due to their light weight, these anodes are the preferred choice as deep well anodes. The current loading of these anodes, in different electrolytes, is in the following range: 100 A m^{-2} in soil with coke backfill, 600 A m^{-2} in seawater, and 100 A m^{-2} in freshwater [7].

- Polymer cable anodes

These anodes are manufactured from a conducting, stabilised and modified plastic. Graphite is incorporated into this plastic and acts as the conducting material within the anode. This type of anodes is known for their flexibility, mechanical resistance, and chemical stability. A copper cable core serves as the means of current lead [7]. It is suggested that these anodes can have a current delivery of up to 20 mA per meter of cable, with an expected service lifetime of up to10 years.

During the anodic reactions, that were discussed earlier, graphite is consumed. This graphite consumption at certain areas of the anode, over a period of time, causes the anode resistance to increase at these areas. This process is dependent on the current densities at the different anode areas and therefore directly dependable on the specific soil resistivity. The service lifetime of these anodes is determined, not by their mechanical stability, but more specifically by their electrical effectiveness in installed capacity.

D.2.2 Forms of impressed current anodes

Impressed current anodes are available in variety of shapes and sizes. Different forms of impressed current anodes are used in different applications. The available forms and the most common applications of these forms are to be discussed.

- Anodes suitable for soil

Anodes that are best fitted to be buried in soil, are cylindrical in shape, and manufactured from high-silicon iron. The weight, diameter, and length of these anodes will vary according to application and the acidity of the soil in which they are to be buried. Commonly, these anodes are manufactured to be slightly conical. Furthermore, the anodes have a thicker end in which an iron connector is embedded. This iron connector is referred to as the current lead and is used to make a cable connection by either brazing or wedging.

As cable connection problems are mostly responsible for premature anode failure in impressed current CP systems, some precautions are necessary. The connection between the cable and iron connector is typically sealed by using cast resin. This part of the anode is then generally referred to as the anode head. Installation and assembly costs form the largest part of the total expenses regarding anode system installation. Therefore special attention should be given whenever cable connections are made to anodes to ensure that the anode head is both durable and reliable.

Figure D-2: Impressed current anode manufactured from silicon iron **[33]**

The typical shape of impressed current anodes suitable for burying in soil is displayed in Figure D-2. The iron tip, to which the cable connection is to be made, can be seen at the top of the anode and is on the left hand side of the figure. The anode being displayed in Figure D-2 is manufactured from silicon iron and is available in different sizes. The anode sizes generally vary in the following categories: length, diameter and weight.

- Anodes suitable for water

Anodes suitable for use in water are similarly shaped than those discussed in the preceding section. Also, anodes that are used in soil can be implemented in water without any significant

difficulties. These anodes are predominantly used in water to protect steel-water constructions, offshore installations, and internal protection of tanks. Anodes suitable for use in soil are predominantly manufactured from graphite, magnetite, and high-silicon iron. In addition to these materials, anodes suitable for use in water are also manufactured from lead-silver alloys. Furthermore, titanium, niobium or tantalum coated with platinum or lithium ferrite is also common materials used in the manufacturing of anodes suitable for use in water.

Although anodes suitable for soil can be used in water as well, most anodes suitable for use in water are not solid, but rather manufactured in tubular form. The tubular shape of these anodes is preferred because of the larger surfaces that are provided by this shape. The larger surfaces lead to higher currents being delivered by the anodes.

The same type of cable connection that was discussed in the previous section is applicable to lead-silver anodes. In this case the cable is soft soldered to the anode in applications where the reduction in the tensile load is required. The same type of cable connection cannot be used on titanium anodes. Therefore, this type of anodes is available with a screw connection. The screw connection is welded onto the anode by the manufacturer where applicable. The screw connector is also manufactured from titanium. The titanium anode configuration is finally coated with cast resin or the whole tube is filled with a suitable sealing compound [7]. In some instances where the titanium anodes are long and highly loaded, they are manufactured with current connections at both ends of the anode. This is necessary because of the poor conductivity of titanium.

Other anode shapes that are suitable for use in water include: disc, ingot-shaped, rod, and hurdle-shaped anodes. Rod and hurdle-shaped anodes are often parallel-connected, if sufficient space is available, to protect larger objects such as sheet steel linings and loading bridges. Floating anodes are also available and is generally used to protect offshore structure. These anodes are available in cylindrical as well as spherical forms. Floating anodes are attached to the seabed to float at a predetermined depth, by means of an anchor. Some advantages that floating anodes hold over other forms of anodes includes: repairs can be carried out without interrupting the operation of the offshore installation, and uniform current distribution can be achieved. The uniform current distribution is achieved by distancing the anode at an optimal distance from the protected structure.

- Anodes for internal protection

Titanium rod anodes, the same as those already discussed, are commonly used for the internal protection of pipes, tanks, condensers, and other process equipment. Rod anodes are not stable

enough in cases where the rods are too long, and therefore other forms of anodes are also common in internal protection. Plate anodes, along with basket anodes are generally installed on the base of tanks to provide internal corrosion protection.

(a) **(b)**

Figure D-3: Forms of anodes generally used for the internal protection of tanks **[33]**

Special forms of impressed current anodes are displayed in Figure D-3. A screw-in type rod anode is displayed in Figure D-3 (a), while a plate anode is displayed in Figure D-3 (b). These types of anodes are generally used for the internal protection of structures like tanks, pipelines etc. The rod anode displayed in the figure can be seen to have a pressure resistant head structure, which allows for the anode to be used in structures that operate under pressure. Plate anodes are generally installed on the bottom of tanks. The structure of the plate anode consists of an anode plate that is assembled and sealed inside a support frame. The support frame of the plate anode is manufactured from impact resistant plastic material. Other uses of plate anodes include the protection of offshore structures and sluices.

- Other forms of impressed current anodes

Other forms of impressed current anodes are also available on the market and are used in a wide range of applications. The materials, from which these anodes are manufactured, are the same as the range already discussed throughout the text. One special form in which impressed current anodes are produced in is mesh anodes. Mesh anodes are mostly used for the protection of steel reinforced concrete structures. Furthermore, wire anodes, which are manufactured from platinised titanium/niobium/tantalum, are also used for the internal protection of water tanks and pipelines.

D.3 Insulating materials

It is necessary to insulate impressed current anodes from the structure that is being protected by means of an impressed current CP system. The current connections between the cable and the impressed current anodes are also needed to be well insulated. This insulation is required to prevent the free ends of the cable from being attacked and destroyed by the corrosive elements present in the electrolyte.

Electrolytes known to be not too demanding on insulating materials include soil and freshwater. On the other hand, electrolytes containing halides are known to be way more demanding on insulating materials, and include seawater. The high demands on the insulating material are due to the anodic chloride that is formed in these electrolytes.

Insulating materials that are commonly used for the purpose of providing sufficient insulation between the anodes and the structure being protected can be any of the following:

- Special types of rubber (neoprene)
- Stabilised plastics of polyethylene and polyvinylchloride
- Cast resins such as acrylate, epoxy, polyester and many others.

Insulating materials that can be used in halide containing electrolytes, and that is chloride resistant include the following:

- Polypropylene
- Neoprene
- Chloroprene
- Special types of polyvinylchloride
- Special variations of epoxy and unsaturated polyesters
- Fluorinated plastics, e.g. polytetrafluoroethylene (Teflon)

The abovementioned insulating materials are rather important to the success of the CP system, especially in the case of SACP systems where the anodes are fixed to the structure. Failure to provide efficient insulation between the impressed current anodes and the structure being protected can result in the breakdown of the anode in a short time.

E

ANNEXURE

CATHODIC PROTECTION CRITERIA

E.1 Protection criterion for cathodic protection

Assurance is needed that CP systems provide sufficient protection to the structures it is meant to protect. Different criteria are used to determine if sufficient protection is delivered by a given system. The different criteria that are commonly used for this purpose shall be discussed in greater detail. The entire criteria to be discussed are included in the 1996 revision of NACE Standard RP-01-69. The criteria to follow are applicable to steel and cast iron piping unless stated otherwise.

E.1.1 -850 mV with cathodic protection applied criterion

“The full criterion states that adequate protection is achieved with:

A negative (cathodic) potential of at least 850 mV with the CP applied. This potential is measured with respect to a saturated copper/copper sulphate reference electrode contacting the electrolyte. Voltage drops other than those across the structure-to-electrolyte boundary must be considered for valid interpretation of this voltage measurement. Consideration is understood to mean application of sound engineering practice in determining the significance of voltage drops by methods such as:

- measuring or calculating the voltage drop(s),
- reviewing the historical performance of the CP system,
- evaluating the physical and electrical characteristics of the pipe and its environment,
- determining whether or not there is physical evidence of corrosion.” [8, 20, 28]

Different criterion is used for different applications of CP. The different applications associated with the different criterion shall be discussed along with the limitations of each criterion. The limitations of the different criterion will determine when the different criterion will be implemented.

- Applications

The -850 mV with CP applied criterion is the most widely used criterion for determining whether the level of CP applied to a submerged structure is acceptable and sufficient. The criterion is based on potential measurements taken with respect to a copper/copper sulphate reference electrode that is placed as close as possible to the structure. The reference electrode is typically placed directly above the submerged structure when potential measurements are taken. It is accepted that the level of CP is acceptable when the potential difference between the submerged structure and the reference electrode is equal to or more negative than -850 mV.

Important to note, is the fact that certain current flow in the electrolyte can influence the potential measurements that is taken. The mentioned current flow directly results into ohmic or IR voltage drops. Voltage drops will also be present in the structure-to-electrolyte boundary, but won't affect the potential measurements as much. The IR voltage drops require valid interpretation for the criterion to be accurate. IR voltage drops are typically much higher in close proximity of anode ground beds and in areas where stray currents are present. As the soil resistivity increases, the IR voltage drops are also known to increase.

It is possible to reduce the IR voltage drops and the affect it will have on potential drops through the placement of the reference electrode. By placing the reference electrode as close as possible to the submerged structure, IR voltage drops become negligible. This is especially important when assessing bare or poorly coated pipelines, as the IR voltage drop will be greatest for these types of pipelines. When coated pipelines are considered, the majority of the IR voltage drop appears across the coating.

It is also possible to completely eliminate IR voltage drops and its influence on potential measurements. This is done through the interruption of all DC current sources within the CP system. The potential measurements are to be taken instantaneously after the interruption of the current sources and are known as the instantaneous off-potential. These potential measurements are free of IR voltage drops, if and only if all the current sources have been interrupted properly.

The IR voltage drop error can be calculated by calculating the difference between the "on"- and off-potentials respectively. This difference will represent the magnitude of the error that is made, with regard to the IR voltage drop, whenever potentials measurements are taken with the protective current applied.

The criterion of -850 mV was adopted to provide a 50 mV margin of protection as the highest native potential measurement on submerged structures was in the range of -800 mV. The effectiveness of the criterion has been demonstrated over many years of application [8, 20, 28]

- Limitations

Although the -850 mV with CP applied criterion is the most widely used of the criteria, it is associated with a number of limitations. As previously stated, this criterion's use can be limited if the measurements are not taken directly above, and as close as possible to, the submerged structure. Furthermore, it is required that the reference electrode be in direct contact with the respective electrolyte. If this is not possible, alternative criteria may be required as the IR voltage drops will influence potential measurements. The majority of IR voltage drops occur on the boundary of the coatings of well-coated structures therefore this criterion is mostly used for well-coated pipelines [8, 20, 28].

It is possible that potentials more positive than -850 mV (CSE) can exist between measuring points if the distance between the measuring points is too extensive. To avoid this problem, close-interval surveys are recommended when this criterion is used. The criterion requires some adjustment in the presence of bacteria and hot pipelines. The adjustment is required due to the increased anodic current kinetics that is associated with the two aforementioned scenarios. This adjustment states that a minimum of -950 mV (CSE) is used in these cases.

Overprotection on the other hand can accelerate the corrosion process and needs to be avoided. The potential measurements acquired through using this criterion can be used to identify areas where overprotection occurs. Polarised potentials that is more negative than -1.05 to -1.1 mV should be avoided. This is also the general consensus in the industry [8, 20, 28]. As the soil moisture content is dependent on seasonal changes, the potentials are known to vary according to the soil moisture content.

This criterion has further limitations in the presence of telluric currents or where shielding has occurred. The mentioned shielding can be the cause of disbonded coatings, rocks, thermal insulation, etc. Stray currents and variations in coating conditions of a structure is also a limitation of this criterion as the accuracy of the potential measurements is compromise [8, 20, 28] d. Stray currents also influence the polarised potential of the structure and will have an effect on the off-potential measurements. Areas where stray current activity is expected to have an effect it is recommended that the potential values are measured for the entire duration of the stray current

activity. The duration in which these measurements are to taken can be anything from 24 hours or longer [8, 20, 28].

Although stray currents can influence the potential measurements, this criterion is the most widely used criterion in areas where stray current activity is suspected. Whenever the potential measurement of a structure remains more negative than -850 mV at a test location at all times, it is accepted that the structure is protected at that given test location.

E.1.2 Polarized potential of -850 mV criterion

“This criterion states that adequate protection is achieved with a negative polarised potential of at least 850 mV relative to a saturated copper/copper sulphate reference electrode. The polarized potential that is referred to is defined as the potential across the structure/electrolyte interface that is the sum of the corrosion potential and the cathodic polarisation [8, 20, 28].”

The off-potential, which is often used to describe the polarised potential, is measured directly after all the current sources have been interrupted. After the interruption of the current sources, two measurable potentials exist. There is the native potential of the structure, and the off potential. The purpose of this criterion is to establish the amount of polarisation that has occurred as a result of the application of CP. The amount of polarisation is determined by the difference in potential between the native and off potentials respectively.

Differences in potential between the on- and off potentials are the result of various voltage drops. These differences are an error brought about by the voltage drops in the electrolyte and the metallic return path in the measuring circuit. The data required for determining the amount of polarization achieved by a given CP system is acquired through a close interval survey [8, 20, 28].

An example of the potential measurements taken during a close-interval survey on a stretch of pipeline is displayed in Figure E-1. The on-, off-, and native potentials of the pipeline are displayed respectively. This is figure will aid in better understanding the error that is made during measurements due to the respective IR voltage drops previously explained.

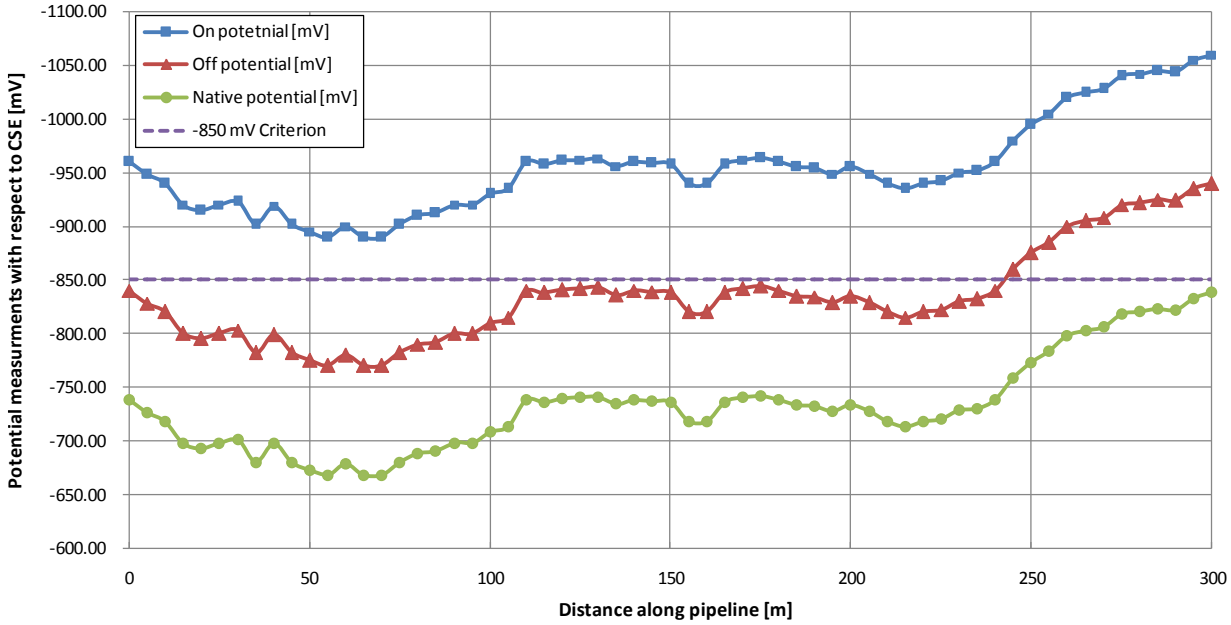

Figure E-1: Example of results obtained from close-interval survey performed on a pipeline

- Applications

This criterion clearly defines the way in which the error regarding the IR voltage drops are considered. These voltage drop errors are minimised or eliminated by using this criterion. The cause of the voltage drops have already been discussed along with the previous criterion.

The voltage drops are measurement errors. This is because the cathodic polarisation at the structure-to-electrolyte interface is the only part of the on-potential measurement that contributes to a reduction in the rate of the corrosion of the structure [8, 20, 28]. Once the polarisation causes the potential shift to be in the negative direction, it is referred to as cathodic polarisation. This criterion, as with the previous criterion, is mostly applied on structures that is well coated, and where all the DC current sources can be readily interrupted.

- Limitations

This criterion is dependent on the fact that all DC current sources require interruption for this criterion to be effectively applied. This is an important limitation of the criterion. When implementing standard survey techniques, it is important to consider that the interruption of all the current sources in the system must occur simultaneously. Several rectifiers, sacrificial anodes, and bonds can be present on a section of pipeline and will require interruption. Experimental verification may sometimes be required in order to determine the number of rectifiers that has an influence on a specific test section.

In cases where the electrical leads of sacrificial anodes are directly bonded to the structure, it is almost impossible to perform interruptions to the system. This is especially true for gas distribution systems. In these cases, the criterion cannot be used and an alternative criterion is advised.

Overprotection can occur through achieving this criterion. This is due to the high currents that need to be applied in some cases for the criterion to be achieved. Further limitations of the polarised potential of -850 mV criterion are included in the limitations of the -850 mV with cathodic protection applied criterion.

E.1.3 100 mV of polarization criterion

“This criterion states that adequate protection is achieved with a minimum of 100 mV of cathodic polarization between the structure surface and a stable reference electrode contacting the electrolyte. The formation or decay of polarization can be measured to satisfy this criterion [8, 20, 28]”.

Considering all of the criteria that have been discussed up to this point, it is adjudged that this criterion has the soundest fundamental basis. When applying this criterion, the rate of corrosion and the rate of the reduction reaction, on the surface of the structure being protected, need to be kept in mind. This is especially important as the corrosion rate can be expressed as a current along with the rate of the reduction reaction. The applied CP current is equal is equal to the difference between the two aforementioned currents.

The anodic Tafel slope is generally used for reference to the anodic reaction’s slope. The Tafel slope generally has a value of approximately 100 mV per decade of current [8, 20, 28]. Whenever a structure experiences a negative shift of 100 mV in the polarised potential, the rate of corrosion experienced by the structure will decrease. According to the Tafel slope, the rate of the corrosion will decrease by a factor of 10. The factor of 10 is referred as an order of magnitude. Typically, when the corrosion rate is decreased by one order of magnitude, corrosion will be mitigated efficiently.

The cathodic polarisation that is brought about by the application of this criterion also has beneficial influences on the environment directly surrounding the structure. The changes in the surrounding environment, further decreases the corrosion rate and is referred to as environmental polarisation. Environmental polarisation results in a potential shift in the free corrosion potential of the submerged structure in the negative direction. The total polarisation experienced by the structure is thus attributable to cathodic – and environmental polarisation.

It is possible to determine the magnitude of the polarisation through measuring the formation or decay of the polarisation. The formation of polarisation is measured by first determining the native potential of the submerged structure at the test locations and is done before CP is applied. Measurements of the potential are then taken again after the CP system had been energised. The time between the measurements must allow sufficient time for polarisation to occur. The design of the CP system along with the nature of the structure will have the greatest effect on the time that the structure requires for sufficient polarisation to occur.

Continuous measurements of the on-potential are required at one test location after the CP system had been energised. When no measurable shift in the on-potential is measured, the off-potential is measured instantaneously after the interruption of current sources. The off-potential measurements are then compared with the native potential measurements of the structure. Once the difference between the off-potential and the native potential exceeds 100 mV, this criterion has been met and sufficient CP is supplied to the structure. Other test locations are to be assessed in the same manner in order to verify the level of CP across the entire structure.

The structure-to-soil potential as a function of time following energising the CP system is displayed in Figure E-2. Important periods during the polarisation period are displayed along with the potential curve typically associated with this process. The curve that is displayed is typically used to determine whether or not the 100 mV polarisation criterion has been met.

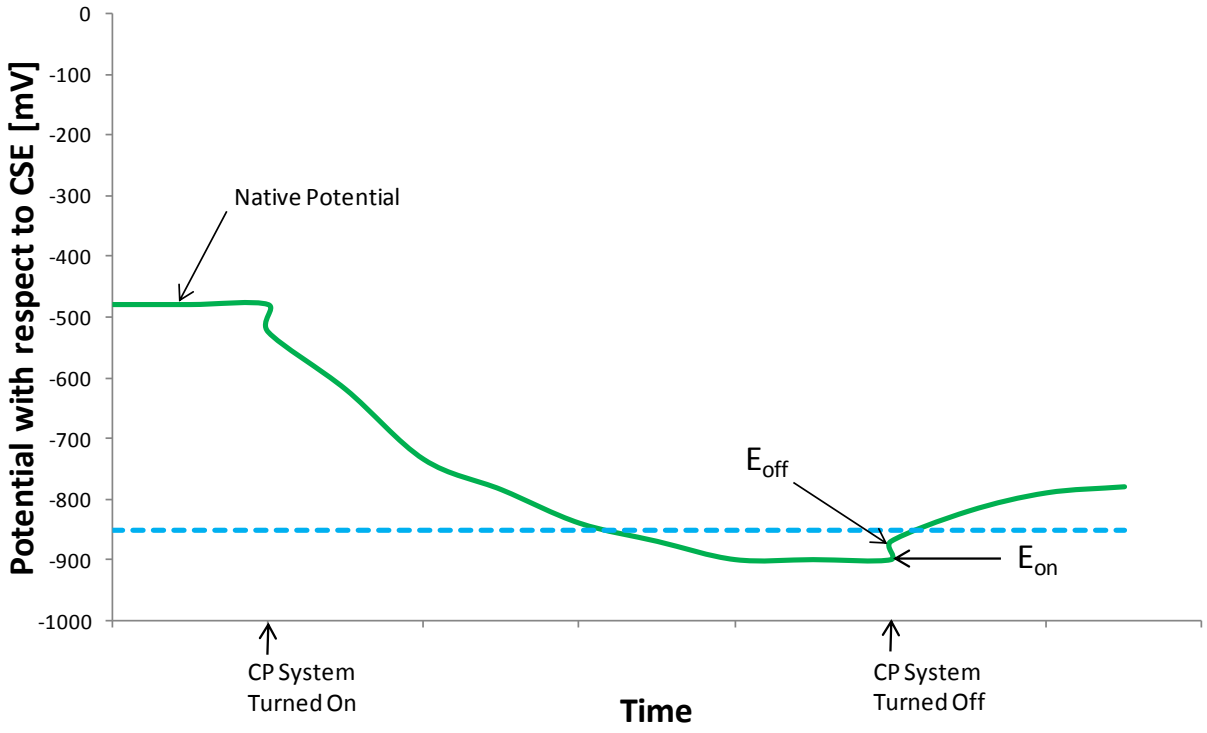

Figure E-2: Structure-to-soil potential as a function of time following energising CP system **[20]**

The formation of cathodic polarisation can be assessed through the use of an alternative method. This method is only dependent on on-potential measurements. The first measurement is taken immediately after the CP system had been energised. Allowing for a few hours or days, depending on the nature of the structure and the CP system design, the on-potential is measured once more. If the on-potential shifted more than 100 mV in the negative direction, it is conservatively accepted that the criterion has been met [8, 20, 28].

This method of verification is only valid if it can be confirmed that the total shift in the on-potential is a result of the sum of the cathodic polarisation and environmental polarisation. Whenever this method is utilised, it is the responsibility of the respective engineer to confirm that the applied CP current decreased with time [8, 20, 28].

Polarisation decay is associated with the de-energising of the CP system. During this period, the potential experiences a shift in the positive direction. This is the most common method that is used to determine the amount of polarisation. The potential shift in the positive direction is due to the elimination of the IR voltage drop in the surrounding environment when the CP system is de-energised. The off-potential is considered the starting point in the assessment of the polarisation shift.

The inductive effects of the pipeline and the CP system can cause a spike in the potential readings directly after the interruption of the CP system. Thus, the respective potential readings are to be taken a few hundred milliseconds after the CP system had been interrupted. Thereafter the potential will experience an exponential decay with time in the positive direction. The exponential decay of the potential is due to the discharge of the capacitor that exists across the structure-to-electrolyte boundary. This component of the potential shift is known as the cathodic polarisation.

The other component of the potential shift, the environmental polarisation, will cause the decay to take a more linear approach. This is a result of the environment surrounding the structure returning to its native condition. This criterion has been satisfied if the difference between the potential measured after polarisation decay and the off-potential is more than 100 mV.

The spike that the potential reading will experience immediately after the interruption of the CP system is displayed in Figure E-3. Furthermore, the cathodic and environmental depolarisation is indicated respectively on the potential profile. The dashed blue line indicates the -850 mV potential, which is the potential where corrosion is effectively mitigated.

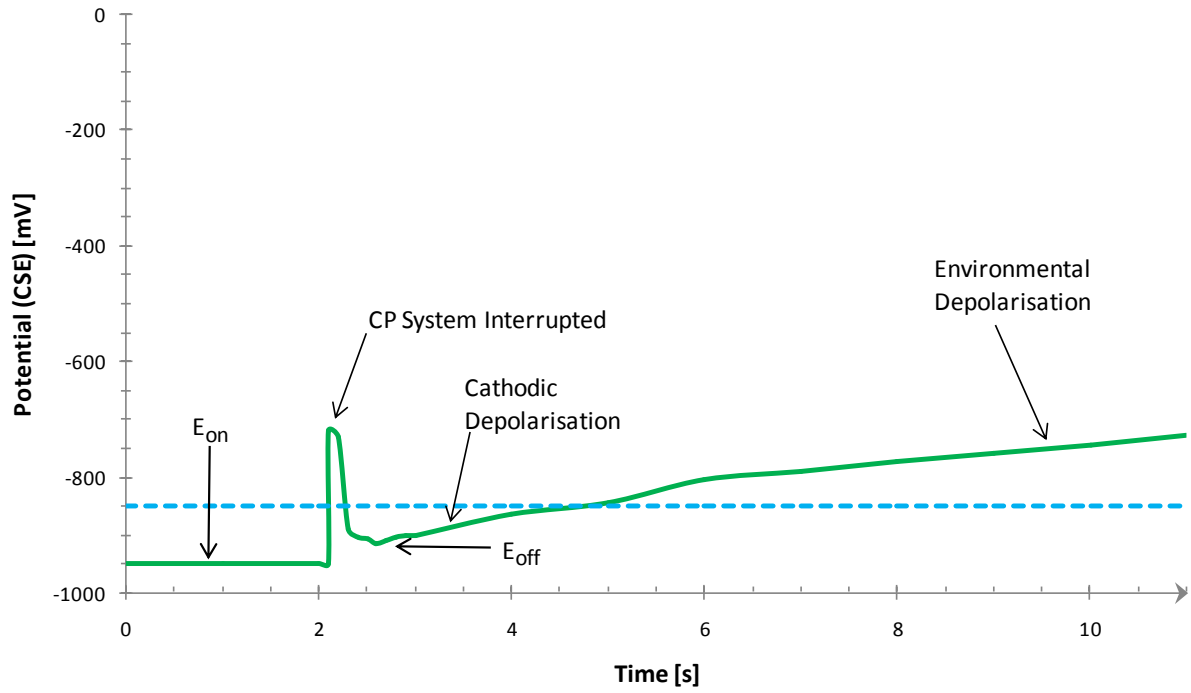

Figure E-3: Potential profile of structure following de-energising CP system **[8, 20, 28]**

- Applications

Of the three criteria discussed, this is the criterion that is mostly used in the assessment of CP systems applied to poorly coated or bare structures. This is due to the fact that it can be difficult and expensive to meet the -850 mV criteria on poorly coated or bare structures. This criterion holds an advantage over the -850 mV criteria, as 100 mV of polarisation is achievable in most cases where the off-potential is less negative than -850 mV. Overprotection and the effects it generally has on the structure, these include coating degradation and hydrogen embrittlement, is minimised through the use of this criterion.

Generally, whenever sections of old pipelines are replaced, different criteria are used on the different sections. The 100 mV polarisation criterion is preferred for the older sections, while either of the -850 mV criterion is preferred for the new sections of the pipeline.

- Limitations

Although this criterion is widely used, it has its limitations. Depolarisation of certain structures can be very time consuming, especially poorly coated or bare structures. This can leave the structure unprotected for several days or weeks. Normally in cases where the criterion has been met within a few hours of the moment at which the CP system had been interrupted, further waiting on

depolarisation is unnecessary. Waiting periods for depolarisation can be lengthy though, especially where the total polarisation is very close to 100 mV [8, 20, 28].

It is questionable if the criterion will be achieved if a depolarisation potential of less than 50 mV is measured after a few hours of interruption of the CP system. The costs associated with the upgrading of CP systems, in areas where the -850 mV criteria were not achieved, are frequently reduced through the use of the 100 mV polarisation criterion. It is recommended though that a proper economical analysis is performed in order to determine if this application will cut the costs.

Further limitations of the 100 mV polarisation criterion include areas subject to stray currents. In such areas, 100 mV of polarisation is not enough to mitigate the corrosion associated with stray currents. This criterion is also not recommended for use on structures that may experience galvanic corrosion. The 100 mV of polarisation may not be adequate to protect the active metal in the galvanic couple.

Careful consideration and knowledge of the different criteria is required before applying it in practice. It may be required that other criteria are to be used in certain installations and this will depend on the different specifications of the sites and environments where CP is to be installed.

The criteria that had been discussed are to be kept in mind when CP systems are designed for different applications and environments. These criteria can be instrumental to the success of the overall CP system and the different applications and limitations of the respective criteria will determine the effectiveness of the protection provided to a given structure.